

Aus dem Institut für Prophylaxe und Epidemiologie der Kreislaufkrankheiten (IPEK)
der Ludwig-Maximilians-Universität München
Direktor: Univ.-Prof. Dr. med. Christian Weber

Role of serotonin and antidepressants targeting serotonin transporters in atherosclerosis

Dissertation

zum Erwerb des Doktorgrades der Naturwissenschaften

an der Medizinischen Fakultät

der Ludwig-Maximilians-Universität zu München

vorgelegt von

Martina Rami

aus Augsburg

2018

**Gedruckt mit Genehmigung der Medizinischen Fakultät
der Ludwig-Maximilians-Universität München**

Betreuerin: Prof. Dr. rer. nat. Sabine Steffens

Zweitgutachter: Prof. Dr. rer. nat. Jürgen Bernhagen

Dekan: Prof. Dr. med. dent. Reinhard HICKEL

Tag der mündlichen Prüfung: 04.12.2018

Eidesstattliche Versicherung

Rami, Martina

Name, Vorname

Ich erkläre hiermit an Eides statt,
dass ich die vorliegende Dissertation mit dem Thema

**Role of serotonin and antidepressants targeting serotonin transporters in
atherosclerosis**

selbständig verfasst, mich außer der angegebenen keiner weiteren Hilfsmittel bedient und alle Erkenntnisse, die aus dem Schrifttum ganz oder annähernd übernommen sind, als solche kenntlich gemacht und nach ihrer Herkunft unter Bezeichnung der Fundstelle einzeln nachgewiesen habe.

Ich erkläre des Weiteren, dass die hier vorgelegte Dissertation nicht in gleicher oder in ähnlicher Form bei einer anderen Stelle zur Erlangung eines akademischen Grades eingereicht wurde.

München, 20.12.2018

Ort, Datum

Martina Rami

Unterschrift Doktorandin

The results of this work were published in:

Rami M, Guillamat-Prats R, Rinne P, Salvermoser M., Ring L, Bianchini M, Blanchet X, Megens RTA, Döring Y, Walzog B, Soehnlein O, Weber C, Faussner F, Steffens S. Chronic Intake of the Selective Serotonin Reuptake Inhibitor Fluoxetine Enhances Atherosclerosis. *Arteriosclerosis, Thrombosis, and Vascular Biology*. 2018;38:1007-1019.

The article was highlighted by the journal with an editorial:

Wang J & Eitzman DT. Do Selective Serotonin Reuptake Inhibitor Antidepressant Drugs Promote Atherosclerosis? *Arteriosclerosis, Thrombosis, and Vascular Biology*. 2018;38:978-979.

The results of this work were presented at the following conferences:

ORAL PRESENTATIONS

- 04/2018 **Young-DZHK Meeting**, Munich, Germany
Title: "Chronic intake of the antidepressant fluoxetine enhances atherosclerosis"
- 03/2017 **Immuno-Metabolic Mechanisms of Atherosclerosis: Novel critical mediators and therapeutic targets Conference**, Cancun, Mexico
Title: "Chronic treatment with antidepressant fluoxetine promotes atherogenesis in apolipoprotein e-deficient mice"
- 07/2016 **Frontiers in CardioVascular Biology 2016**, Florence, Italy
Title: "Pharmacological depletion of serotonin promotes atherosclerotic plaque formation in *ApoE*^{-/-} mice"

POSTER PRESENTATIONS

- 10/2016 **International Symposium SFB1123**, Munich, Germany
- 06/2016 **Cardiac Regeneration and Vascular Biology Conference 2016**, San Servolo, Italy
Title: "Pharmacological depletion of platelet serotonin promotes atherosclerosis"
- 09/2015 **2nd Young-DZHK-Retreat/3rd DZHK-Retreat (Jahrestagung des Deutschen Zentrum für Herz-Kreislauf-Forschung)**, Potsdam, Germany
Title: "Pharmacological depletion of platelet serotonin promotes atherogenesis in *ApoE*^{-/-} mice"
- 07/2015 **Munich Heart Alliance - Summer Meeting 2015**, Höhenried, Germany
Title: "Pharmacological depletion of platelet serotonin promotes plaque formation in *ApoE*^{-/-} mice"

TABLE OF CONTENTS

LIST OF FIGURES	V
LIST OF TABLES	VII
ABBREVIATIONS	VIII
1 SUMMARY	1
2 ZUSAMMENFASSUNG	3
3 INTRODUCTION.....	5
3.1 Cardiovascular diseases.....	5
3.2 Atherosclerosis	5
3.2.1 Pathogenesis of atherosclerosis.....	5
3.2.2 Mouse model of atherosclerosis.....	8
3.2.3 Leukocyte trafficking – recruitment into the vessel wall.....	8
3.2.3.1 Leukocyte adhesion cascade	9
3.2.3.2 Role of integrins in leukocyte recruitment during atherogenesis.....	12
3.2.3.3 Platelet-mediated leukocyte recruitment	15
3.3 The serotonergic system	18
3.3.1 Central versus peripheral serotonin.....	18
3.3.2 Components of the serotonergic system.....	20
3.3.2.1 Serotonin receptors	20
3.3.2.2 Serotonin transporter.....	21
3.3.3 Impact of platelet serotonin on immune function.....	23
3.4 Antidepressants and cardiovascular diseases.....	24
3.4.1 Depression – a cardiovascular risk factor.....	24
3.4.2 Selective serotonin reuptake inhibitors – good or bad?.....	25
3.5 Aim of the study	30
4 MATERIALS AND METHODS.....	31
4.1 Materials	31
4.1.1 Chemicals and reagents.....	31
4.1.2 Buffers and solutions	32
4.1.3 Kits	33
4.1.4 Primers	34
4.1.5 Plasmids	35
4.1.6 Bacteria	36

TABLE OF CONTENTS

4.1.7	Cell lines.....	36
4.1.8	Antibodies	36
4.1.9	Enzymes and recombinant proteins.....	38
4.1.10	Consumables	39
4.1.11	Equipment.....	39
4.1.12	Software	40
4.2	Methods.....	41
4.2.1	Mouse model.....	41
4.2.1.1	Mice	41
4.2.1.2	Mouse dissection	41
4.2.1.3	Platelet 5-HT depletion via FLX treatment	42
4.2.1.4	Pharmacological peripheral 5-HT depletion via TPH1 inhibition.....	42
4.2.1.5	5-HTR1b antagonism.....	43
4.2.1.6	Induced peritonitis.....	43
4.2.1.7	Intravital microscopy	43
4.2.1.8	<i>In vivo</i> permeability assay	44
4.2.2	Lipid analysis.....	44
4.2.2.1	Plasma cholesterol measurement.....	44
4.2.2.2	Lipid analysis of blood leukocytes.....	44
4.2.3	Enzyme-linked immunosorbent assay (ELISA).....	45
4.2.3.1	5-HT ELISA.....	45
4.2.3.2	CXCL4 and CCL5 ELISA	45
4.2.3.3	Multiplex immunoassay.....	46
4.3	Histology and immunohistochemistry	46
4.3.1.1	Oil Red O staining.....	47
4.3.1.2	Sirius Red staining	47
4.3.1.3	Immunohistochemistry	47
4.3.1.3.1	Macrophage staining	47
4.3.1.3.2	Smooth muscle cell staining	48
4.3.2	Flow cytometry	48
4.3.2.1	Determination of leukocyte counts in bone marrow and spleen	49
4.3.2.2	Protein expression on arterial endothelial cells and leukocytes.....	49
4.3.2.3	Assessment of platelet-leukocyte aggregates	49
4.3.3	Murine cell isolation.....	50
4.3.3.1	Platelet isolation and <i>in vitro</i> stimulation	50
4.3.3.2	Isolation of monocytes and neutrophils from bone marrow	50

TABLE OF CONTENTS

4.3.4	Biomolecular methods.....	50
4.3.4.1	RNA isolation	50
4.3.4.2	Reverse transcription	51
4.3.4.3	Quantitative real-time PCR (TaqMan).....	51
4.3.5	Generation of a 5-HTR2a-overexpressing cell line.....	52
4.3.5.1	Restriction digest.....	53
4.3.5.2	Agarose gel electrophoresis and gel extraction	53
4.3.5.3	Ligation.....	53
4.3.5.4	Bacterial transformation	54
4.3.5.5	Colony PCR	54
4.3.5.6	Plasmid amplification and purification	54
4.3.5.7	Sequencing	55
4.3.5.8	Cell transfection	55
4.3.6	Cell-based <i>in vitro</i> assays.....	55
4.3.6.1	Calcium assay.....	55
4.3.6.2	GloSensor cAMP assay	56
4.3.6.3	Stimulation of SVEC4-10 cells	56
4.3.6.4	Integrin activation assay.....	57
4.3.6.4.1	Murine ICAM1/VCAM1 binding assay.....	57
4.3.6.4.2	Assessment of human high-affinity β 2-integrin conformation	57
4.3.7	Statistics	58
5	RESULTS	59
5.1	Atherogenesis modulates the serotonergic system.....	59
5.2	Chronic FLX treatment leads to platelet 5-HT depletion without affecting 5-HT plasma levels.....	60
5.3	FLX leads to reduced leukocyte extravasation in wild type mice.....	61
5.4	Chronic FLX treatment aggravates atherosclerosis.....	61
5.5	FLX transiently lowers circulating leukocyte and platelet counts.....	66
5.6	FLX does not affect myelopoiesis and mobilization from bone marrow and spleen	67
5.7	Arterial adhesion of myeloid cells is enhanced by FLX	68
5.8	5-HTR1b antagonism has no influence on atherogenesis.....	69
5.9	FLX does not alter platelet characteristics.....	70
5.10	FLX enhances vascular permeability.....	72
5.11	FLX does not affect adhesion molecule expression	72
5.12	FLX amplifies chemokine-mediated integrin activation on myeloid cells.....	74

TABLE OF CONTENTS

5.13	FLX does not induce a calcium response via 5-HTR2a	77
5.14	FLX co-stimulation of chemokine receptors reveals inconclusive findings.....	80
5.15	Pharmacologic TPH1 inhibition does not enhance atherogenesis	81
6	DISCUSSION	85
6.1	FLX treatment enhances atherogenesis by promoting leukocyte recruitment	85
6.2	Atherosclerosis affects the serotonergic system	88
6.3	The underlying molecular mechanism of FLX-mediated integrin activation requires further investigation	89
6.4	TPH1 inhibition as therapeutic target	91
6.5	FLX-mediated aggravation of atherosclerosis – a drug class specific effect?.....	92
6.6	Conclusion and future perspectives	92
7	REFERENCES	94
8	ACKNOWLEDGEMENTS	111

LIST OF FIGURES

Figure 1: Development and progression of atherosclerosis.....	6
Figure 2: Leukocyte mobilization.....	9
Figure 3: Leukocyte adhesion cascade.	10
Figure 4: Integrin activation.....	13
Figure 5: Integrin heterodimers in myeloid cells.....	14
Figure 6: Pathways of platelet-mediated leukocyte recruitment.....	17
Figure 7: The effects of peripheral and central 5-HT.	18
Figure 8: Comparison of 5-HT in neurons and platelets.	19
Figure 9: 5-HTR subtypes and their main signaling pathways.....	20
Figure 10: Structure of FLX enantiomers and escitalopram.....	26
Figure 11: SERT-inhibition by SSRIs.	26
Figure 12: Impact of SSRI intake on neurons and platelets.....	27
Figure 13: Schematic structure of the pcDNA5/FRT/TO expression vector.....	35
Figure 14: Experimental setups for platelet 5-HT depletion.....	42
Figure 15: Experimental setup for pharmacological 5-HT depletion.	42
Figure 16: Experimental setup for antagonism of 5-HTR1b.....	43
Figure 17: Experimental setup for induced peritonitis.	43
Figure 18: Atherosclerosis affects the 5-HT system.	59
Figure 19: Atherosclerosis leads to reduced 5-HT levels in serum.....	60
Figure 20: FLX treatment leads to platelet 5-HT depletion.	60
Figure 21: FLX impairs leukocyte extravasation in wild type mice.....	61
Figure 22: FLX does not affect body weight and cholesterol levels.....	61
Figure 23: FLX treatment enhances atherosclerosis.	62
Figure 24: FLX has no effect on lipid loading in circulating leukocytes.....	63
Figure 25: FLX does no effect the progression of already established plaques.	63
Figure 26: Pre-treatment with FLX reveals similar results to standard experimental setup. ...	64
Figure 27: IL22 plasma levels were elevated by FLX treatment while the abundance of other cytokines was not affected.....	64
Figure 28: FLX treatment leads to elevated macrophage content in aortic lesions.	65
Figure 29: FLX does not affect composition of advanced plaques.	65
Figure 30: FLX leads to a transient decline in blood cell counts in <i>ApoE^{-/-}</i> mice.....	66
Figure 31: FLX treatment has no impact on myelopoiesis and mobilization from bone marrow and spleen.	67
Figure 32: FLX enhances arterial adhesion of myeloid cells.....	68
Figure 33: Injection of 5-HTR1b antagonist does not alter atherosclerosis.	69
Figure 34: FLX does no effect platelet characteristics.	70

LIST OF FIGURES

Figure 35: FLX does not affect PLA formation.....	71
Figure 36: FLX aggravates vascular permeability.	72
Figure 37: FLX does not induce expression of molecules involved in adhesion.	73
Figure 38: FLX-treated mice show enhanced CCL5-mediated integrin activation.....	74
Figure 39: <i>In vitro</i> stimulation with FLX, but not 5-HT promotes CCL5-mediated integrin binding activity of murine blood leukocytes.	75
Figure 40: FLX triggers CCL5-mediated integrin activation in human neutrophil-like cells. ..	76
Figure 41: Escitalopram induces CCL5-evoked β 1-integrin activation on mouse blood leukocytes after <i>in vitro</i> stimulation.....	77
Figure 42: Monocytes and neutrophils express <i>5-Htr1b</i> , <i>5-Htr2a</i> and <i>Sert</i>	78
Figure 43: FLX treatment alters expression of <i>5-Htrs</i> and <i>Sert</i> in aorta.	78
Figure 44: Generation of a 5-HTR2a-overexpressing HEK-293 cell line.	79
Figure 45: FLX does not trigger a calcium response via 5-HTR2a.....	80
Figure 46: Measurement of CCR1 and CCR5 signaling.....	81
Figure 47: TPH1 inhibition does not promote atherosclerosis.	82
Figure 48: Effect of TPH1 inhibition on blood cell counts and adhesion molecule levels.	83
Figure 49: Summary of the effect of chronic SSRI intake on atherosclerosis in a mouse model.....	93

LIST OF TABLES

Table 1: Main adhesion molecules involved in leukocyte adhesion.....	11
Table 2: Major types of granules in platelets with their main cargos.....	16
Table 3: Serotonergic components in immune cells	23
Table 4: FDA-approved SSRIs	26
Table 5: Selected clinical studies showing controversial findings regarding the effect of SSRI intake on CVD risk.....	29
Table 6: Chemicals and reagents	31
Table 7: Buffers, solutions and their composition	32
Table 8: Kits	33
Table 9: Primers for qPCR analysis.....	34
Table 10: PCR primer	35
Table 11: Plasmids used for generation of a 5-HTR2a overexpressing cell line.....	35
Table 12: Overview and description of cell lines	36
Table 13: Murine FACS antibodies	36
Table 14: Human FACS antibody	37
Table 15: Antibodies for intravital microscopy	37
Table 16: Antibodies used for immunohistochemistry.....	37
Table 17: Isotype controls.....	38
Table 18: Secondary antibodies	38
Table 19: Enzymes	38
Table 20: Recombinant proteins	38
Table 21: Material	39
Table 22: Equipment.....	39
Table 23: Software	40
Table 24: Dehydration protocol.....	47
Table 25: RT reaction mix.....	51
Table 26: RT program.....	51
Table 27: Primer-probe mix	52
Table 28: qPCR reaction mix.....	52
Table 29: qPCR FAST program.....	52
Table 30: Digestion mix	53
Table 31: Ligation reaction mix	53
Table 32: Colony PCR mix.....	54
Table 33: Colony PCR program.....	54

ABBREVIATIONS

5-HIAA	5-hydroxyindoleacetic acid
5-HT	Serotonin/5-hydroxytryptamine
5-HTP	5-hydroxytryptophan
5-HTR	Serotonin receptor
5-HTT	Serotonin transporter
5-HTTLRP	Serotonin-transporter-gene-linked polymorphic region
AADC	Aromatic L-amino acid decarboxylase
ABC	ATP-binding cassette
AC	Adenylyl cyclase
ACD	Acid citrate dextrose
ACK	Ammonium chloride potassium
ACS	Acute coronary syndromes
ADP	Adenosine diphosphate
AF	AlexaFluor
ANOVA	Analysis of variance
APC	Allophycocyanin
ApoE	Apolipoprotein E
ATP	Adenosine triphosphate
BSA	Bovine serum albumin
BV	Brilliant violet
CAM	Cell adhesion molecule
cAMP	Cyclic adenosine monophosphate
CCL	C-C motif chemokine ligand
CCR	C-C motif chemokine receptor
cDNA	Complementary DNA
CMV	Cytomegalovirus
CNS	Central nervous system
CVD	Cardiovascular disease
CVE	Cerebrovascular events
CXCL	C-X-C motif chemokine ligand
Cy	Cyanine
DAG	Diacylglycerol
DMEM	Dulbecco's modified eagle medium
DMSO	Dimethylsulfoxid
DNA	Deoxyribonucleic acid
DNase	Deoxyribonuclease
dNTP	Deoxynucleotide triphosphate
EDTA	Ethylenediaminetetraacetic acid
ELISA	Enzyme-linked immunosorbent assay
eNOS	Endothelial nitric oxide synthase
ESL1	E-selectin ligand 1
eYFP	Enhanced yellow fluorescent protein
FACS	Fluorescence-activated cell sorting
FBS	Fetal bovine serum
FDA	Food and Drug Administration
FITC	Fluorescein isothiocyanate
FLX	Fluoxetine

ABBREVIATIONS

FRT	Flp recombination target
Fwd	Forward
Gapdh	Glyceraldehyde 3-phosphate dehydrogenase
GM-CSF	Granulocyte-macrophage colony-stimulating factor
GPCR	G protein-coupled receptor
GTPase	Guanosine triphosphatase
H&E	Hematoxylin and eosin
HBSS	Hank's balanced salt solution
HDL	High density lipoprotein
HEK	Human embryonic kidney
HEPES	4-(2-hydroxyethyl)-1-piperazineethanesulfonic acid
HF	High fidelity
HFD	High fat diet
Hprt	Hypoxanthine-guanine phosphoribosyltransferase
HRP	Horseradish peroxidase
HSPC	Hematopoietic stem cell
i.p.	Intraperitoneal
i.v.	Intravenous
ICAM1	Intercellular adhesion molecule 1
IEL	Internal elastic lamina
IFN γ	Interferon gamma
IgG	Immunoglobulin G
IL	Interleukin
IP3	Inositol 1,4,5-triphosphate
JAM	Junctional adhesion molecule
JIR	Jackson ImmunoResearch
LB	Lysogeny broth
LDL	Low density lipoprotein
LDLR	Low density lipoprotein receptor
LFA1	Lymphocyte function-associated antigen 1
mAb	Monoclonal antibody
MAC	Macrophage antigen
MACS	Magnetic cell separation
MAO	Monoamine oxidase
MAPK	Mitogen-activated protein kinase
M-CSF	Macrophage colony-stimulating factor
MDD	Major depressive disorder
MFI	Mean fluorescence intensity
MI	Myocardial infarction
MMP	Matrix metalloproteinase
MPV	Mean platelet volume
mRNA	Messenger RNA
NC	Nanocrystals
NO	Nitric oxide
OD	Optical density
ORO	Oil red O
oxLDL	oxidized low density lipoprotein
PBS	Phosphate buffered saline
PCR	Polymerase chain reaction

ABBREVIATIONS

PE	Phycoerythrin
PerCP	Peridinin chlorophyll
PIP2	Phosphatidylinositol 4,5-bisphosphate
PLA	Platelet-leukocyte aggregate
PLC	Phospholipase C
PSGL1	P-selectin glycoprotein ligand 1
qPCR	Quantitative PCR
RBC	Red blood cell
Rev	Reverse
RNA	Ribonucleic acid
RNase	Ribonuclease
RPMI	Roswell Park Memorial Institute
RT	Reverse transcription
RT	Room temperature
SEM	Standard error of the mean
SERT	Serotonin transporter
SLC6A4	Solute carrier family 6 member 4
SMA	Smooth muscle actin
SMC	Smooth muscle cell
SSRI	Selective serotonin reuptake inhibitor
TACE	TNF α -converting enzyme
TAE	Tris-acetate-EDTA
TetO ₂	Tetracycline operator 2
TGF β	Transforming growth factor beta
TNF α	Tumor necrosis factor alpha
TPH	Tryptophan hydroxylase 1
Trp	Tryptophan
VCAM1	Vascular cell adhesion molecule 1
VLA4	Very late antigen 4
VLDL	Very low density lipoprotein
VMAT	Vesicular monoamine transporter
VWF	Von Willebrand factor
WHO	World Health Organization

1 SUMMARY

Atherosclerosis is a chronic inflammatory disease of the arterial vessel wall and the primary underlying maladaptive mechanism for developing cardiovascular events, with myocardial infarction or stroke being the most life-threatening ones. Another major contributor to the overall global burden of disease is depression with more than 300 million people worldwide suffering from this common mental disorder. Numerous studies strongly suggest an association between both diseases. Clinical data on potential cardiovascular effects of the most commonly used group of antidepressant drugs, selective serotonin reuptake inhibitors (SSRIs), are controversial. Beyond the antidepressant effect, which is considered to depend on the increased serotonin (5-hydroxytryptamine; 5-HT) concentration in the synaptic cleft through inhibition of the serotonin transporter (SERT), SSRIs also deplete the major peripheral 5-HT storage in platelets by blocking SERT-mediated uptake.

Based on the inconclusive findings in humans, the aim of this thesis was to investigate the effect of chronic intake of SSRIs on the onset and progression of atherosclerosis in a mouse model. To this end, the common SSRI fluoxetine (FLX) was administered orally to apolipoprotein E-deficient (*ApoE*^{-/-}) mice accompanied by high fat diet feeding for 2, 4 or 16 weeks. Drug efficiency was confirmed by an observed 88%-reduction of platelet-derived 5-HT measured in serum after 2 weeks of FLX treatment. Interestingly, atherosclerosis, determined by plaque size in the aortic roots, was aggravated at all stages upon treatment, with the strongest effect on early lesion formation. FLX-treated *ApoE*^{-/-} mice exhibited a transient reduction of circulating leukocyte and platelet numbers after 2 weeks, which was not present at later time points. Changes in myelopoiesis or mobilization from bone marrow and spleen were excluded as possible causes. Notably, wild type mice receiving FLX for 2 weeks did not show the drop in circulating cell counts, suggesting that inflammatory conditions such as hypercholesterolemia are crucial. Plaques of FLX-treated mice revealed a more pronounced macrophage infiltration during early atherogenesis due to increased adhesion of myeloid cells in carotid arteries. A mechanistic explanation may reside in the enhanced vascular permeability and increased chemokine-mediated integrin binding capability discovered in FLX-treated mice. *In vitro* stimulation of blood leukocytes revealed that FLX, but not 5-HT, directly promoted CCL5-evoked β 1- and β 2-integrin activation. Of note, FLX did not trigger integrin binding capability in the absence of CCL5, suggesting that the drug FLX directly alters leukocyte adhesion properties in an inflammatory setting in presence of enhanced chemokine levels, independent of 5-HT platelet depletion. Similar results were obtained with another SSRI escitalopram. Furthermore, augmented CCL5-induced integrin activation by FLX was also verified in human neutrophil-like HL-60 cells. The hypothesis that the pro-atherogenic effect of FLX is independent of platelet 5-HT depletion was corroborated by the observation that

SUMMARY

inhibition of the 5-HT synthesizing enzyme tryptophan hydroxylase 1 did not aggravate atherogenesis. Instead, the pharmacological 5-HT depletion even caused a reduced lesion size at the early time point. In conclusion, the findings reveal a pro-atherogenic effect of the SSRI FLX in a mechanism independent of serotonin, which is of high clinical relevance in view of the increasing prescription of antidepressant drugs. Thus, chronic use of SSRIs should be carefully reconsidered and at least carefully monitored in patients with multiple cardiovascular risk factors.

2 ZUSAMMENFASSUNG

Atherosklerose ist eine chronische Entzündung der arteriellen Gefäßwand und die häufigste Ursache für die Entstehung von Herz-Kreislauf-Erkrankungen. Myokardinfarkt und Schlaganfall sind die lebensbedrohlichsten Folgen der Atherosklerose und gehören weltweit zu den häufigsten Todesursachen. Neben diesen zählt die Depression mit derzeit mehr als 300 Millionen Betroffenen ebenfalls zu einer der am meistverbreiteten Erkrankungen. Es gibt viele Hinweise darauf, dass das Auftreten von Depressionen das Risiko für Herz-Kreislauf-Erkrankungen erhöht. Klinische Studien über die Auswirkungen der am häufigsten verordneten Antidepressiva, den Selektiven Serotonin-Wiederaufnahmehemmern (SSRIs), auf das Herz-Kreislauf-System sind kontrovers. Die antidepressive Wirkung ist sehr wahrscheinlich bedingt durch erhöhte Serotonin (5-Hydroxytryptamin; 5-HT)-Spiegel im synaptischen Spalt als Folge der Hemmung des Serotonintransporters (SERT). Da SERT allerdings auch eine wichtige Rolle für die 5-HT Aufnahme in Thrombozyten spielt, führt die Behandlung mit SSRIs auch zur Depletion von 5-HT in den Thrombozyten, dem Hautspeicherort in der Peripherie.

Aufgrund der widersprüchlichen Daten klinischer Studien war das Ziel dieser Arbeit, die Auswirkungen von SSRIs auf die Entstehung und den Verlauf der Atherosklerose im Mausmodell zu untersuchen. Hierfür wurden Apolipoprotein E-defiziente Mäuse mit dem weitverbreiteten SSRI Fluoxetin (FLX) parallel zu einer fettreichen Diät für 2, 4 oder 16 Wochen behandelt. Die Wirkung des Medikaments konnte nach zweiwöchiger Behandlung anhand einer 88%igen Senkung des thrombozytären 5-HT bestätigt werden. Interessanterweise führte die Behandlung zu vergrößerten atherosklerotischen Läsionen in den Aortenwurzeln. Diese proatherogene Wirkung von FLX konnte in allen Phasen der Atherogenese (2, 4 und 16 Wochen) beobachtet werden, wobei der Unterschied im frühen Stadium besonders ausgeprägt war. Nach 2 Wochen wiesen FLX-behandelte Mäuse zudem eine verminderte Anzahl an Leukozyten und Thrombozyten im Blut auf. Da an späteren Behandlungszeitpunkten die Zellzahlen zwischen den Gruppen vergleichbar waren, ist von einem transienten Effekt auszugehen. Als Ursachen konnten Unterschiede in der Myelopoese sowie in der Rekrutierung aus dem Knochenmark oder der Milz ausgeschlossen werden. Da die FLX-vermittelte transiente Reduktion der Zellzahlen im Blut nicht in Wildtyp-Mäusen, sondern nur in atherosklerotischen Mäusen beobachtet werden konnte, ist davon auszugehen, dass hierfür ein inflammatorisches Milieu, wie im Falle einer Hypercholesterinämie, ausschlaggebend ist. In frühen atherosklerotischen Plaques der FLX-behandelten Gruppe war eine vermehrte Akkumulation an Makrophagen festzustellen. Dies war durch eine verstärkte Adhäsion von myeloischen Zellen an das Endothel bedingt. Die vermehrte Rekrutierung lässt sich durch eine in FLX-behandelten Mäusen beobachtete erhöhte vaskuläre Permeabilität und verstärkte

Chemokin-induzierte Integrinaktivität erklären. Die *in vitro* Stimulation von Mausblut mit FLX oder 5-HT zeigte, dass lediglich FLX direkt die CCL5-vermittelte β 1- und β 2-Integrinbindungsaktivität von Leukozyten verstärkte. Allerdings konnte in Abwesenheit von CCL5 keine Steigerung der Integrinaktivität gemessen werden. Diese Beobachtungen lassen vermuten, dass das Medikament FLX einen direkten, 5-HT-unabhängigen Effekt auf die Leukozytenadhäsion hat und dieser nur im Chemokin-reichen Milieu und somit unter inflammatorischen Bedingungen zum Tragen kommt. Zusätzliche *in vitro* Versuche mit Escitalopram, dem derzeit wirksamsten und für Patienten bestverträglichsten SSRI, führten zu vergleichbaren Ergebnissen. Zudem konnte der Effekt in der humanen Neutrophil-ähnlichen HL-60 Zelllinie reproduziert werden. Die Hypothese der 5-HT-unabhängigen, proatherogenen Wirkung von FLX, konnte darüber hinaus mit einem weiteren *in vivo* Experiment untermauert werden. In diesem pharmakologischen Ansatz wurde das periphere 5-HT durch die Injektion eines Inhibitors des peripheren 5-HT-synthetisierenden Enzyms Tryptophanhydroxylase 1 depletiert. Im Gegensatz zur FLX-Behandlung führte die Inhibition der Tryptophanhydroxylase 1 nicht zur Steigerung der Atherosklerose, sondern verringerte sogar die Plaquentwicklung bei zweiwöchiger Behandlung. Zusammenfassend zeigen die Ergebnisse dieser Arbeit eine proatherogene, 5-HT-unabhängige Wirkung von FLX. Diese Erkenntnis ist aufgrund der zunehmenden Verbreitung von SSRIs von hoher klinischer Relevanz. Die chronische Einnahme von SSRIs sollte demnach vor allem bei Patienten mit kardiovaskulärer Risikofaktoren neu bedacht oder diese Patienten zumindest umfassend überwacht werden.

3 INTRODUCTION

3.1 Cardiovascular diseases

Cardiovascular diseases (CVDs) generally encompass disorders affecting the heart and blood vessels. According to the World Health Organization (WHO), CVDs bear the blame for more than 30 % of deaths worldwide with annually more people dying from them than from any other diseases.¹ The most life-threatening complications of CVDs are myocardial infarction and stroke, which are mainly caused by thrombotic occlusion of a coronary artery or cerebral microvessel preventing the blood flow to the heart or brain, respectively. The primary underlying mechanism in the blood vessels resulting in these severe acute cardiovascular events is referred to as atherosclerosis.^{1,2} Today, peoples' lifestyle is marked by behavioral cardiovascular risk factors such as unhealthy diet, lack of physical exercise, smoking, or alcohol consumption. The long-term exposure to these behavioral risk factors gives rise to an enhanced prevalence for obesity, hypertension, diabetes and high blood cholesterol, which in turn lead to the increasing incidence of CVDs.¹⁻³ So far, primary prevention is the most sustainable solution for CVDs,² while the translation of therapeutic approaches from bench to bedside has been disappointing so far. A better understanding of the underlying mechanisms of atherosclerosis is urgently needed to discover novel therapies for the treatment of CVDs.

3.2 Atherosclerosis

Atherosclerosis, the most common underlying cause of CVDs, is a complex pathological process in the artery wall that develops over many years. It is characterized by a chronic inflammation of the vessel wall with subendothelial plaque formation. Typically, atherosclerosis remains unnoticed at the beginning of the development until severe stenosis causing ischemic episodes or plaque rupture leading to thrombus formation and subsequently to vessel occlusion.⁴

3.2.1 Pathogenesis of atherosclerosis

The pathogenesis of atherosclerosis can be divided in three different stages: the initiation including plaque formation, plaque progression and plaque rupture (Figure 1). Normal arteries comprise three layers (Figure 1A). The inner layer, called intima, is separated from the vascular lumen via a monolayer of endothelial cells. The middle layer, the media, is rich in smooth muscle cells (SMCs) and embedded in a complex extracellular matrix. It is surrounded by the outer layer, the adventitia, which contains different leukocyte cell types, mast cells, fibroblasts, nerve endings and microvessels embedded in a collagen-rich matrix.⁵ Under steady state conditions, the endothelium is a protective barrier preventing leukocyte adhesion. It reacts on hemodynamic forces such as high pressure and shear to maintain vascular integrity. This is achieved by suppressing inflammation through high endothelial nitric oxide synthase (eNOS)

expression, by decreasing cell turnover and by strengthening of endothelial cell-cell interaction, which in turn leads to diminished vascular permeability.^{6,7}

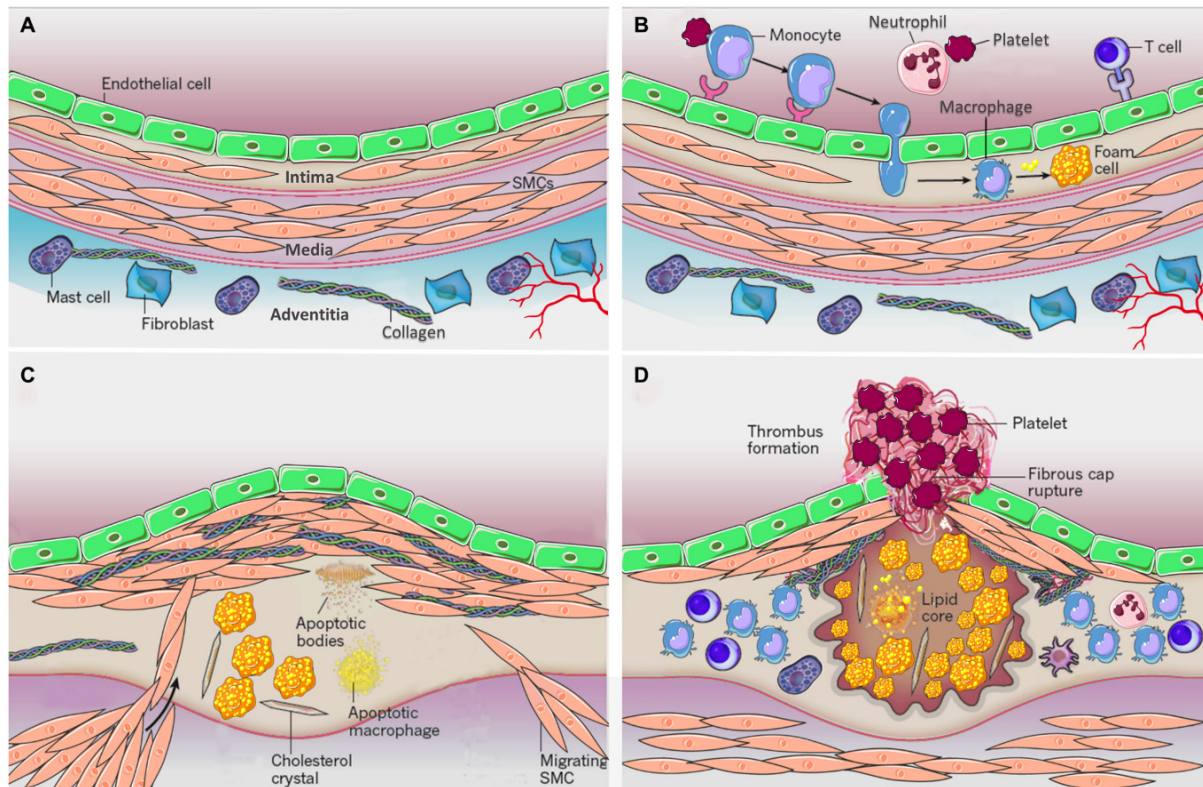


Figure 1: Development and progression of atherosclerosis.

(A) The normal artery comprises three layers: intima, media and adventitia. The inner layer, the intima, is lined by a monolayer of endothelial cells as a border between vessel wall and vascular lumen. In humans the intima contains resident SMCs compared to many other species such as mice. The middle layer, the media, harbors SMCs surrounded by an extra cellular matrix. The outer layer, the adventitia, comprises collagen, nerve endings and microvessels and several cell types like mast cells and fibroblasts. (B) Atherosclerosis is initiated at sites of dysfunctional endothelium. Loss of endothelium integrity, for example as a consequence of pro-inflammatory stimuli, low shear stress or hyperlipidemia, results in increased permeability and upregulation of adhesion molecules. Lipids accumulate in the intima and circulating leukocytes, mainly monocytes, are recruited to the site of inflammation, followed by binding to adhesion molecules and subsequently transmigration to the intima. Monocytes differentiate to macrophages, which engulf lipids, thereby transforming into foam cells. (C) During lesion progression, SMCs migrate from the media to the intima, proliferate and synthesize collagen resulting in the formation of the fibrous cap. Dying SMCs and foam cells, extracellular lipids derived from dead cells, cholesterol crystals and other extracellular matrix material cause the development of the necrotic core. (D) Loss of cap stability due to collagen degradation leads to plaque rupture. The subsequent exposure of pro-thrombotic material to blood triggers thrombus formation, which can cause vessel occlusion. (Adapted from Libby *et al.*)⁵

At sites of disturbed blood flow, such as atheroprone arterial branching points, the endothelium is chronically inflamed characterized by an upregulation of adhesion molecules including intercellular adhesion molecule 1 (ICAM1) and vascular cell adhesion molecule 1 (VCAM1), enhanced turnover (proliferation and apoptosis) and subsequently enhanced permeability.⁷ Endothelial dysfunction is additionally promoted by pro-atherogenic stimuli including dyslipidemia or oxidative stress.⁶ Disruption of the endothelial integrity leads to subendothelial accumulation of lipids, especially under hypercholesterolemia. The retention of infiltrating cholesterol-containing particles such as low density lipoprotein (LDL) particles is an initiating

step in the development of atherosclerosis.⁴ Thus, high blood lipid levels, more precisely LDL, have been shown to strongly correlate with the development of atherosclerosis.⁸ Trapped LDL is modified to oxidized LDL (oxLDL), which triggers inflammation by initiating the formation of chemotactic gradients. Circulating leukocytes including lymphocytes, neutrophils and predominately monocytes are recruited from the circulation to the site of inflammation. Recruited leukocytes bind to upregulated ICAM1 and VCAM1 on the activated endothelium, followed by transmigration through the endothelium into the intima triggered by a chemotactic gradient (Figure 1B).⁹ In response to granulocyte-macrophage colony-stimulating factor (GM-CSF) and macrophage colony-stimulating factor (M-CSF) infiltrating monocytes differentiate into macrophages, which engulf oxLDL through the expression of scavenger receptors such as CD36 or SR-A1 leading to foam cell formation.⁴ As the so-called fatty streak progresses, the plaque becomes more complex (Figure 1C). SMCs migrate from the media into the intima upon secretion of inflammatory mediators by endothelial cells and macrophages. There, SMCs proliferate, produce extracellular matrix components such as collagen and form the fibrous cap covering the plaque.⁵ SMCs and collagen are essential for plaque stability. Transforming growth factor (TGF) β , known to be secreted by SMCs, endothelial cells and several immune cells,¹⁰ promotes collagen production by SMCs as well as collagen maturation providing mechanical strength to the fibrous cap.⁴ During lesion progression, continuous lipid-uptake by macrophage-derived foam cells eventually promotes cell death leading to accumulation of extracellular lipids. Likewise, SMCs may undergo apoptosis in advanced lesions. The inefficient clearance of dead cells by efferocytosis leads to the formation of the necrotic core consisting of apoptotic and necrotic cells as well as extracellular lipids, cell debris, cholesterol crystals and other extra cellular material, which in turn provokes further recruitment of immune cells.^{4,5} Counteracting the production of pro-inflammatory cytokines such as interferon (IFN) γ and tumor necrosis factor (TNF) α , distinct subsets of macrophages and T cells secrete anti-inflammatory mediators like TGF β and Interleukin (IL) 10. The balance between pro- and anti-inflammatory agents elicits the slowly progressive chronic inflammation.¹¹ Plaques generally cause symptoms either by stenosis leading to chronic tissue ischemia or plaque rupture causing an acute ischemic event. The latter occurs when the fibrous cap fails to withstand the force from the blood stream and ruptures, thereby leading to thrombus formation (Figure 1D). So far, the reason for plaque rupture is not completely understood. Vulnerable plaques, which are prone to rupture, are characterized by a collagen-poor thin fibrous cap, a large lipid-rich necrotic core, less SMC content and ongoing inflammation.^{4,5} It is believed that the release of IFN γ and other cytokines by activated T cells and macrophages inhibit SMC proliferation and subsequently the presence of mature collagen. Additionally, plaque cells secrete matrix metalloproteinases (MMPs) promoting collagen degradation. The loss of collagen together with the growing necrotic core cause plaque instability and eventually plaque rupture.^{4,11} Upon

plaque rupture, the highly pro-thrombogenic material of the plaque's core is exposed to the blood stream rapidly triggering platelet activation, coagulation and ultimately thrombus formation. The thrombus possibly leads to vessel occlusion either locally at the site of plaque rupture or embolizes and block the blood stream in distal arteries causing life-threatening events such as myocardial infarction or stroke.¹¹

3.2.2 Mouse model of atherosclerosis

To study atherogenesis, the mouse has become the predominant species for preclinical research because of its ease of breeding, rapid reproduction and therefore the benefit to explore the pathogenesis of atherosclerosis in a reasonable time frame. An additional advantage is the ease of genetic manipulation to investigate the contribution of cell types and proteins to the process of atherogenesis.¹² Compared to humans with LDL being the main subfraction, the lipid profile of wild type mice reveals high density lipoprotein (HDL) as the major subset.¹³ Thus, wild type mice do not develop atherosclerosis and genetic manipulation is mandatory to study atherogenesis. The two major mouse models frequently used are based on a genetic modified cholesterol metabolism: *Apolipoprotein E*-deficient (*ApoE*^{-/-}) and *LDL receptor* (*Ldlr*^{-/-})-deficient mice.¹² With LDLR being the receptor for the clearance of LDL and ApoE being a ligand for LDLR, both gene knockouts lead to an increase in plasma cholesterol. Likewise, the models develop atherosclerotic plaques preferentially in aortic roots, the aortic arch and at branching points of the aorta. Compared to *Ldlr*^{-/-} mice, *ApoE*^{-/-} mice have some disadvantages such as a nonhuman-like lipid profile with very low density lipoprotein (VLDL) being the major subfraction¹³ and the loss of ApoE, which is a multifunctional protein that might affect atherosclerotic plaque development independent of plasma lipid levels. However, the advantages of *ApoE*^{-/-} mice are the spontaneously and more rapid development of atherosclerosis with a more advanced, human-like plaque phenotype.¹² Nevertheless, both models have the limitation that plaques do not rupture spontaneously, thus the mouse is a suitable model to study atherogenesis, but not plaque instability (at least not without surgical manipulation such as placement of a flow modifying tube around the carotid artery).^{12,14} In this study all atherosclerosis experiments were performed in *ApoE*^{-/-} mice.

3.2.3 Leukocyte trafficking – recruitment into the vessel wall

Leukocyte trafficking from the bone marrow or the spleen into the vessel wall is an essential part of the pathogenesis of atherosclerosis. Under steady state, monocytes and neutrophils derive from hematopoietic stem cells (HSPCs) located in the bone marrow. However, during atherogenesis, secondary lymphoid organs such as spleen represent additional reservoirs for leukocytes, where extramedullary hematopoiesis occurs. In response to hypercholesterolemia, HSPC proliferation is induced and myeloid cell mobilization into the circulation is enhanced, which leads to monocytosis and neutrophilia (Figure 2). Subsequently, myeloid cells are

recruited to the site of inflammation resulting in lesional cell accumulation and increased atherosclerosis.^{15,16}

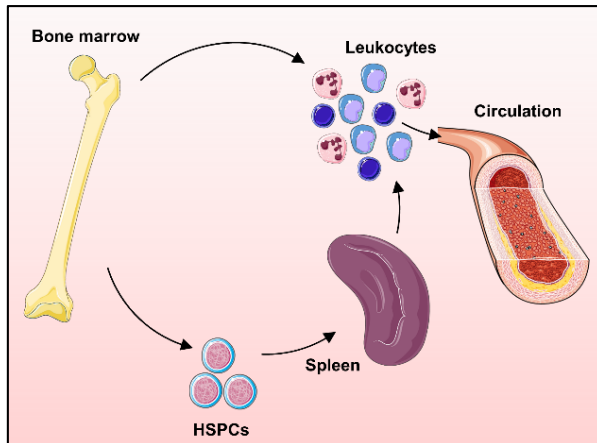


Figure 2: Leukocyte mobilization.

During atherogenesis, HSPCs in the bone marrow (medullary hematopoiesis) and spleen (extra-medullary hematopoiesis) proliferate and differentiate followed by mobilization into the circulation and subsequently recruitment to the site of inflammation. (Adapted from Swirski & Nahrendorf)¹⁵

Although only few neutrophils are detectable within atherosclerotic lesions, several studies demonstrate the importance of neutrophils during atherogenesis.^{17,18} They are suggested to promote early lesion formation by releasing inflammatory mediators, thereby paving the way for monocytes.¹⁹ Studies in mice have shown that mainly bone-marrow derived circulating monocytes rather than resident macrophages give rise to lesional macrophages, which are the predominant cell type in the plaque.²⁰ Moreover, monocyte recruitment is enhanced by hypercholesterolemia and accumulation increases in proportion to lesion size.²¹ Thus, circulating monocytes not only participate importantly in the pathogenesis of atherosclerosis but also have an active role and may commit for specific functions while still in circulation. Indeed, at least two phenotypically distinct subsets of monocytes are described in mice and humans: classical Ly6C^{high} monocytes in mice corresponding to human CD14^{high}CD16⁻ blood monocytes and murine non-classical Ly6C^{low} monocytes corresponding to CD14⁺CD16⁺ monocytes in humans. While classical monocytes are known to be pro-inflammatory and rapidly infiltrate injured tissues, non-classical monocytes are considered as patrolling cells with an anti-inflammatory phenotype.²² In response to high fat diet (HFD), mice revealed induced patrolling activity of non-classical monocytes along the vascular wall during early atherogenesis.²³ However, the exact role of these vascular housekeepers still needs to be explored.

3.2.3.1 Leukocyte adhesion cascade

Circulating leukocytes are recruited to the activated arterial endothelium. This requires a coordinated interplay of endothelial adhesion molecules with their counterparts on leukocytes (Table 1). The development of intravital microscopy imaging techniques, which enables live imaging of leukocyte trafficking in the microvasculature, yielded groundbreaking insights into this multistep process. The interaction of leukocytes with the vessel wall occurs in a series of events, the so-called leukocyte adhesion cascade, which starts with capture and rolling of

leukocytes, followed by slow rolling, arrest, crawling and ultimately transmigration, also known as extravasation (Figure 3).²⁴ Because imaging in large arteries is technically challenging due to respiratory and pulsatile movements of these vessels,²⁵ leukocyte-endothelium interactions are mainly studied in post-capillary venules of the microvasculature, accordingly the mechanism in large arteries is less well understood. The homing of leukocytes to sites of inflammation not only requires the expression of adhesion molecules on the part of the activated endothelium but also the activation of leukocytes themselves, which is mainly achieved by a local secretion of chemokines. These chemotactic mediators, released upon activation from endothelial cells, platelets, lymphocytes or macrophages, provoke local gradients by binding to glycosaminoglycans on cell surfaces leading to leukocyte activation and migration.²⁶ Monocyte trafficking to inflamed arteries is mainly dependent on C-C motif chemokine ligand (CCL) 2 and CCL5.²⁷

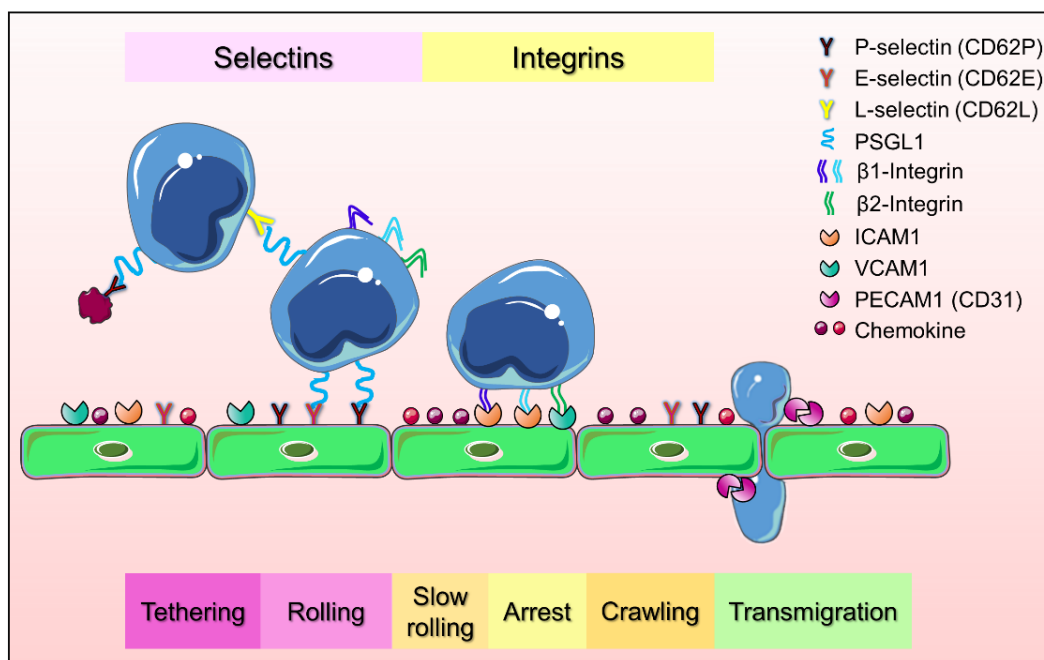


Figure 3: Leukocyte adhesion cascade.

Inflammation provokes the release of pro-inflammatory mediators causing the activation of the endothelium by upregulation of adhesion molecules, which in turns triggers a cascade of events leading to leukocyte adhesion: capture, rolling, firm adhesion and transmigration. Selectins and PSGL1 are the key players in capture of leukocytes followed by rolling on the endothelium, whereas integrins and cell adhesion molecules (CAMs) are mainly mediating the firm adhesion. The transmigration generally occurs at endothelial junctions and involves several adhesion molecules like PECAM1 and junctional adhesion molecules (JAMs).²⁴

The initial steps in leukocyte adhesion, serving as a tether system to capture circulating leukocytes from the rapid flowing blood, are primarily mediated by selectins (P-, E-, and L-selectin) binding to glycosylated ligands. Their main ligand is P-selectin glycoprotein ligand-1 (PSGL1), which is constitutively expressed on all leukocytes.²⁸ E-selectin (CD62E) is solely found on endothelial cells and upregulated by enhanced transcription in the presence of inflammatory cytokines such as TNF α and IL1 β . Aside from PSGL1, E-selectin also binds to

glycosylated CD44 and E-selectin ligand 1 (ESL1). In contrast, P-selectin (CD62P), which is stored in Weibel-Palade bodies of endothelial cells and in α -granules of platelets, is rapidly translocated to the cell surface in response to an inflammatory stimulus. L-selectin (CD62L), however, is expressed on several leukocytes, such as lymphocytes and neutrophils, and is shed upon activation.²⁹

Table 1: Main adhesion molecules involved in leukocyte adhesion

Class	Common name	Immunological name	Gene name (mouse)	Main ligands	Expressed on
Selectins	E-selectin	CD62E	<i>Sele</i>	PSGL1, ESL1, CD44	Endothelial cells
	L-selectin	CD62L	<i>Sell</i>	PSGL1	Endothelial cells Leukocytes
	P-selectin	CD62P	<i>Selp</i>	PSGL1	Endothelial cells Platelets
CAMs	ICAM1	CD54	<i>Icam1</i>	LFA1	Endothelial cells
	VCAM1	CD106	<i>Vcam1</i>	VLA4	Endothelial cells
	PECAM1	CD31	<i>Pecam1</i>	PECAM1	Endothelial cells Platelets Leukocytes
Integrins	LFA1	CD11a/CD18	<i>Itgal/Itgb2</i>	ICAM1	Leukocytes
	MAC1	CD11b/CD18	<i>Itgam/Itgb2</i>	several	Leukocytes
	p150,95	CD11c/CD18	<i>Itgax/Itgb2</i>	ICAM1, VCAM1	Leukocytes
	VLA4	CD49d/CD29	<i>Itga4/Itgb1</i>	VCAM1	Leukocytes

Adapted from Gerhardt *et al.*²⁷

The binding of PSGL1 on leukocytes to endothelial P-selectin plays a key role for the rolling on the endothelium,³⁰ while the interaction of leukocytic PSGL1 with L-selectin on other leukocytes or activated platelets promotes the capture on the endothelium (secondary leukocyte capture).^{28,31} Classical monocytes express PSGL1 with a much higher abundance compared to non-classical monocytes, and thus reveal an enhanced binding to E-, P- and L-selectin. Impaired recruitment of classical monocytes to lesions in *ApoE*^{-/-} mice lacking PSGL1 likely explains the preferential homing to atherosclerotic plaques of classical over non-classical monocytes.³² The expression of both E-selectin and P-selectin on the endothelium was shown to be enhanced during atherogenesis.³³ The selectin-mediated leukocyte-endothelium interaction is rather weak and easily breaks due to the rapid blood stream causing the leukocyte rolling along the luminal surface. Chemoattractants deposited on the endothelium, mainly chemokines, stimulate the rolling of leukocytes, leading to the activation of integrins.²⁴ Chemokines are either released from endothelial cells or produced by proteolytic cleavage in activated mast cells or platelets and signal through binding to G protein-coupled receptors (GPCRs) on the target cell. Platelets for instance are known to induce leukocyte adhesion by depositing C-X-C motif chemokine ligand (CXCL) 4 or CCL5 on the inflamed endothelium. The integrin activation on leukocytes results in firm adhesion on the endothelial cell surface by

binding to ICAM1 and VCAM1. Most relevant integrins involved in leukocyte arrest are β 1- and β 2-integrins, of which very late antigen 4 (VLA4) and lymphocyte function-associated antigen 1 (LFA1) are the best studied.²⁸ Leukocytes crawl along the endothelium until they transmigrate, which mainly takes place at endothelial cell junctions (paracellular diapedesis). Several molecules such as platelet-endothelial cell adhesion molecule 1 (PECAM1; CD31) or junctional adhesion molecules (JAMs) are involved in this process.²⁴

Although most research on leukocyte trafficking was performed in the microvasculature, several *in vivo* studies inhibiting molecules or interactions involved in the leukocyte adhesion cascade have highlighted a key role of these players also during atherogenesis. For instance, the absence of P-selectin decreased fatty streak formation in cholesterol-rich-fed *Ldlr*^{-/-} mice and mitigated advanced atherosclerosis in *ApoE*^{-/-} mice under chow diet, suggesting an important role for P-selectin during early and advanced atherogenesis.^{34,35} Mice lacking L-selectin, however, revealed aggravated plaque formation, proposing an atheroprotective role of L-selectin through an alteration of the immune cell composition within the peripheral blood and aortic wall.³⁶ An additional study demonstrated that *ApoE*^{-/-} mice deficient for E-, P-selectin or ICAM1 exhibited a reduction in atherosclerotic lesion sizes.³⁷ Although animal studies aiming to suppress atherogenesis by targeting arterial recruitment were encouraging, testing candidate drugs in humans is still in early stages. This failure in clinical translation might be caused, among other, by the redundancy of molecules involved in adhesion. Consequently, selective inhibition of a single adhesion molecule might be insufficient. Additionally, targeting an adhesion molecule might interfere with other leukocyte functions, because ligand binding also initiates intracellular signaling aside from adhesion. Moreover, other inflammatory processes, which are essential for tissue injury healing and defense against pathogens, might also be affected by drugs targeting leukocyte adhesion. Further investigation of the molecular structure and function of involved molecules are needed for the design of more selective small-molecule inhibitors.²⁹ Advancements in live cell imaging enabled high-resolution imaging of leukocyte movement on the endothelium in atherosclerotic arteries in living mice.²⁵ The improvement of intravital microscopy combined with flow cytometry and transcriptomics will shed further light on the understanding of how leukocyte recruitment drives atherogenesis.³⁸ In summary, leukocyte trafficking to atherogenic lesions including adhesion and extravasation is a complex mechanism depending on the interaction of numerous molecules.

3.2.3.2 Role of integrins in leukocyte recruitment during atherogenesis

Integrins are transmembrane receptors which play a crucial role during leukocyte recruitment in atherogenesis and in particular during the rolling and adhesion phase as described above. These adhesion receptors facilitate cell-extracellular matrix or cell-cell interactions by binding to extracellular matrix ligands or to the counterpart on the surface of other cells,

respectively.^{39,40} Their presence on almost all cell types and the underlying complex signaling highlights the importance of integrins in a large variety of biological processes. Integrins are heterodimers assembled through non-covalent binding of one α -subunit with one β -subunit.⁴¹ Currently, 18 α - and 8 β -subunits are known that assemble to 24 heterodimers.³³ Both integrin subunits have a cytoplasmic tail, a transmembrane domain and a large extracellular domain. The activation of integrins is highly regulated and involves large conformational changes in the extracellular domains leading to an opened ligand-binding pocket which enables the cell to interact with their local environment. Integrins occur in at least two different conformational stages: an inactive bent conformation with low ligand affinity and an active, extended state with high affinity for the ligand (Figure 4). Since this transition process is triggered by signaling molecules inside the cell, it is referred to as inside-out signaling.⁴⁰

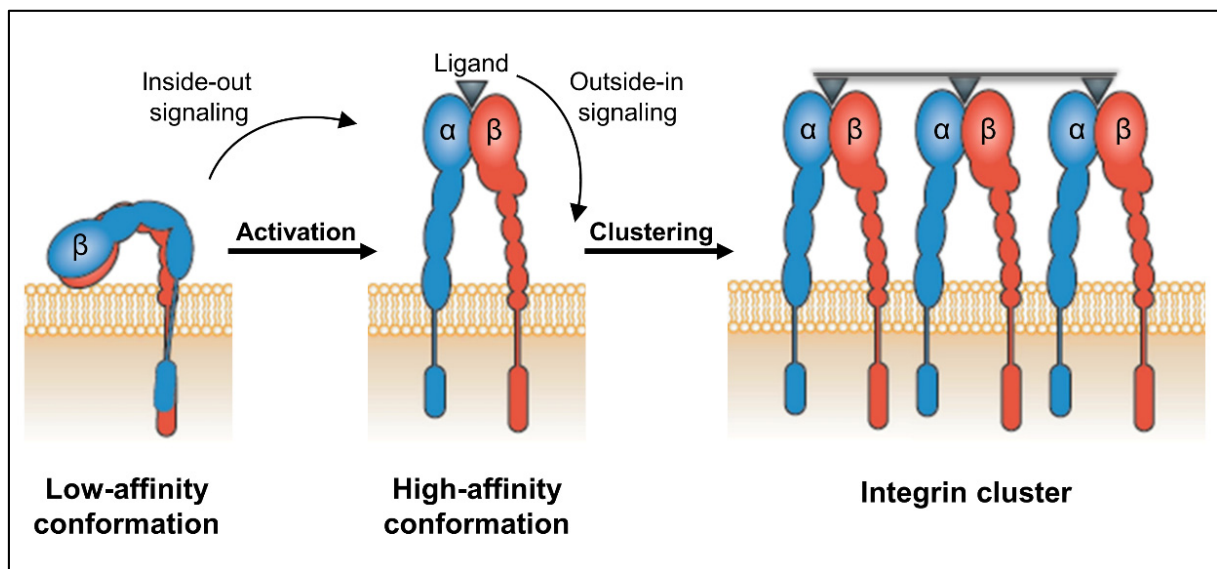


Figure 4: Integrin activation.

Intracellular signals lead to activation of integrins by conformational changes from bent low-affinity state to extended high-affinity state (inside-out signaling). This conformational transition characterized by dramatic changes in the extracellular domain leads to the exposure of the ligand-binding pocket. The binding to the counterpart on the cell surface of other cells or to extracellular matrix ligands promotes cell adhesion. Besides adhesion, extracellular ligand binding can also induce intracellular signal transduction (outside-in signaling). By lateral movement, activated integrins can form clusters, which promote adhesion and further signaling.⁴² (Adapted from Ley *et al.*)⁴⁰

The exact molecular activation mechanism of integrins in atherogenesis is not well defined. Generally, it is suggested that chemokine-induced GPCR stimulation leads to phospholipase C (PLC)-mediated activation of the small guanosine triphosphatase (GTPase) Rap1, a member of the Ras family. Rap1 transmits downstream signaling through several effectors, which in turn leads to binding of cytoskeletal adapter proteins to the cytoplasmic tail. The interaction of the adapter molecules, of which talin and kindlin are the best studied, with the intracellular domain of the β -subunit breaks the salt bridge between the cytoplasmic tails of both subunits, resulting in integrin extension and consequently activation.^{33,39} The binding of the extracellular ligand also triggers an integrin-specific signal transduction inside the cell, a

process referred to as outside-in signaling that can regulate cell function.^{33,41} The initial interaction of leukocyte integrins to CAMs on the endothelium is not strong enough to prevent leukocytes from being carried away by the blood flow. Thus, ligand binding also stimulates the formation of hetero-oligo clusters, caused by the lateral movement of integrin heterodimers on the cell surface to the site of binding.²⁴ This process known as integrin clustering leads to adhesion strengthening, which is particularly important during adhesion in large arteries.¹⁸ Several adapter proteins have been linked to enhancing integrin clustering, but the molecular mechanism still remains to be uncovered.³⁷

In circulating cells such as platelets and leukocytes, integrins are mostly found in the bent conformation, masking the ligand binding pocket. The activation through inside-out signaling enables rapid initiation of adhesion of circulating leukocytes and platelets inducing leukocyte recruitment and thrombosis, respectively.³³ Leukocytes express several integrin subsets that are involved in leukocyte-endothelium interaction (Figure 5). Integrins are dynamically up- or down-regulated depending on the leukocyte activation stage and each integrin exhibits a specific function in leukocyte recruitment.⁴³ Among these integrins, six are exclusively expressed in leukocytes: the $\beta 2$ -subunit (CD18) with its four α -subunit binding partners αL (LFA1), αM (MAC1), αX (p150,95), αD and the $\beta 7$ -subunit with its two α -subunit binding partners $\alpha 4$ and αE . In addition to these six, leukocytes also express the $\beta 1$ -subunit (CD29) coupling to $\alpha 4$ (VLA4).⁴⁰

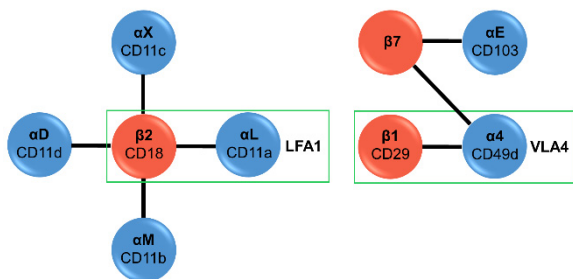


Figure 5: Integrin heterodimers in myeloid cells.

Integrins are heterodimers composed of one α -subunit coupling to one β -subunit. Leukocytes express numerous integrins of which the displayed ones except for VLA4 are exclusively expressed by leukocytes. They all mediate leukocyte-endothelial interaction, of which LFA1 and VLA4 are the best studied in atherogenesis.^{33,40}

While monocytes possess $\beta 1$ - and $\beta 2$ -integrins, neutrophils predominantly express $\beta 2$ -integrins and only a low amount of $\beta 1$ -integrins, whereas lymphocytes show a pattern of $\beta 1$ -, $\beta 2$ - and $\beta 7$ -integrins dependent on their activation state.⁴⁴ From these, LFA1 and VLA4 as well as p150,95 were shown to play a prominent role in leukocyte recruitment during atherogenesis. Like all $\beta 2$ -integrins, LFA1 binds to ICAM1, whereas the $\beta 1$ -integrin VLA4 functions as the primary leukocyte VCAM1 counterpart (Table 1). However, p150,95 has been shown to interact with VCAM1 as well. While genetic knockout of *Vla4* was reported to be lethal,⁴⁵ blocking VLA4 revealed reduced myeloid cell adhesion as well as attenuated neointimal growth and fatty streak formation in atherosclerotic mice.^{46–48} Similarly, blocking antibodies against LFA1 significantly limited mononuclear cell recruitment in early atherogenesis and deletion of $\beta 2$ -integrins reduced early plaque formation, indicating that $\beta 2$ -integrins are also important in

monocyte homing to the plaque.^{49–51} In addition, integrin p150,95 was shown to be upregulated during hypercholesterolemia and the deletion decreased atherosclerosis.^{52,53} These studies are consistent with reduced plaque formation in mice lacking functional VCAM1 or ICAM1, thus highlighting the importance of those interactions during atherogenesis.^{33,37,54}

The essential role of integrins becomes evident in human genetic disorders. Inherited mutations in the *Itgβ2* gene are known to give rise to a severe immunodeficiency named Leukocyte Adhesion Deficiency Type I (LADI), which is characterized by the insufficient or aberrant expression of the β2-subunit. Subsequently, leukocytes from patients suffering from this rare disease lack the ability to extravasate into tissue and fight against bacteria making this genetic deficiency a life-threatening disease.²⁴ Leukocyte adhesion is the basis of any type of immune response, targeting this process to either boost a defective immune system or to suppress exaggerated inflammation is thus of high biomedical interest.⁴⁰ So far, drugs against leukocyte integrins are applied in diseases such as multiple sclerosis and inflammatory bowel diseases. The benefit of integrin-based drugs in these patients leads to continued medical interest with currently around 80 clinical trials being listed involving integrin-interfering therapeutics.⁴⁰

3.2.3.3 Platelet-mediated leukocyte recruitment

Platelets, also known as thrombocytes, are the smallest (2-3 μm) cells in circulation. These anucleate, megakaryocyte-derived cells are essential for maintaining vascular integrity. Platelets are mostly known for their role in blood clot formation (hemostasis) to stop bleeding after vessel injury. Their function is marked by exocytosis of their granules upon stimulation. The three major types of granules are α-granules, dense granules and lysosomes, which are packed with distinct cargos (Table 2).⁵⁵ α-Granules, the most abundant secretory vesicles in platelets, carry mainly proteins comprising transmembrane receptors and soluble cargos including the chemokines CCL5 and CXCL4. Proteomic analysis revealed more than 300 soluble proteins, which are involved in several processes such as wound healing, hemostasis and inflammation.⁵⁶ The α-granule cargo protein P-selectin is widely used to determine platelet activation, since it is rapidly translocated to cell surface upon activation, and therefore easy to measure with flow cytometry.⁵⁷ Dense granules are ten times less present than α-granules and mainly contain bioactive amines such as serotonin (5-HT), a high concentration of cations, mainly Ca²⁺, adenine nucleotides and polyphosphates.⁵⁶ Platelet lysosomes are packed with several digestive enzymes such as cathepsin and collagenase. Their exact function, however, is not well understood.^{55,57} The initial formation of platelet granules starts in megakaryocytes with endogenous cargos or from endocytic origin. Though, the granule maturation continues in circulating platelets and includes cargo uptake from plasma.⁵⁶ For instance, circulating platelets take up plasma 5-HT followed by translocation from platelet cytosol into dense granules.⁵⁵

Table 2: Major types of granules in platelets with their main cargos

Type	α -Granules	Dense granules	Lysosomes
Number/platelet	50-80	3-8	1-3
Cargo	Chemokines (e.g. CCL5, CXCL4) Coagulation factors Adhesion molecules (e.g. P-selectin, VWF) Immune mediators Growth factors Angiogenic factors/inhibitors	ADP, ATP Cations (e.g. Ca ²⁺ , Mg ²⁺) Bioactive amines (e.g. 5-HT, histamine) Polyphosphates	Acid proteases (e.g. cathepsins, collagenases) Glycohydrolases (e.g. Glucosidases)

ADP = Adenosine diphosphate; ATP = Adenosine triphosphate; VWF = Von Willebrand factor; Adapted from Fitch-Tewfik *et al.*⁵⁵

Platelets have a lifespan of only 8-10 days after which they are removed from the circulation by phagocytosis in spleen or liver. In humans, to maintain the normal platelet count of 150-400 x 10⁶ cells/mL blood, 100 billion new platelets must be generated daily from megakaryocytes in the bone marrow. Of note, platelet counts in mice are with 900-1600 x 10⁶ cells/mL blood around 5 times higher than in humans.⁵⁸

Under steady state, they circulate at high shear stress as discoid cells. Following vessel injury marked by the exposure of extra cellular matrix material to the vascular lumen, platelets get activated and undergo drastic morphological changes.^{55,58} The initial step in platelet-endothelial adhesion is the interaction of platelet glycoprotein (GP) Ib-V-IX complex with collagen-bound von Willebrand factor (VWF). This transient interaction enables stable platelet adhesion to collagen, which stimulates the release of platelet-stored effector molecules with high local concentrations, leading to further platelet recruitment and initiation of the coagulation cascade.^{58,59} In the context of atherosclerosis, platelets are activated when a plaque ruptures because of the exposure to highly pro-thrombogenic plaque-components such as collagen or VWF. Platelet aggregation and activation leads to thrombus formation and eventually to vessel occlusion.¹¹

Beyond their role in thrombosis and hemostasis, it is now widely recognized that platelets also promote endothelial leukocyte recruitment in diverse ways during inflammation. Activated platelets express P-selectin by which they can interact with the activated endothelium via VWF or PSGL1. However, leukocytes also express the P-selectin ligand PSGL1, thereby enabling activated platelets to capture leukocytes. On the one hand, they can interact in circulation forming so-called platelet-leukocyte aggregates (PLAs) and, on the other hand, endothelium-bound platelets can facilitate leukocyte recruitment by forming an adhesive bridge between endothelium and blood leukocytes (Figure 6A,B).⁶⁰ Furthermore, platelet-mediated deposition of effector molecules such as CCL5 on the endothelium can enable leukocyte recruitment (Figure 6C). Several *in vivo* studies reported that enhanced platelet-leukocyte interactions

promote atherogenesis. For instance, the injection of activated platelets derived from wild type mice induced monocyte arrest on atherosclerotic lesions, which was not observed with P-selectin deficient platelets.⁶¹ In line with these results, platelet-specific *P-selectin* knockout reduced atherogenic lesions in *ApoE*^{-/-} mice.⁶²

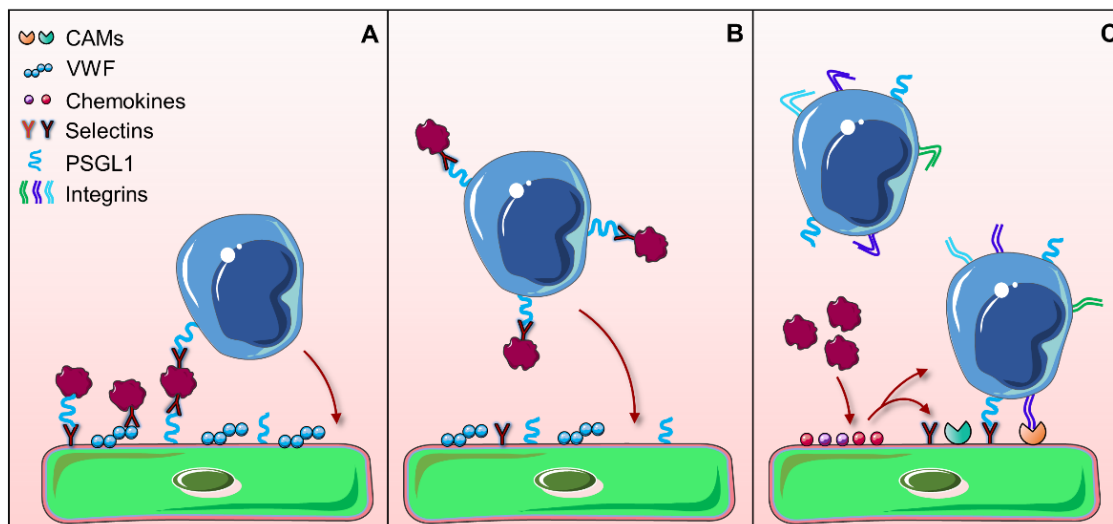


Figure 6: Pathways of platelet-mediated leukocyte recruitment.

Platelets can mediate leukocyte recruitment and adhesion to the endothelium in different ways. **(A)** The activated endothelium expresses factors such as VWF, PSGL1 or P-selectin leading to platelet recruitment, binding and subsequently activation. Platelets can capture leukocytes by P-selectin-PSGL1 binding, thereby forming a bridge between the immune cells and the endothelium. **(B)** Activated platelets can form aggregates with leukocytes in circulation in a P-selectin-mediated manner enhancing the recruitment to the activated endothelium. **(C)** Inflammatory chemokines deposited by platelets can induce the activation on the one side of endothelial cells, and on the other side of leukocytes leading to leukocyte adhesion.⁶³

The formation of PLAs is also observed in healthy individuals, albeit with low frequency. Interestingly, the amount of PLAs positively correlated with the severity of inflammation. For instance, an augmented incidence was observed in stable coronary artery disease or during myocardial infarction and stroke.⁶³ In mice, it was demonstrated that PLAs promote atherogenesis and P-selectin on activated platelets is crucial for their formation.⁶¹ Further studies showed that the deposition of chemokines by platelets provokes atherogenesis.^{61,64–66} More precisely, deposition of platelet-derived CCL5 and CXCL4 is P-selectin-dependent and triggers integrin-mediated monocyte activation and recruitment to atherosclerotic lesions which in turn leads to aggravated atherosclerosis.^{61,64,65} Moreover, genetic ablation of CXCL4 protected mice from atherosclerosis.⁶⁶ Interestingly, CCL5 and CXCL4 were shown to form heteromers, which in turn promote monocyte arrest on the endothelium.⁶⁷ Moreover, disruption of this interaction mitigated atherogenesis.^{68,69}

In summary, platelets can mediate leukocyte recruitment either by chemokine deposition or by direct leukocyte interaction. The latter can occur in three different ways during atherogenesis: First, activated, endothelium-adherent platelets can bind to blood leukocytes and thereby form a bridge between leukocytes and vessel wall; second, the formation of platelet-leukocyte

aggregates in circulation promotes leukocyte recruitment; third, during hemostasis leukocytes are recruited to the growing thrombus. Whether these interactions are causal or consequential in inflammatory disease still remains to be addressed.⁶³

3.3 The serotonergic system

3.3.1 Central versus peripheral serotonin

Serotonin (5-hydroxytryptamine, 5-HT), discovered by Rapport *et al.* 1948 as a vasoconstrictor compound,⁷⁰ has two distinct sites of action: one as a neurotransmitter regulating mood, behavior, sleep, appetite and other brain functions, and one as a peripheral hormone (Figure 7). Although 5-HT is mainly known for its role as neurotransmitter in the brain, the vast majority of 5-HT (~95 %) is found in the periphery, where it is involved in a variety of different functions such as the regulation of the vascular tone,⁷¹ platelet aggregation and degranulation,⁷² vascular permeability,⁷³ intestinal motility⁷⁴ or immune-modulation.⁷⁵ 5-HT is synthesized from the essential amino acid tryptophan (Trp) in two steps with the initial and rate-limiting step being the hydroxylation to 5-hydroxytryptophan (5-HTP) by the enzyme tryptophan hydroxylase (TPH), followed by decarboxylation through the catalytic action of aromatic amino acid decarboxylase (AADC).⁷⁶

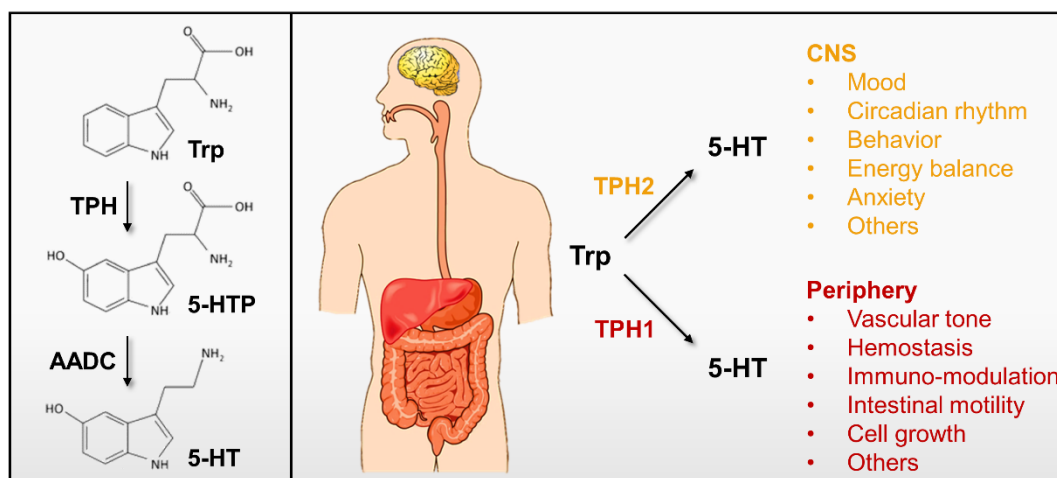


Figure 7: The effects of peripheral and central 5-HT.

5-HT is synthesized from the amino acid tryptophan (Trp) in two steps: hydroxylation to 5-hydroxytryptophan (5-HTP) by the rate-limiting enzyme tryptophan hydroxylase (TPH) followed by decarboxylation through the aromatic L-amino acid decarboxylase (AADC) to 5-HT. Because 5-HT cannot pass the blood brain barrier, the central and peripheral pools are synthesized via two different enzyme isoforms: TPH1, which is found in the periphery, and TPH2, which is only expressed in neurons. In the central nervous system (CNS), 5-HT is associated with the regulation of several behaviors such as mood, sleep and anxiety. However, most of the body's 5-HT can be found in the periphery where the majority is stored in circulating platelets. Peripheral 5-HT is involved in the regulation of a variety of different processes such as vascular tone, hemostasis and intestinal motility.^{75,76}

5-HT cannot pass the blood-brain barrier yielding two isolated 5-HT pools - one in the brain and one in the periphery. These are synthesized by two different TPH isoenzymes: TPH1, primarily localized in enterochromaffin cells in the gastrointestinal tract, and TPH2, exclusively

expressed in neurons.⁷⁷ Once synthesized, 5-HT is packed into vesicles mediated by the vesicular monoamine transporter (VMAT) and stored until targeted secretion through exocytosis.⁷⁶ The bioavailability of 5-HT is dependent on synthesis and metabolism. It is mainly degraded by monoamine oxidase (MAO) to the end product 5-hydroxyindoleacetic acid (5-HIAA) followed by excretion through the kidneys. Besides, 5-HT can be metabolized to melatonin, known to be involved in the circadian rhythm regulating sleep-wake timing. Age-related decline in 5-HT might correlate with changes in sleep behavior linked with aging.⁷⁶

In neurons, upon activation, synthesized 5-HT is released into the synaptic cleft, where signaling takes place by binding to one of the several 5-HT receptors (5-HTRs) either in an autocrine or paracrine fashion (Figure 8). The signaling can be regulated by 5-HT reuptake through the serotonin transporter (SERT). Abnormalities in 5-HT signaling are associated with several neuropsychological conditions such as depression, anxiety disorders or schizophrenia.⁷⁶

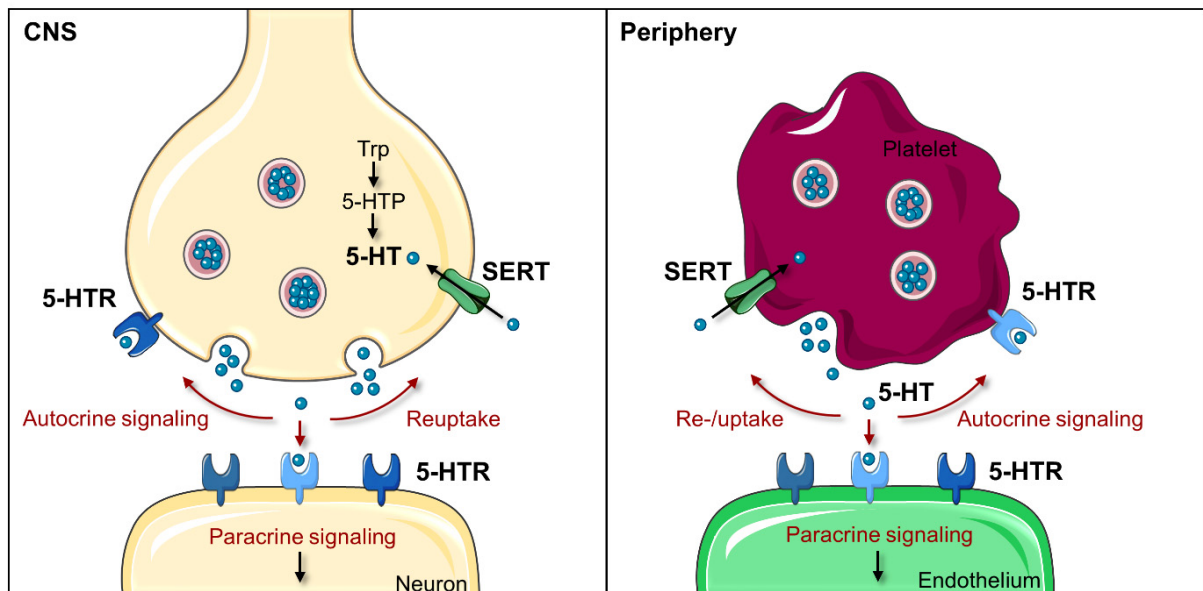


Figure 8: Comparison of 5-HT in neurons and platelets.

In neurons, 5-HT is synthesized from tryptophan (Trp) via 5-hydroxytryptophan (5-HTP) within the cell and stored in vesicles. In contrast, platelets do not synthesize 5-HT. Here, enterochromaffin cell-derived 5-HT is taken up from plasma via SERT and stored in the dense granules. In both cell types, activation leads to 5-HT release by exocytosis and autocrine and/or paracrine signaling by binding to several 5-HTRs. 5-HT signaling can be regulated on the part of the ligand 5-HT through 5-HT reuptake by SERT.

Platelets represent the major storage site for peripheral 5-HT. However, they lack the enzyme TPH1 and thus cannot synthesize 5-HT themselves. Instead, they take up enterochromaffin cell-derived 5-HT from the plasma through SERT and store it in their dense granules.⁷⁸ The translocation from the cytosol into the dense granules is mediated by VMAT2, which is driven through an electrochemical proton gradient.⁵⁵ Under steady state, the 5-HT plasma concentration is very low (~10 nM). Upon platelet activation, the targeted release of 5-HT through exocytosis leads to rapidly increased levels of up to 10 μ M and more.⁷⁵ Secreted 5-HT

provokes signaling by binding to one of the 5-HT receptors (5-HTR), which is terminated on the part of the ligand by 5-HT-reuptake via SERT (Figure 8). Elevated plasma 5-HT levels have been associated with CVDs, including myocardial infarction, coronary artery disease, atherothrombosis and stroke.⁷⁹

Although most platelet 5-HT is stored in the dense granules, Walter *et al.* stated that cytoplasmic platelet 5-HT can be transamidated to small GTPases, a process named serotonylation. The covalent binding of 5-HT leads to the activation of GTPases resulting in α -granule secretion, representing a receptor-independent intracellular 5-HT signaling pathway.⁸⁰ So far, this process has also been demonstrated in pancreatic β -cells and vascular SMC. Thus, serotonylation may also occur in other cell types such as leukocytes.⁸¹ Pathological function of peripheral 5-HT was shown to be implicated in several inflammatory diseases such as colitis,⁸² asthma,⁸³ inflammatory bowel disease,⁸² and obesity.⁸⁴

3.3.2 Components of the serotonergic system

3.3.2.1 Serotonin receptors

The wide range of functions mediated by 5-HT results from the existence of several 5-HTRs. In mammals, seven distinct 5-HTRs (5-HTR1-7) are described with at least fourteen known subtypes (Figure 9). All 5-HTRs are GPCRs with the exception of 5-HTR3, which is a ligand-gated cation channel (Na^+ and Ca^{2+} influx, K^+ efflux). GPCRs are seven transmembrane receptors characterized by the ability to activate heterotrimeric G proteins comprised of the three subunits α , β and γ . The complexity of the serotonergic system is further amplified by the fact that the 5-HTRs couple to different G proteins and may also assemble to receptor homo- and heterodimers.⁸⁵

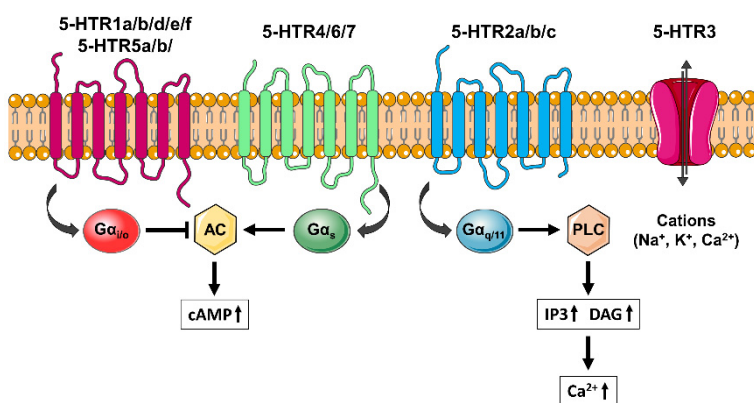


Figure 9: 5-HTR subtypes and their main signaling pathways.

Overview about the main signaling pathways of the different 5-HTRs. All 5-HTRs are GPCRs with the exception of 5-HTR3, which is a ligand-gated cation channel. 5-HTR1 and 5-HTR5 are associated with coupling to $\text{G}\alpha_{i/o}$ causing a decrease in cAMP, whereas 5-HTR4, 5-HTR6 and 5-HTR7 are known to increase cAMP by activation of $\text{G}\alpha_s$. 5-HTR2, however, couples to $\text{G}\alpha_{q/11}$ leading to the release of intracellular calcium.⁸⁶

5-HTR1 and 5-HTR5 couple to $\text{G}\alpha_{i/o}$, which inhibits adenylyl cyclases (ACs), resulting in downregulation of cyclic adenosine monophosphate (cAMP).⁸⁶ The 5-HTR1 subfamily, which is linked with migraine and anxiety, consists of five subtypes: 5-HTR1a, 5-HTR1b, 5-HTR1d, 5-HTR1e, 5-HTR1f. The subtype 5-HTR1c was reassigned to 5-HTR2c because of its different signaling. Little is known about the 5-HTR5 subfamily, which is comprised of 5-HTR5a and

5-HTR5b, mainly due to the lack of selective agonists.⁸⁷ 5-HTR4, 5-HTR6 and 5-HTR7 are known to activate ACs via $G\alpha_s$ causing an increase in cAMP. The 5-HTR2 subfamily encompasses the three subtypes 5-HTR2a, 5-HTR2b and 5-HTR2c and is associated with coupling to $G\alpha_{q/11}$. This signaling pathway leads to the activation of PLC, which in turn hydrolyzes phosphatidylinositol 4,5-bisphosphate (PIP2) to diacylglycerol (DAG) and inositol 1,4,5-triphosphate (IP3), triggering the release of intracellular calcium.⁸⁶ However, in cell culture 5-HTR2a and 5-HTR2c were also shown to exhibit $G\alpha_{i/o}$ activation.⁸⁷

To define a specific function for each 5-HTR is difficult, at least based on the current literature. For instance, contradictory reports were published about the role of 5-HTR2a in inflammation. On the one hand, 5-HT2a stimulation was shown to trigger a pro-inflammatory response by IL6 release in vascular SMCs.⁸⁸ In line with these findings, inhibition of 5-HTR2 blocked the TNF α -induced ICAM1 expression in human umbilical vein endothelial cells via nitric oxide (NO) release.⁸⁹ On the other hand, a different report revealed anti-inflammatory properties of 5-HTR2a in primary aortic SMCs. Specific activation led to the inhibition of TNF α -mediated inflammation including a decrease in the expression of ICAM1 and IL6.⁹⁰ The little consistency in studies arise through the complexity of the serotonergic system. As different cell types express a different 5-HTR expression pattern, 5-HT function is diverse. For instance, 5-HT seems to have two faces in the regulation of the vascular tone. Firstly, 5-HT acts as a vasoconstrictor via the 5-HT2A receptor in VSMC. Secondly, 5-HT induces vasodilation through eNOS production via 5-HTR1b present on endothelial cells.⁹¹ Even within the same organ, different receptors can be stimulatory or inhibitory, leading to the bivalent action of increased or decreased 5-HT.⁷⁶ Conflicting results in cell culture experiments may be explained by contaminations of 5-HT since fetal bovine serum (FBS) contains ~300 nM 5-HT, which is enough to stimulate most 5-HTRs.⁹² Moreover, the absence of sufficiently selective ligands makes it difficult to attribute a specific function to a receptor.⁹³ A few years ago Wang *et al.* and Wacker *et al.* deciphered the GPCR crystal structures of the 5-HT subtypes 5-HTR1b and 5-HTR2b.^{94,95} While both receptors show high similarity in the structure of the 5-HT binding site, there is a subtle difference in the width of the binding pocket, which is already enough to cause differences in signaling. This paved the way for the development of novel more selective compounds for these two receptors. Further research on 5-HTR crystal structures will provide a better understanding of the serotonergic receptor function and will enable the design of more selective compounds and thereby more specific drugs.⁹⁶

3.3.2.2 Serotonin transporter

The 5-HT transporter (SERT or 5-HTT) is a Na⁺/Cl⁻-dependent twelve transmembrane domain spanning monoamine transporter, which is encoded in humans by the gene *solute carrier family 6, member 4* (SLC6A4).⁸¹ It is a key regulator for 5-HT signaling, which terminates signaling by removing extracellular 5-HT through transportation across the plasma membrane

into the cell. In this way, the 5-HT reuptake can mediate the duration as well as the strength of the autocrine and paracrine signaling of 5-HT. After reuptake, 5-HT is either recycled and packed into vesicles by VMAT or degraded by MAO. Although SERT is mainly studied and therapeutically targeted for controlling the 5-HT concentration in the synaptic cleft, it is also crucial for platelet function including the regulation of plasma 5-HT levels.^{76,79,81} Because of its important function, SERT is regulated in several ways. Like many receptors, SERT is not constitutively located on the plasma membrane but dynamically traffics due to post-translational modifications such as phosphorylation. Apart from trafficking, phosphorylation was also postulated to modulate SERT activity. Thus, p38 mitogen activated protein kinase (MAPK)-dependent phosphorylation, induced by the pro-inflammatory cytokines IL1 β and TNF α , enhances SERT activity.⁹⁷ Moreover, 5-HT itself regulates the density of SERT on the plasma membrane. Increased 5-HT concentrations display a bivalent effect on SERT. In neurons, high extracellular 5-HT levels decrease the density of SERT on the membrane, whereas SERT on the surface of platelets is initially upregulated with increasing plasma 5-HT levels.⁹⁸ However, with continuously rising plasma levels, the SERT density on platelets falls below normal levels, suggesting that 5-HT limits its own uptake into platelets by down-regulating SERT.⁷⁹ This is further supported by the observation that high intracellular 5-HT levels in platelets result in SERT internalization, which is dependent on GTPase serotonylation.⁸¹

It is well established that SERT is implicated in mental disorders such as depression, although the precise mechanism is still debated.⁹³ This is further supported by the observation that genetic variations and altered SERT expression are associated with behavioral phenotypes and disorders. Clinical evidence arises from polymorphisms in the promoter region of SERT, the so-called serotonin-transporter-gene-linked polymorphic region (5-HTTLRP), which has been associated with neuropsychiatric disorders.⁹⁹ In accordance, mice deficient for SERT exhibit behavioral abnormalities linked to anxiety and depression. As a result, SERT is the primary target of many antidepressant medications. The most common antidepressants are the selective serotonin reuptake inhibitors (SSRIs). The effectiveness of SSRIs is assumed to be mediated by enhanced serotonergic neurotransmission. More precisely, SSRIs block SERT and thereby the 5-HT reuptake, resulting in an increased 5-HT concentration in the synaptic cleft and subsequently to an amplified signaling. Just recently, Coleman and colleagues were the first who described a high resolution structure of the human SERT bound to two different SSRIs.^{100,101} While others suggest that SERT functions by forming oligomers, Coleman *et al.* postulate that SERT-dimers observed in crystal form are unlikely to occur under physiological conditions in the cell membrane because the predicted membrane-spanning regions of each protomer are not properly aligned.¹⁰⁰

3.3.3 Impact of platelet serotonin on immune function

Davis and colleagues already stated in 1960 that platelet-derived 5-HT is linked to inflammation based on the observation that inflammation triggered by *E. coli* endotoxin coincided with a decrease in circulating platelet counts and serum 5-HT.¹⁰² In fact, platelets represent the main source of 5-HT for immune cells. Apart from mast cells, monocytes/macrophages and T cells are described to have the ability to synthesize small amounts of 5-HT, representing an additional but smaller 5-HT source for the immune system.⁹² The expression of 5-HTRs was determined on several immune cells as well as on platelets, endothelial cells and vascular SMCs (Table 3). Additionally, most immune cells were proposed to express SERT. However, the presence of serotonergic components on different cell types is rather controversial between studies, especially when it comes to neutrophils.⁷⁵ This might be due to methodical problems based on unspecific primers or contaminations by other cell types during cell isolation.

Table 3: Serotonergic components in immune cells ^{75,81,85,103–105}

Cell type	5-HTR	SERT	TPH1
Monocytes	1a, 1e, 2a, 3, 4, 7	+	+
Neutrophils	(1a, 1b, 2, 7)	?	-
T cells	1a, 1b, 2a, 2c, 3, 7	+	+
Platelets	2a, 3	+	-
Endothelial cells	1b, 2b, 4	+	+
Vascular SMCs	1b, 2a, 2b, 7	+	+

Activated platelets release 5-HT locally at the site of acute or chronic inflammation, leading to autocrine signaling or stimulation of other cell types such as leukocytes, SMCs and endothelial cells.⁹⁸ Although the 5-HTR3 receptor was also reported to be expressed on platelets, the effects of 5-HT on platelets so far are assigned to serotonylation and mainly to the activation of 5-HTR2a.⁷⁵ The latter induces a positive feedback loop by PLC-mediated increase of intracellular calcium. This in turn leads to amplified platelet activation and the recruitment of other circulating platelets.¹⁰⁶ Contrariwise, 5-HTR2a activation without further platelet stimulation was shown to activate TNF α -converting enzyme (TACE), resulting in reduced platelet adhesiveness through shedding of GP Iba and V from the VWF receptor complex GPIb–IX–V.¹⁰⁷

Several studies reported that platelet-derived 5-HT is implicated in multiple immune reactions, mainly caused by the regulation of cytokine secretion and alteration of leukocyte function.^{88–90,98,108–110} The immunomodulatory effects of 5-HT depend on the different expression of the serotonergic components by immune cells. Thereby, the regulation can differ in terms of pro- or anti-inflammatory action depending on the cell type and the environment.⁸¹ For instance, it was shown that 5-HT induces proliferation of lymphocytes.¹⁰⁸ Moreover, 5-HT enhances the phagocytotic activity of macrophages¹⁰⁹ as well as the polarization to a more anti-inflammatory

phenotype.¹¹⁰ However, Sternberg *et al.* reported that 5-HT had inhibitory or stimulator effects on murine macrophage activity depending on the dose of IFN γ . At high concentrations, 5-HT suppressed the IFN γ -mediated phagocytotic activity, while at lower levels, it revealed stimulatory effects.^{75,111,112} Others showed that 5-HT promotes the LPS-induced release of cytokines such as IL1 β and IL6 in human blood monocytes.¹⁰⁵ However, TPH1 deficient mice, which lack non-neuronal 5-HT, are not immunocompromised, suggesting that 5-HT is not essential for immune response but rather has an immunomodulatory role.^{76,92} These data further illustrate the complexity of 5-HT signaling.

It becomes even more complicated when considering endothelial inflammation. In this context, Cloutier *et al.* discovered an unpredicted role for platelets by amplifying vascular permeability in inflammatory arthritis in a 5-HT dependent manner.⁷³ *In vitro* studies showed that 5-HT stimulates the release of Weibel-Palade bodies from endothelial cells,^{113,114} which are known to be packed with P-selectin and may thereby promote leukocyte rolling. In line with this mechanism, Duerschmied and coworkers reported that platelet 5-HT promotes E- and P-selectin-mediated neutrophil rolling and adhesion on the endothelium of mesenteric veins.^{115,116} In addition, they showed that TPH1 deficient mice revealed improved wound healing and mitigated neutrophil extravasation in response to an acute inflammation, suggesting a pro-inflammatory role for 5-HT.¹¹⁵

Although the reported immunomodulatory effects of 5-HT are somewhat controversial, they highlight that 5-HT is more than just a neurotransmitter for mood modulation. However, it is difficult to pinpoint a specific mode of 5-HT action, as it regulates several processes at multiple steps through different receptors, often with opposing mechanisms. Thus, even drugs targeting a specific 5-HTR are likely to have off-target effects, which is challenging for drug development. But at the same time, this may offer a pharmacologic opportunity.⁷⁸ Hence, drugs targeting the serotonergic systems should be examined carefully. Michael Gershon, the so-called “father of neurogastroenterology”, once ironically stated that 5-HT has delighted every pharmacologist because something always happens and that the attempts to define the exact function of 5-HT is bedeviled because it has the ability to do too much.¹¹⁷ Thus, the knowledge about the 5-HT function remains poorly understood. Nevertheless, it is clear that 5-HT plays an important role as an immunomodulator.

3.4 Antidepressants and cardiovascular diseases

3.4.1 Depression – a cardiovascular risk factor

Depression can affect anyone. According to the WHO depression is the leading cause of disability with more than 300 million people globally suffering from this mental disorder.¹¹⁸ Interestingly, persons suffering from depression are more likely to develop CVDs and possess a higher mortality rate compared to healthy individuals.¹¹⁹ Moreover, Ladwig and colleagues

published a report in 2017 based on the data set from the MONICA/KORA study, where 3428 male patients were monitored for ten years.¹²⁰ They surprisingly found that depression represents a cardiovascular risk factor which is just as great as that posed by obesity and high cholesterol levels. Based on their findings, only hypertension and smoking are associated with a higher risk.¹²⁰ Given that depression represents a widely accepted risk factor for CVDs the question is emerging if the treatment of depression may reduce the risk for CVDs.

Depression has been implicated with a dysregulation of the serotonergic system. However, years of research still do not clarify which precise role 5-HT is playing in depression. Thus, the 50 years ago proposed “serotonin hypothesis”, which says that a 5-HT deficiency is causal for the development of depression, is still highly debatable.^{121,122} Indeed, there are some arguments against this theory. For instance, the measurements of brain 5-HT levels are not feasible in living individuals. Given that 5-HT cannot pass the blood brain barrier, the measurement of 5-HT blood levels may not exactly reflect brain levels. Furthermore, carriers of the short (s) variant of the 5-HTTLRP polymorphism, which results in decreased expression of SERT and thereby higher extracellular 5-HT levels, are likely to suffer from depression. However, it seems too simplistic that a single neurotransmitter is the only cause for developing depression.¹²² Nevertheless, there is substantial evidence for an association of imbalanced 5-HT signaling, and targeting the serotonergic system in depressed patients displays beneficial effects. With the increasing incidence of depression, antidepressants are one of the most prescribed drug classes nowadays.¹²³

3.4.2 Selective serotonin reuptake inhibitors – good or bad?

The serotonergic system turned out to be an effective target for the treatment of depression. The most widely prescribed antidepressants are the SSRIs. They are a newer class of antidepressants targeting SERT and display higher efficacy and lower adverse effects, compared to the first generation drugs, the tricyclic antidepressants, even though their exact mechanism is not entirely elucidated.¹²⁴ It is assumed that the antidepressant effect of SSRIs is caused by preventing the SERT-mediated 5-HT reuptake, which leads to an increase of extracellular 5-HT and in turn to an enhanced 5-HT signaling.⁷⁶ Table 4 shows the U. S. Food and Drug Administration (FDA)-approved SSRIs and their most common trade names,¹²⁵ of which fluoxetine (FLX) and escitalopram are those who were used in this work (Figure 10). FLX, better known with its trade name Prozac, was approved as one of the first SSRIs for the treatment of depression. It is a racemic mixture of the (S)- and the (R)-enantiomer, of which the (S)-enantiomer is slightly more potent. Interestingly, the metabolite of FLX, norfluoxetine, is even more potent and has an extremely long biological half-life of 7-15 days.¹²⁶ Escitalopram is the active (S)-enantiomer of the racemic citalopram and is the newest marketed SSRI.¹²⁷

Table 4: FDA-approved SSRIs¹²⁵

Generic name	Trade name
Fluoxetine	Prozac
Citalopram	Celexa
Escitalopram	Lexapro
Fluvoxamine	Luvox
Paroxetine	Paxil
Sertraline	Zoloft
Vilazodone	Viibryd

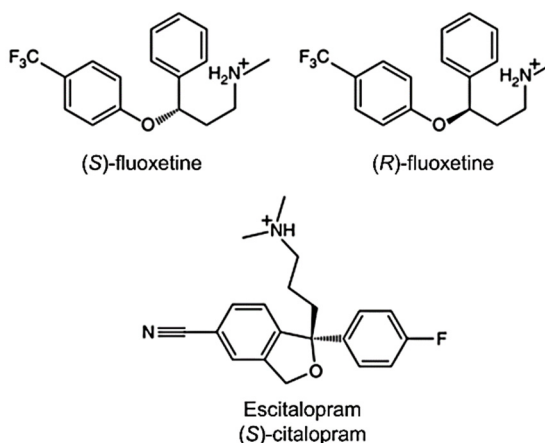


Figure 10: Structure of FLX enantiomers and escitalopram.¹²⁸

All SSRIs are small molecules with diverse chemical structures and different functional groups, leading to different affinities to SERT.¹²⁸ So far, little was known about the structural basis of how the diverse SSRIs bind to SERT, until Coleman and coworkers recently provided the structures of the human SERT bound to different SSRIs. More precisely, two years ago they were the first to describe X-ray crystallographic structures of human SERT bound to the SSRI escitalopram or paroxetine.¹⁰⁰ More recently, they were also able to crystallize human SERT occupied with sertraline and fluvoxamine. This enables new insights into the interaction of different pharmacophores within the central cavity, paving the way for the development of new and better drugs.¹²⁸ By binding in the central cavity, SSRIs lock SERT in an outward-open position, directly inhibiting 5-HT binding (Figure 11A-D).

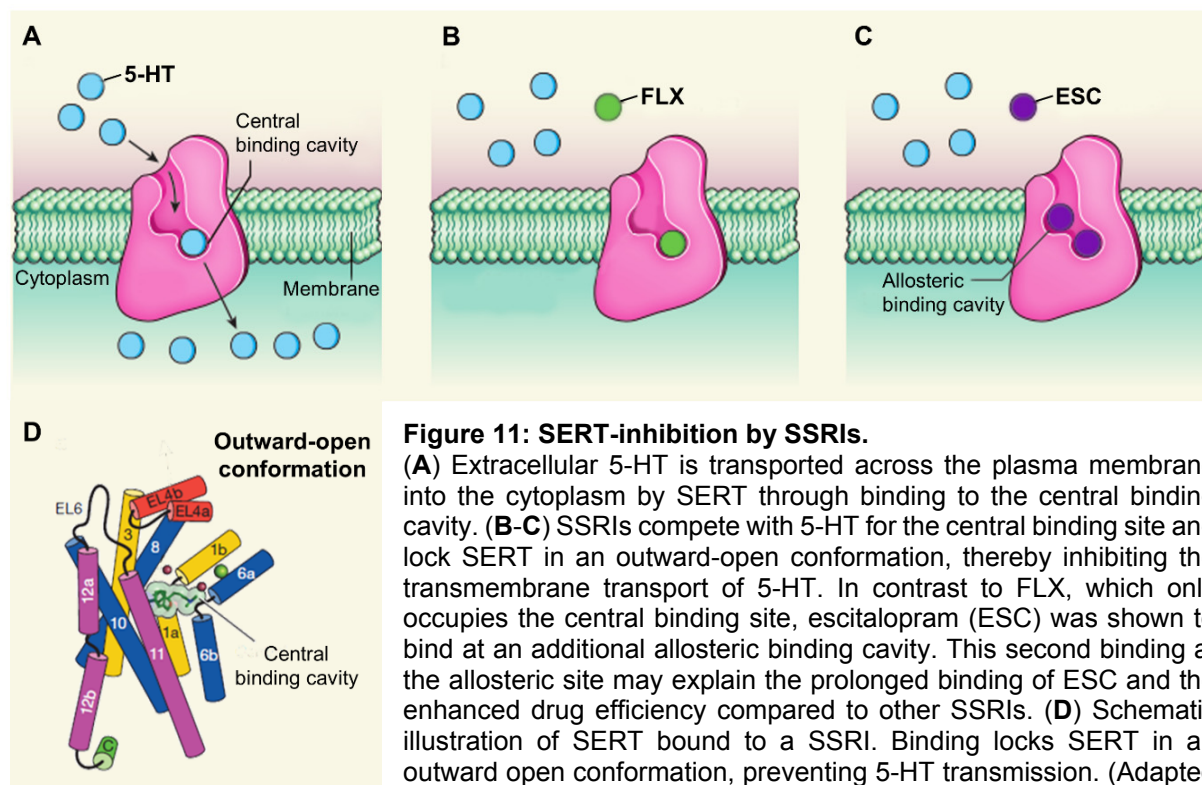


Figure 11: SERT-inhibition by SSRIs.

(A) Extracellular 5-HT is transported across the plasma membrane into the cytoplasm by SERT through binding to the central binding cavity. (B-C) SSRIs compete with 5-HT for the central binding site and lock SERT in an outward-open conformation, thereby inhibiting the transmembrane transport of 5-HT. In contrast to FLX, which only occupies the central binding site, escitalopram (ESC) was shown to bind at an additional allosteric binding cavity. This second binding at the allosteric site may explain the prolonged binding of ESC and the enhanced drug efficiency compared to other SSRIs. (D) Schematic illustration of SERT bound to a SSRI. Binding locks SERT in an outward open conformation, preventing 5-HT transmission. (Adapted from Caron & Gether and Coleman *et al.*)^{100,130}

Escitalopram differs from the other SSRIs because two molecules bind to SERT at the same time. In addition to the central cavity, escitalopram also binds “above” at an allosteric site. This additional occupancy sterically prevents dissociation of the drug from the central binding site and thereby prolongs the blocking activity of escitalopram. The additional binding at the allosteric site probably explains the higher efficacy of escitalopram compared to other SSRIs.^{100,101} Thus, escitalopram has a recommended therapeutical range of 15-80 ng/mL, which is much lower compared to the one for FLX (120-300 ng/mL).¹²⁹

Although SSRIs are the first-line therapy for depression, the treatment is ineffective in one-third of the patients. One of the underlying causes might be related to polymorphisms of the SERT gene.¹²⁴ Another important issue in terms of SSRI intake is that SERT is not only expressed on neurons but also on the plasma membrane of several other cell types such as platelets (Table 3). As platelets are not able to synthesize 5-HT, chronic SSRI intake leads to the depletion of platelet 5-HT and thereby to the depletion of the major 5-HT storage in the periphery (Figure 12). Indeed, depressed patients taking SSRI have decreased intra-platelet 5-HT content.¹³¹ The same was observed in mice treated with the SSRI FLX.¹¹⁵ Because released platelet 5-HT is known to provoke a positive feedback mechanism, thereby enhancing platelet activation, it is conceivable that SSRI treatment is associated with bleeding disorders. However, studies investigating the bleeding risk in patients taking SSRIs present contradictory results.^{132,133} Ideally, randomized double-blind studies would be important to determine the link between SSRI and bleeding risk.¹³⁴

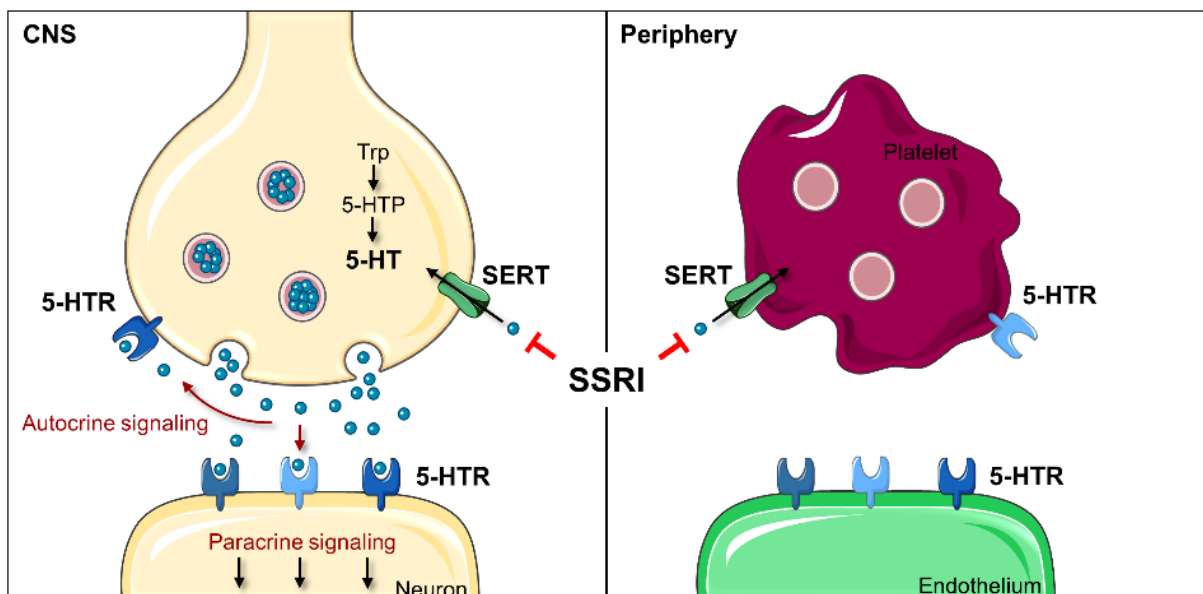


Figure 12: Impact of SSRI intake on neurons and platelets.

The antidepressant effect of SSRIs is supposed to underlie in blocking the SERT-mediated 5-HT uptake, thereby leading to increased 5-HT levels in the synaptic cleft and subsequently to an amplified 5-HT signaling. However, SERT is expressed by several other cell types and SSRIs are not selective for neuronal SERT. For instance, intake of SSRIs leads to the inhibition of 5-HT uptake in platelets and thereby to the depletion of the platelet 5-HT storage, which is the major source of 5-HT in the periphery.

The fact that depression poses a widely accepted risk factor for CVD raises the question if antidepressant medication reduces the risk for the incidence of a cardiovascular event. So far, there is still no clear answer to this question because clinical studies investigating the effect of SSRI intake on CVD risk are controversial (Table 5). Data from observational and experimental studies showed indeed a reduced cardiovascular risk for patients taking SSRIs.^{135–141} In contrast, other case-control and cohort studies claim that SSRI intake increases the risk for CVD,^{142–146} while some reports show no influence at all.^{147–155} An important issue of these conflicting results are the confounding effects by depression and behavioral risk factors. Given the rising number of people suffering from depression and SSRIs being the first-line therapy, answering the question if SSRIs treatment has an impact on the risk for the incidence of a cardiovascular event is of great importance and requires further investigation. Ideally, more randomized double-blinded controlled trials without depression as a confounding variable would be needed to address this issue.

Table 5: Selected clinical studies showing controversial findings regarding the effect of SSRI intake on CVD risk

Observational studies					
Risk	Study design	Study group		Cohort (SSRIs)#	Ref
↑↓	Case-control study	Stroke patients		44765* ¹ (3520)	147
↑↓	Case-control study	MI patients GPRD (General Practice Research Database)		16458* ² (221)	148
↑↓	Cohort study	Subjects without a history of CVDs		14784 (299)	149
↑↓	Cohort study	MESA (Multi-Ethic Study of Atherosclerosis)		6814 (324)	150
↑↓	Case-control study	Patients with stroke recurrence		19825* ³ (239)	151
↑	Cohort study	ACS patients		457 (58)	142
↑	Cohort study	Postmenopausal women		136293 (3040)	143
↑	Case-control study	MI patients		442398* ⁴ (12988)	144
↑	Case-control study	Patients with depression +/- CVE		7601 (2632)	145
↑	Case-control study	Patients with out-of-hospital cardiac arrest		19110 (1696)	146
↓	Observational secondary analysis	MI patients		1834 (301)	135
↓	Case-control study	MI patients		3465* ⁵ (586)	136
↓	Case-control study	MI patients		5336* ⁶ (223)	137
↓	Cohort study	Stroke patients		36175 (5833)	138
Experimental studies					
Risk	Study design	Study group	Intervention	Sample size	Ref
↑↓	Randomized controlled trial (double-blinded)	Depressed heart failure patients	Escitalopram vs. placebo	3720	152
↑↓	Randomized controlled trial (double-blinded)	Non depressed ACS patients	Escitalopram vs. placebo	240	153
↑↓	Randomized controlled trial (double-blinded)	MDD patients	Sertraline vs. placebo	369	154
↑↓	Randomized controlled trial (double-blinded)	Depressed heart failure patients	Sertraline vs. placebo	469	155
↓	Randomized controlled trial (double-blinded for SSRI treatment)	MDD patients	Sertraline, placebo, supervised exercise, home-based exercise	202	139
↓	Randomized controlled trial (single-blinded)	Stroke patients	FLX vs. no intervention	404	140
↓	Randomized controlled trial (double-blinded)	Depressed MI patients	Sertraline vs. placebo	38	141

ACS = Acute coronary syndromes; CVE = Cerebrovascular events; MDD = Major depressive disorder; MI = Myocardial infarction

Number of patients in total cohort receiving SSRIs.

*The cohort includes the following number of controls: *¹ 40000, *² 13139, *³ 7779, *⁴ 378886, *⁵ 2772, *⁶ 4256.

3.5 Aim of the study

Depression is the leading cause of disability worldwide that can affect anyone. The WHO estimated that from 2030 onwards depression will not only be the largest contributor to global disease burden but also the illness that will be the number one financial health burden. With more than 300 million people worldwide being affected, it is not surprising that antidepressant medication finds widespread use.^{118,156} Several studies suggest an association between depression and CVDs.^{119,120} However, clinical studies investigating potential cardiovascular effects of SSRIs, the most common antidepressants, are controversial.^{135,136,145–154,137,155,138–144} A confounding factor is that depression *per se* is a well-established cardiovascular risk factor.^{119,157} Considering the rising importance of this disease and given the inconclusive findings in human studies, the aim of the thesis was to shed light on this topic by investigating the effect of chronic SSRI intake on the onset and progression of atherosclerosis in a mouse model. In particular, the impact of short- and long-term treatment of *ApoE*^{-/-} mice with the common SSRI FLX on atherogenesis and underlying mechanisms were explored.

4 MATERIALS AND METHODS

4.1 Materials

4.1.1 Chemicals and reagents

Table 6: Chemicals and reagents

Chemical /Reagents	Company
1 kb Plus DNA ladder	Invitrogen AG, Carlsbad, USA
2-Methylbutane	Sigma-Aldrich Chemie GmbH, Munich, Germany
2-Propanol	Sigma-Aldrich Chemie GmbH, Munich, Germany
Agar	AppliChem GmbH Darmstadt, Germany
Agarose	Sigma-Aldrich Chemie GmbH, Munich, Germany
Albumin	Carl Roth GmbH + Co. KG, Karlsruhe, Germany
Ampicillin	Sigma-Aldrich Chemie GmbH, Munich, Germany
Aqua ad injectabilia	B. Braun AG, Puchheim, Germany
Citric Acid	Merck KGaA, Darmstadt, Germany
CountBright absolute counting beads	Thermo Fisher Scientific, Waltham, USA
Direct Red 80	Sigma-Aldrich Chemie GmbH, Munich, Germany
DMEM	Thermo Fisher Scientific, Waltham, USA
DMSO	Carl Roth GmbH + Co. KG, Karlsruhe, Germany
DPX Mountant	Sigma-Aldrich Chemie GmbH, Munich, Germany
EcoTransfect	OZ Biosciences, Marseille, France
EDTA	Sigma-Aldrich Chemie GmbH, Munich, Germany
Escitalopram oxalate	Sigma-Aldrich Chemie GmbH, Munich, Germany
Ethanol 99%	Klinikum der Universität München
Ethanol 99% (absolute)	VWR International, Radnor, USA
Ethidium bromide	Sigma-Aldrich Chemie GmbH, Munich, Germany
Evans blue	Sigma-Aldrich Chemie GmbH, Munich, Germany
FBS	Sigma-Aldrich Chemie GmbH, Munich, Germany
Fluoxetine (Prozac)	Eli Lilly and Company, Neuilly-sur-Seine Cedex, France
Fluoxetine hydrochloride	Sigma-Aldrich Chemie GmbH, Munich, Germany
Formamide	Merck KgaA, Darmstadt, Germany
Forskolin	Sigma-Aldrich Chemie GmbH, Munich, Germany
Gel Loading Dye 6x	New England Biolabs, Ipswich, USA
Glucose	Merck KgaA, Darmstadt, Germany
HBSS with Ca/Mg (10x)	Thermo Fisher Scientific, Waltham, USA
HCl 37 %	Merck KGaA, Darmstadt, Germany
Hematoxylin solution according to Mayer	Sigma-Aldrich Chemie GmbH, Munich, Germany
HEPES solution 1 M	Sigma-Aldrich Chemie GmbH, Munich, Germany
Hygromycin	InvivoGen, San Diego, USA
Immu-Mount	Thermo Fisher Scientific, Waltham, USA
Ketamine	WDT eG, Garbsen, Germany

Luciferin-EF	Promega GmbH, Madison, USA
NAS-181	Tocris Bioscience, Bristol, United Kingdom
Oil Red O	Sigma-Aldrich Chemie GmbH, Munich, Germany
Paraformaldehyde	Merck KGaA, Darmstadt, Germany
PBS	Biochrom GmbH, Berlin, Germany
Penicillin-Streptomycin	Sigma-Aldrich Chemie GmbH, Munich, Germany
PeqGold Trifast	Peqlab Biotechnologie GmbH, Erlangen, Germany
Picric acid solution	Sigma-Aldrich Chemie GmbH, Munich, Germany
Poly-D-Lysine	Sigma-Aldrich Chemie GmbH, Munich, Germany
Prostaglandin E1	Cayman Chemical, Ann Arbor, USA
RBC Lysis/Fixation Solution (10x)	BioLegend, San Diego, USA
Roti-Histofix 4 %	Carl Roth GmbH + Co. KG, Karlsruhe, Germany
RPMI-1640	Thermo Fisher Scientific, Waltham, USA
Serotonin hydrochloride	Sigma-Aldrich Chemie GmbH, Munich, Germany
S.O.C. medium	Thermo Fisher Scientific, Waltham, USA
Sodium citrate tribasic dihydrate	Sigma-Aldrich Chemie GmbH, Munich, Germany
Sodiumchlorid 0.9%	B. Braun AG, Puchheim, Germany
TAE buffer (50X)	AppliChem GmbH Darmstadt, Germany
Tetracycline	Sigma-Aldrich Chemie GmbH, Munich, Germany
Thioglycolate broth	Sigma-Aldrich Chemie GmbH, Munich, Germany
Tissue-Tek O.C.T	Sakura Finetek Germany GmbH, Staufen, Germany
Tryptone	AppliChem GmbH Darmstadt, Germany
Tween 20	Sigma-Aldrich Chemie GmbH, Munich, Germany
Tween 80	Sigma-Aldrich Chemie GmbH, Munich, Germany
Xylazine	WDT eG, Garbsen, Germany
Xylene	Sigma-Aldrich Chemie GmbH, Munich, Germany
Yeast extract	AppliChem GmbH Darmstadt, Germany

DMEM = Dulbecco's modified Eagle's Medium; DMSO = Dimethyl sulfoxide; DNA = Deoxyribonucleic acid; EDTA = Ethylenediaminetetraacetic acid; HBSS = Hanks' balanced salt solution; HEPES = 4-(2-hydroxyethyl)-1-piperazineethanesulfonic acid; PBS = Phosphate buffered saline; RBC = Red blood cell; RPMI = Roswell Park Memorial Institute; TAE = Tris-acetate-EDTA

4.1.2 Buffers and solutions

Table 7: Buffers, solutions and their composition

Buffers and solutions	Composition
0.1% Sirius Red solution	0.1 % (w/v) Direct Red 80 in picric acid solution
1x TAE buffer	50x TAE diluted in H ₂ O
4 % Thioglycolate	4 % (w/v) thioglycolate broth in dH ₂ O, autoclaved and allowed to stand for at least one week.
ACD buffer	75 mM trisodium citrate, 38 mM citric acid, 139 mM glucose dextrose, pH 5.4
ACK lysis buffer	150 mM NH ₄ Cl, 10 mM KHCO ₃ , 0.1 mM Na ₂ EDTA, pH 7.4
Adhesion medium	1.2 mM CaCl ₂ , 1 mM MgCl ₂ , 0.25 % (w/v) BSA, 0.1 % (v/v) glucose, 20 mM HEPES, pH 7.4 in HBSS

MATERIALS AND METHODS

Antigen retrieval buffer	1.4 mM citric acid, 5.74 mM sodium citrate tribasic dihydrate, 0.035 % (v/v) tween 20
Aortic digestion cocktail	10 mg/mL collagenaseIV, 20 U/mL DNase I in PBS
Blocking buffer	10 % (v/v) serum, 0.1% (v/v) Tween 20 in PBS
Ethidium bromide solution	Spatula tip of ethidium bromide in 15 mL H ₂ O
FACS buffer	0.5 % (w/v) albumin in PBS
HBSS/HEPES buffer	20 mM HEPES in HBSS
Integrin assay buffer	0.5 % (w/v) BSA in 1x HBSS(+Ca ²⁺ /Mg ²⁺), pH 7.4
LB medium	1 % (w/v) Trypton, 0.5 % (w/v) yeast extract, 1 % (w/v) NaCl, pH 7.0, autoclaved For agar: 1.5 % (w/v) agar and 50 µg/mL ampicillin were added and poured into petridishes
MACS buffer	0.5 % (w/v) BSA, 2 mM EDTA in PBS
ORO stock solution	0.5 % (w/v) ORO in 99 % 2-propanol
Tyrode buffer	0.14 M NaCl, 3 mM KCl, 12 mM NaHCO ₃ , 0.6 mM NaH ₂ PO ₄ H ₂ O, 5 mM HEPES, 0.2 % (w/v) albumin, 0.09 % (w/v) glucose

ACD = Acid citrate dextrose; ACK = Ammonium chloride potassium; BSA = Bovine serum albumin; DNase = Deoxyribonuclease; FACS = Fluorescence-activated cell sorting; LB = Lysogeny broth; MACS = Magnetic cell separation; ORO = Oil Red O

4.1.3 Kits

Table 8: Kits

Kit	Company
Amplex Red Cholesterol Assay kit	Invitrogen, Carlsbad, USA
Cholesterol CHOP-PAP kit + Calibrator	Roche, Basel, Switzerland
Serotonin Fast Track ELISA	Labor Diagnostika Nord, Nordhorn, Germany
Mouse CCL5 DuoSet ELISA	R&D Systems, Inc., Minneapolis, USA
Mouse CXCL4 DuoSet ELISA	R&D Systems, Inc., Minneapolis, USA
Monocyte Isolation kit	Miltenyi Biotec GmbH, Bergisch Gladbach, Germany
Neutrophil Isolation kit	Miltenyi Biotec GmbH, Bergisch Gladbach, Germany
peqGOLD Total RNA kit	Peqlab Biotechnologie GmbH, Erlangen, Germany
KAPA PROBE FAST Universal qPCR kit	Peqlab Biotechnologie GmbH, Erlangen, Germany
FLPR Calcium 5 Assay kit	Molecular Devices, LLC, USA
PrimeScript RT Reagent kit	TaKaRa Bio Inc., Kusatsu, Japan
Cytokine&Chemokine Mouse ProcartaPlex Panel 1	eBioscience Inc, San Diego, USA
VECTOR Red AP Substrate kit	Vector Laboratories, Burlingame, USA
QIAquick Gel Extraction kit	Qiagen, Hilden, Germany
QIAprep Spin Miniprep kit	Qiagen, Hilden, Germany
VECTASTAIN ABC-AP Staining kit	Vector Laboratories, Burlingame, USA
Vector Red AP Substrate kit	Vector Laboratories, Burlingame, USA

ELISA = Enzyme-linked immunosorbent assay; HRP = Horseradish peroxidase; qPCR = quantitative polymerase chain reaction; RNA = Ribonucleic acid

4.1.4 Primers

Primers and probes for qPCR were either self-designed and purchased from MWG-Biotech AG or bought as a pre-made primer-probe mix from Life Technologies. Sequences or Assay IDs of primer-probe mixes are listed in Table 9.

Table 9: Primers for qPCR analysis

Gene	Accession no	5'-3' primer sequence or Assay ID
<i>5-Htr1b</i>	NM_010482.1	Fwd: GAGCAGGGTATTCAGTGCG Rev: GAGTCCTGGTAAATGTAGCCG P: FAM-TGTGGGAGAGGTTGGTGAGAGGTA-TAMRA
<i>5-Htr2a</i>	NM_172812.2	Mm00555764_m1
<i>5-Htr2b</i>	NM_008311.2	Mm00434123_m1
<i>5-Htr2c</i>	NM_008312.4	Mm00434127_m1
<i>5-Htr4</i>	NM_008313.4	Mm00434129_m1
<i>5-Htr7</i>	NM_008315.2	Mm00434133_m1
<i>Ccl2</i>	NM_009915	Fwd: GAGCATCCACGTGTTGGCT Rev: TGGTGAATGAGTAGCAGCAGGT P: FAM-AGCCAGATGCAGTTAACGCCCCACT-TAMRA
<i>Ccl3</i>	NM_011337	Fwd: CAGCCAGGTGTCATTTTCCT Rev: CCAAGACTCTCAGGCATTTCAG P: FAM-AAGAGAAACCGGCAGATCTGCGCT-TAMRA
<i>Ccl5</i>	NM_013653.3	Mm01302427_m1
<i>Ccr1</i>	NM_009912.4	Mm00438260_s1
<i>Ccr2</i>	NM_009915	Fwd: AGTAACTGTGTGATTGACAAGCACTTAGA Rev: CAACAAAGGCATAAATGACAGGAT P: FAM-ACAGAGACTCTTGAATGACACACTGCTGC-TAMRA
<i>Ccr5</i>	NM_009917.5	Fwd: AATATTTCTTGAAAGTATTTTTCAGCCGT Rev: TTAATACTCTTTTGATTGAGAGTAAGCA P: FAM-AGATGTTATGTCCAAGCATG CAGTTTCGGA-TAMRA
<i>Cxcl1</i>	NM_008176	Fwd: CATAGCCACACTCAAGAATGGT Rev: TGAACCAAGGGAGCTTCAG P: FAM-CGCGAGGCTTGCCTTGACC-TAMRA
<i>Cxcl2</i>	NM_009140	Fwd: AGTGAAGTGGCTGTCAATG Rev: GCCCTTGAGAGTGGCTATGA P: FAM-AAGACCTGCCAAGGGTTGACTTC-TAMRA
<i>Gapdh</i>	NM_001289726.1/ NM_008084.3	Mm99999915_g1
<i>Hprt</i>	NM_013556	Fwd: GACCGGTCCCGTCATGC Rev: TCATAACCTGGTTCATCATCGC P: VIC-ACCCGAGTCCAGCGTCGTG-TAMRA
<i>Icam1</i>	NM_010493.2	Mm00516023_m1
<i>Sert</i>	NM_010484.2	Mm00439391_m1
<i>Vcam1</i>	NM_011693.3	Mm01320970_m1

CCR = C-C motif chemokine receptor; Fwd = Forward; Gapdh = Glyceraldehyde 3-phosphate dehydrogenase; Hprt = Hypoxanthine-guanine phosphoribosyltransferase; Rev = Reverse

The following primers were used for colony PCR (4.3.5.5) and sequencing (4.3.5.7).

Table 10: PCR primer

Gene	5'-3' primer sequence
5-HTR2a (rev)	AATTCTCGAGCACACAGCTCACCTTTTCATTCCTCCG
CMV (fwd)	CGCAAATGGGCGGTAGGCGTGTACG

CMV = Cytomegalovirus

4.1.5 Plasmids

The plasmids in Table 11 were used to generate a HEK-293 cell line overexpressing the 5-HTR2a under control of the CMV promoter in a tetracycline-inducible manner.

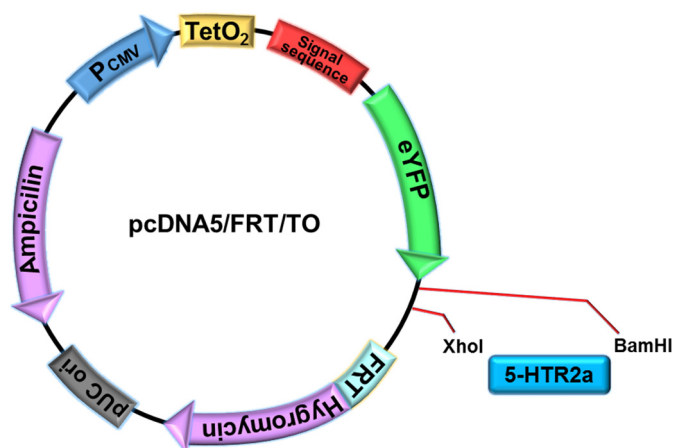
Table 11: Plasmids used for generation of a 5-HTR2a overexpressing cell line

Plasmid	Description	Resistance
pcDNA5/FRT/TO	Expression vector for gene of interest and eYFP under control of the CMV promoter in a tetracycline inducible manner. The Flp recombination target (FRT) site guarantees targeted integration into host cell line.	Ampicillin, hygromycin
pOG44	Coding for Flp recombinase under control of the CMV promoter.	Ampicillin

The pcDNA5/FRT/TO expression vector containing N-terminally the coding sequence for enhanced yellow fluorescent protein (eYFP) was used for incorporation of the 5-HTR2a coding sequence. The expression vector was transfected together with the pOG44 plasmid into the host Flp-In T-Rex-HEK-293 cell line (4.1.7). The pcDNA5/FRT/TO expression vector (Figure 13) comprises the hygromycin resistance gene lacking a promoter and the ATG initiation codon, which becomes active only upon correct integration into the cell genome.

Figure 13: Schematic structure of the pcDNA5/FRT/TO expression vector.

The pcDNA5/FRT/TO expression vector enables integration of the gene of interest (5-HTR2a) within the restriction sites of the enzymes BamHI and XhoI, leading to a fusion protein with eYFP. The expression is under the control of the strong CMV promoter (P_{CMV}), which is regulated by the tetracycline operator 2 (TetO₂). The signal sequence facilitates protein transport to the plasma membrane and finally membrane integration of the eYFP-5-HTR2a fusion protein. The FRT site serves as the binding and cleavage site for Flp recombinase. The hygromycin resistance gene permits selection of stable transfectants in mammalian cells when brought in frame with a promoter and an ATG initiation codon through correct Flp-mediated integration into the cell genome. The pUC origin (pUC ori) allows high-copy number amplification in *E. coli*. The ampicillin resistance gene permits selection of transfectants in *E. coli* cells.



The hygromycin resistance gene permits selection of stable transfectants in mammalian cells when brought in frame with a promoter and an ATG initiation codon through correct Flp-mediated integration into the cell genome. The pUC origin (pUC ori) allows high-copy number amplification in *E. coli*. The ampicillin resistance gene permits selection of transfectants in *E. coli* cells.

4.1.6 Bacteria

For plasmid amplification, the competent *Escherichia coli* (*E. coli*) strain JM109, purchased from Stratagene (San Diego, CA, USA), was used. The cultivation of bacteria was carried out in LB medium or on LB agar plates (Table 7) at 37 °C.

4.1.7 Cell lines

HEK-293 cells (Thermo Fisher Scientific, Waltham, USA), SVEC4-10 cells (American Type Culture Collection, Manassas, USA) and HL-60 cells (American Type Culture Collection, Manassas, USA) were grown in the respective medium listed in Table 12 supplemented with 10 % FBS and 100 U/mL penicillin/streptomycin and cultured at 37 °C and 5 % CO₂ in a humidified incubator. The adherent HEK-293 cells and SVEC4-10 were split 1:10 using trypsin/EDTA solution every 3 days to keep them in culture. HL-60 suspension cells were passaged by splitting 1:10 every 3 days. For storage, cells were frozen in culture medium containing 7.5 % DMSO and kept at -150 °C.

Table 12: Overview and description of cell lines

Cell line	Description	Culture medium
Flp-In T-Rex 293	Human embryonic kidney (HEK) cells containing a FRT site, which allows targeted integration of a Flp-In expression vector (pcDNA5/FRT/TO) leading to stable expression levels of the gene of interest.	DMEM
F20 Flp-In T-Rex 293	Human embryonic kidney cells containing the FRT site and the stably integrated F20-vector, which codes for a luciferase with a cAMP binding site and a G418 resistance.	DMEM
SVEC4-10	SV40 transformed murine endothelial cell line from axillary lymph node vessels.	RPMI-1640
HL-60	human promyelocytic leukemia cell line	RPMI-1640

4.1.8 Antibodies

Most of the antibodies listed in the following tables were purchased from eBioscience (San Diego, USA), BD Bioscience (San Jose, USA) or BioLegend (San Diego, USA).

Table 13: Murine FACS antibodies

Antigen	Clone	Conjugation	Dilution	Provider
ABCA1	polyclonal	AF405	1:100	Novus Biologicals, Littleton, USA
ABCG1	polyclonal	-	1:100	GeneTex, Irvine, USA
CD11a	2D7	PE/Cy7	1:500	BD Bioscience
CD11b	M1/70	PerCP	1:500	BioLegend
CD16/CD32	2.4G2	-	1:1000	BD Bioscience

MATERIALS AND METHODS

CD18	C71/16	FITC	1:500	BD Bioscience
CD31	390	PE/Cy7	1:400	BioLegend
CD36	HM36	PE	1:400	BioLegend
CD41	MWReg30	APC	1:400	eBioscience
CD45	30-F11	APCeFluor780	1:500	eBioscience
CD45.2	104	FITC	1:500	BD Bioscience
CD45.2	104	APC	1:500	BD Bioscience
CD49d	R1-2	PE	1:500	BioLegend
CD62l	MEL-14	FITC	1:400	BD Bioscience
CD62p	RMP-1	PE	1:100	BioLegend
CD107a	1D4B	BV421	1:100	BioLegend
CD115	AFS98	APC	1:500	eBioscience
Gr1	RB6-8C5	APCeFluor780	1:500	eBioscience
ICAM1	Yn1/1.7.4	APC	1:400	BioLegend
Ly6C	AL-21	PE/Cy7	1:500	BD Bioscience
Ly6G	1A8	PE	1:500	BD Bioscience
Ly6G	1A8	ACP/Cy7	1:500	BioLegend
Ly6G	1A8	FITC	1:500	BioLegend
PSGL1	2PH1	PerCP	1:3000	BD Bioscience
SR1	EPR7536	-	1:500	Abcam, Cambridge, UK
VCAM1	429	PerCP/Cy5.5	1:800	BioLegend

AF = AlexaFluor; ABC = ATP-binding cassette; APC = Allophycocyanin; BV = Brilliant violet; PE = Phycoerythrin; FITC = Fluorescein isothiocyanate; PerCP = Peridinin chlorophyll; Cy = Cyanine

Table 14: Human FACS antibody

Antigen	Clone	Source	Dilution	Provider
CD11/CD18 (LFA1)	mAb24	mouse	1:20	Hycult Biotech, Uden, Netherlands

mAb = Monoclonal antibody

Table 15: Antibodies for intravital microscopy

Antigen	Clone	Conjugation	Provider
CD11b	M1/70	eFluor 650NC	eBioscience
Ly6G	1A8	PE	BioLegend

NC = Nanocrystals

Table 16: Antibodies used for immunohistochemistry

Antigen	Clone	Source	Dilution	Provider
MAC2	M3/38	Rat	1:400	Cedarlane, Burlington, Kanada
α -SMA	1A4	Mouse	1:100	Dako Agilent Technologies, Santa Clara, USA

SMA = Smooth muscle actin

Table 17: Isotype controls

Immunoglobulin	Dilution	Provider
Normal rat IgG	1:160	Santa Cruz Biotechnology, Dallas, USA
Normal mouse IgG	1:500	Santa Cruz Biotechnology, Dallas, USA

IgG = Immunoglobulin G

Table 18: Secondary antibodies

Antibody	Source	Conjugation	Dilution	Provider
Anti-rabbit IgG	donkey	BV421	1:20	BioLegend
Anti-rabbit IgG	donkey	AF488	1:400	JIR Inc, West Grove, USA
Anti-mouse IgG	donkey	AF594	1:100	JIR Inc, West Grove, USA
Anti-rat IgG	goat	Biotin	1:100	Vector Laboratories, Burlingame, USA
F(ab)2-anti mouse IgG	goat	AF488	1:100	Invitrogen AG, Carlsbad, USA
Anti-human IgG Fc	goat	PE	1:500	eBioscience

JIR = Jackson ImmunoResearch

4.1.9 Enzymes and recombinant proteins

Table 19: Enzymes

Enzyme	Final concentration	Company
Collagenase IV	10 mg/mL	Worthington Biochemical Corp., Lakewood, USA
DNase I	20 U/mL	Roche, Basel, Switzerland
Thrombin	0.5 U/mL	Sigma-Aldrich Chemie GmbH, Munich, Germany
BamHI-HF	1 U/ μ L	New England Biolabs, Ipswich, USA
XhoI	1 U/ μ L	New England Biolabs, Ipswich, USA
T4 ligase	20 U/ μ L	New England Biolabs, Ipswich, USA
Taq Polymerase	0.05 U/ μ L	QIAGEN N.V, Hilden, Germany

HF = High fidelity

Table 20: Recombinant proteins

Protein	Final concentration	Company
TNF α	10 ng/mL	BioLegend, San Diego, CA, USA
Murine CCL5	5 μ g/mL	PeptoTech, Rocky Hill, NJ, USA
Humane CCL5	5 μ g/mL	AG von Hundelshausen, IPEK, LMU
ICAM1/Fc chimera	2.5 μ g/mL	R&D Systems Inc., Minneapolis, MN, USA
VCAM1/Fc chimera	2.5 μ g/mL	R&D Systems Inc., Minneapolis, MN, USA

4.1.10 Consumables

Table 21: Material

Material	Company
1.3 mL Citrate (3.2 %) micro tube	Sarstedt AG & Co, Nümbrecht, Germany
1.3 mL EDTA micro tubes	Sarstedt AG & Co, Nümbrecht, Germany
1.3 mL Serum Gel Z micro tubes	Sarstedt AG & Co, Nümbrecht, Germany
12-well polystyrene microplate	Corning Inc., NY, USA
384-well flat bottom microplate	Corning Inc., NY, USA
5 mL polystyrene tubes with cell strainer cap	BD Bioscience, San Jose, USA
70-µm cell strainer	BD Bioscience, San Jose, USA
96-well black clear bottom microplate	PerkinElmer Inc., Waltham, USA
96-well half area flat bottom microplate	Corning Inc., NY, USA
96-well white clear bottom microplate	PerkinElmer Inc., Waltham, USA
Disposable Capillaries (30-32 mm, 10 µL)	Hirschmann Laborgeräte GmbH, Eberstadt, Germany
Microlance needles (25 G, 26 G, 27 G)	B. Braun AG, Puchheim, Germany
PE-10 catheter	BD Bioscience, Franklin Lakes, NJ, USA
Qiagen TissueLyser steel beads	Qiagen, Hilden, Germany
Safety scalpel	B. Braun AG, Puchheim, Germany
Semi-skirted 96-well qPCR plates	VWR International, Radnor, USA
Superfrost Plus microscope slides	Menzel-Gläser GmbH, Braunschweig, Germany
Tissue-Tek cryomold	Sakura Finetek Germany GmbH, Staufen, Germany
White adhesive bottom seal	PerkinElmer Inc., Waltham, USA

4.1.11 Equipment

Table 22: Equipment

Equipment	Company
7900 HT Fast Real-Time PCR System	Applied Biosystems, Foster City, USA
Autoclave LTA 400	Zirbus technology GmbH, Bad Grund, Germany
Balance SE 203 LR	VWR International, Radnor, USA
Biorad Mini-Sub Cell GT Cell	Bio-Rad Laboratories GmbH, Munich, Germany
Centrifuges Centrifuge 5418 R Megafuge 1.0R	Eppendorf AG, Hamburg, Germany Heraeus, Hanau, Germany
CO ₂ incubator CB 160	BINDER GmbH, Tuttlingen, Germany
Cryotome CM3050S	Leica Biosystems, Wetzlar, Germany
FACS BD LSRFortessa 5L	BD Bioscience, San Jose, USA

FACS Canto II flow cytometer	BD Bioscience, San Jose, USA
Gel imager INTAS	Intas Science Imaging Instruments GmbH, Göttingen, Germany
Hood HERAsafe	Heraeus, Hanau, Germany
Laboratory pH Meter 766	Knick GmbH, Berlin, Germany
LifeSep Magnetic Plate Holder 96F	Sigma-Aldrich Chemie GmbH, Munich, Germany
Luminex MAGPIX Instrument	Luminex, Austin, USA
Tecan Infinite F200 PRO microplate reader	Tecan Group, Maennedorf, Switzerland
Microscopes	
LEICA DMi1	Leica Biosystems, Wetzlar, Germany
LEICA DMLB	Leica Biosystems, Wetzlar, Germany
LEICA DM6000	Leica Biosystems, Wetzlar, Germany
Olympus BX51	Olympus Corporation, Tokyo, Japan
Leica TCSII SP8 3X	Leica Biosystems, Wetzlar, Germany
Nanodrop ND1000 Peqlab	VWR International, Radnor, USA
PCR Plate Spinners	VWR International, Radnor, USA
PCR Thermocycler Biometra Tpersonal	Biometra GmbH, Göttingen, Germany
Power supply	Kyoritsu Electrical Instruments Works, Tokyo, Japan
Scil Vet ABC Hematology Analyzer	Scil Animal Care Company, USA
Thermomixer F1.5	Eppendorf AG, Hamburg, Germany
TissueLyser LT	Qiagen, Hilden, Germany
Vortex Mixer TX4	VELP Scientifica, Usmate, Italy
Water Purification System Milli-Q	Merck Millipore, Billerica, USA

4.1.12 Software

Table 23: Software

Software	Company
ApE (A plasmid Editor)	-
BD FACSDiva software	BD Bioscience, San Jose, USA
FlowJo v10.3	Tree Star, Inc., OR, USA
GraphPad Prism 7.00	GraphPad Software Inc, USA
Imaris 8.4	Bitplane AG, Zurich, Switzerland
LAS V4.3	Leica Biosystems, Wetzlar, Germany
Olympus Excellence software	Olympus Corporation, Tokyo, Japan
ProcartaPlex Analyst 1.0	Thermo Fisher Scientific, Waltham, USA
SDS2.4 Software	Applied Biosystems, Foster City, USA
xPONENT Software	Luminex, Austin, USA

4.2 Methods

4.2.1 Mouse model

4.2.1.1 Mice

Mice do not develop atherosclerosis spontaneously. Therefore, *ApoE*^{-/-} mice on C57Bl/6 background (stock No. 002052, The Jackson Laboratory, Bar Harbor, ME, USA)¹⁵⁸ were used as a mouse model to study atherosclerosis. To induce atherosclerosis, male mice at the age of 6-8 weeks were fed a HFD (Western type diet TD.88137: 0.21 % cholesterol and 21 % fat, ssniff Spezialdiäten GmbH; Soest, Germany) for different time periods as indicated in the particular experiment. For integrin activation assays, male C57Bl/6 wild type mice were purchased from Janvier Labs. For housing, care and breeding of mice institutional guidelines were followed. All animal experiments were approved by the local ethics committee (District Government of Upper Bavaria; License Number: 55.2-1-54-2532-111-13) and performed according to the national guidelines.

4.2.1.2 Mouse dissection

At the end of each experiment, mice were anesthetized by intraperitoneal (i.p.) injection with ketamine (80 mg/kg) and xylazine (12 mg/kg) using a 1 mL insulin syringe with a 30 G needle. Unless described otherwise, blood was obtained via cardiac puncture using a 26 G microlance needle flushed with 0.5 M EDTA into an EDTA micro tube. To remove remaining blood, mice were perfused with 10 mL of PBS and hearts, spleens and femurs were harvested. Aortas were dissected from the aortic arch to the iliac bifurcation. 20 µL of blood was used for leukocyte count and mean platelet volume (MPV) measurement with a hematology analyzer. Unless otherwise stated, plasma was obtained by centrifugation of EDTA-anticoagulated blood for 10 min at 2500 x g and stored at -80 °C until it was used for analysis. Hearts were frozen in tissue-tek and stored at -20 °C. Organs for RNA extraction were snap-frozen in liquid nitrogen. The organs which were used for flow cytometry analysis were placed in PBS on ice until processing.

4.2.1.3 Platelet 5-HT depletion via FLX treatment

To investigate the effect of platelet 5-HT depletion on atherogenesis, *ApoE*^{-/-} mice were treated with FLX (160 mg/L; Prozac, Lilly) via the drinking water⁷³ in parallel to HFD feeding for 2, 4 or 16 weeks (Figure 14A). As controls, mice received HFD only.

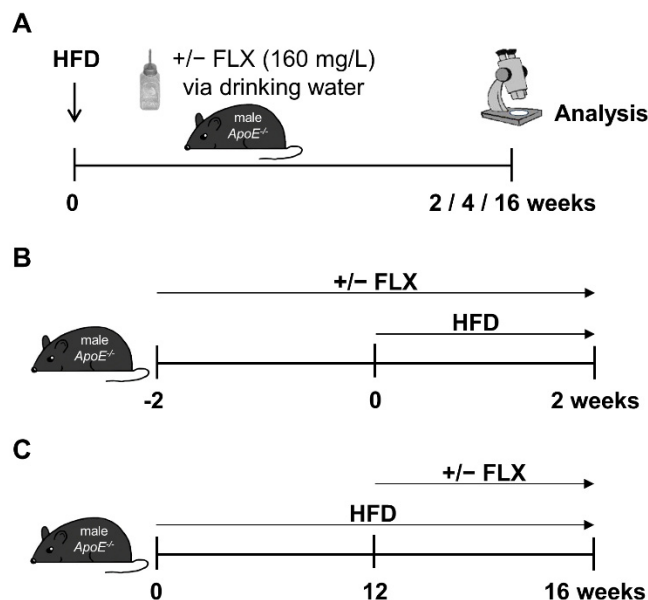


Figure 14: Experimental setups for platelet 5-HT depletion.

In one experiment, mice were pre-treated with FLX for 2 weeks before starting HFD feeding with continuous FLX treatment for 2 weeks (Figure 14B). To assess the effect of FLX on already established plaques, mice were fed a HFD for 16 weeks while receiving FLX treatment only in the last 4 weeks of HFD (Figure 14C). In one experiment, wild type C57Bl/6 mice were treated with FLX for 2 weeks.

4.2.1.4 Pharmacological peripheral 5-HT depletion via TPH1 inhibition

Pharmacological depletion of peripheral 5-HT was assessed via inhibition of the 5-HT-synthesizing enzyme TPH1. Here, *ApoE*^{-/-} mice, receiving a HFD for 2 or 4 weeks, were injected daily with the TPH1 inhibitor LP-533401 (25 mg/kg, i.p.; Dalton Pharma Services, Toronto, Canada) or vehicle (Figure 15).¹⁵⁹ LP-533401 was dissolved in DMSO and diluted in aqua ad injectabilia.

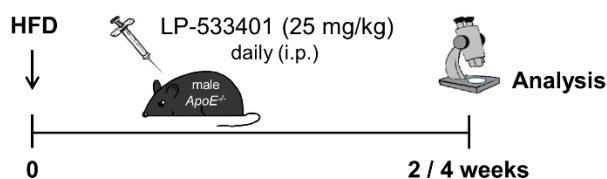


Figure 15: Experimental setup for pharmacological 5-HT depletion.

4.2.1.5 5-HTR1b antagonism

ApoE^{-/-} mice were injected every second day with the 5-HTR1b antagonist NAS-181 (3 mg/kg, i.p.; Tocris Bioscience, Bristol, United Kingdom) dissolved in PBS (Figure 16).¹⁶⁰ As control, an equal volume of PBS was administered.

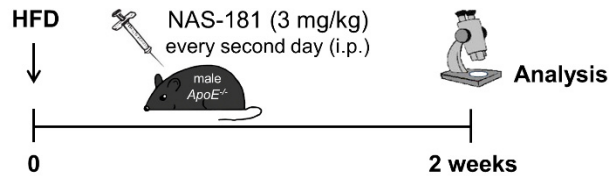


Figure 16: Experimental setup for antagonism of 5-HTR1b.

4.2.1.6 Induced peritonitis

An acute peritonitis was induced to elicit neutrophil extravasation into the peritoneal cavity. For this experiment, FLX-treated (2 weeks) and untreated mice on wild type background were injected with 1 mL sterile 4 % thioglycolate (Table 7) using a 27 G needle (Figure 17). Because the influx of neutrophil peaks 2 h after injection, mice were euthanized at that time point via cervical dislocation. The outer skin of the peritoneum was carefully removed to expose the inner skin. 5 mL of ice cold PBS containing 5 mM EDTA was injected into the peritoneal cavity using a 27 G needle, followed by a gentle massage of the peritoneum for 3 min. The fluid containing the peritoneal cells was collected using a 25 G needle and placed on ice. 4 mL of the peritoneal lavage was centrifuged (400 x g, 5 min, 4 °C) and resuspended in 500 µL PBS/EDTA. The amount of extravasated cells was determined using a hematology analyzer.

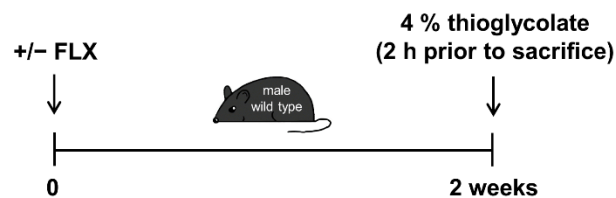


Figure 17: Experimental setup for induced peritonitis.

4.2.1.7 Intravital microscopy

Intravital microscopy of the left carotid artery was performed to examine leukocyte-endothelial interaction *in vivo* by fluorescence labeling of myeloid cells. To this end, control and FLX-treated mice receiving a HFD for 4 weeks were anesthetized with ketamine/xylazine and the right jugular vein was cannulated with a catheter for antibody injection. To stain myeloid cells, antibodies against CD11b and Ly6G were injected and allowed to circulate for 10 min before starting the imaging. Leukocyte-endothelial interactions were examined in exposed left carotid arteries by using an Olympus BX51 microscope. Rolling flux was defined as number of cells passing a reference line perpendicular to blood flow within 30 s, while adhesion was

determined as cells being static for at least 30 s. Image acquisition and analysis was accomplished with the Olympus cell software.¹⁶¹

4.2.1.8 *In vivo* permeability assay

ApoE^{-/-} mice fed a HFD for 2 weeks with or without FLX treatment were injected intravenously (i.v.) with 0.5 % Evans blue solution in 0.9 % saline (40 mg/kg). After 30 min, mice were anesthetized with ketamine/xylazine followed by perfusion with PBS. Hearts, spleens and kidneys were collected, air dried and weighted. Dried organs were incubated with 450 μ L formamide at 56 °C for 24 h for Evans blue extraction.¹⁶² The optical density (OD) of the extracted dye was measured at 620 nm in supernatants using a Tecan Infinite F200 PRO microplate reader. Vascular permeability was defined as ng of Evans blue extravasated per mg tissue using a standard curve of Evans blue in formamide as reference. Vascular leakage in aortic arches was determined by confocal laser scanning microscopy. After dissection, aortic arches were fixed in 4 % paraformaldehyde solution, mounted in PBS on microscopy slides followed by imaging with a Leica TCSII SP8 3X. Whole arches were acquired as a tilescan of 775x775x120-200 μ m xyz stacks. Evans blue was excited with a continuous white-light laser tuned at 580 nm and the emitted fluorescence was collected in the 660-720 nm range. Tilescan volumes were reconstructed and processed using Imaris 8.4. Z-sectioning allowed to remove the external adventitial layer and to expose the underneath Evans blue-positive signal of the endothelium, which was calculated as a volume after application of an ad-hoc mask.

4.2.2 Lipid analysis

4.2.2.1 Plasma cholesterol measurement

Total plasma cholesterol levels were quantified using a colorimetric assay (CHOD-PAP, Roche). Plasma samples were diluted 1:9 with 0.9 % saline. The calibrator was dissolved in 3 mL dH₂O (cholesterol concentration: 160 mg/dL) and standard curve was prepared by serial dilution (undiluted, 1:2, 1:4, 1:8, 1:16) in 0.9 % saline. 5 μ L of each standard and the diluted plasma samples were pipetted in duplicates in a flat bottom 96-well microtiter plate. To increase the range of the assay, 10 μ L of the undiluted standard was also included to the standard curve. 200 μ L of CHOD-PAP CHOL reagent was added and after 30 min incubation at room temperature (RT) absorbance was measured at 450 nm with a Tecan Infinite F200 PRO microplate reader.

4.2.2.2 Lipid analysis of blood leukocytes

Neutral lipid content in circulating cells was measured with the Amplex Red Cholesterol Assay kit (Invitrogen)¹⁶³ and determined as ratio of esterified to total cholesterol. After erythrocyte lysis in ACK lysis buffer (Table 7), cells were washed with cold PBS, resuspended in cold 1x reaction buffer provided by the kit and incubated on ice for 1 h for cell lysis. To degrade

endogenous esterases, samples were heated at 60 °C for 30 min, followed by shaking for 30 min at RT. For measuring total and esterified cholesterol, the assay was performed according to the manufacturer's protocol with and without esterase.

4.2.3 Enzyme-linked immunosorbent assay (ELISA)

ELISAs were performed to quantify the concentration of 5-HT or different cytokines in murine serum, plasma or platelet supernatant.

4.2.3.1 5-HT ELISA

5-HT levels were quantified in serum and plasma. Therefore, blood was taken retro-orbitally using a glass capillary. To verify platelet 5-HT depletion, 5-HT levels were measured in serum. For this purpose, blood was collected in Serum Gel Z tubes and allowed to clot for 30 min at RT. Plasma was obtained by collecting blood in EDTA tubes containing 1 µM prostaglandin E1 to avoid platelet activation. Blood was centrifuged at 1000 x g for 10 min, followed by 16,000 x g for 1 min and stored at -80 °C until usage. 5-HT concentrations were measured using the competitive Serotonin Fast Track ELISA kit (Labordiagnostika Nord) according to the manufacturer's instructions. Briefly, 5-HT was acylated to 5-HIAA by adding 25 µL sample, standards or controls to 500 µL acylation buffer containing 25 µL acylation reagent followed by incubation at RT for 15 min. 25 µL of the acylated samples, standards and controls were pipetted in duplicates on the 5-HIAA pre-coated 96-well plate provided by the kit, 100 µL of 5-HT antiserum was added and the plate was incubated for 1 h at RT. Thereby, free 5-HIAA was competing with the bound 5-HIAA for antiserum binding sites. During washing, the free 5-HIAA and 5-HIAA-antiserum complexes were removed leading to lesser antiserum binding to the solid phase in samples originally containing higher 5-HT amounts. 100 µL anti-rabbit-IgG conjugated with HRP was added and incubated for 15 min at RT. After washing, 100 µL tetramethylbenzidine substrate was incubated for 15 min at RT and subsequently stopped by adding 100 µL of stopping solution. The HRP-mediated substrate conversion was analyzed with a Tecan Infinite F200 PRO microplate reader at 450 nm (reference wavelength: 650 nm). 5-HT sample concentrations were determined by interpolation of the standard curve, obtained by plotting the absorbance readings against the corresponding standard concentrations using a non-linear regression (two-phase decay) for curve fitting.

4.2.3.2 CXCL4 and CCL5 ELISA

CXCL4 and CCL5 concentrations in serum and/or supernatant of activated platelets (4.3.3.1) were assessed with the DuoSet ELISA kits (R&D systems) according to the manufacturer's protocol with slight alterations. To increase the sensitivity of the ELISA, the concentration of detection and capture antibodies were doubled. CXCL4 was measured in a 384-well plate, while CCL5 was determined in a 96-well half area plate, therefore half the reagent volumes were applied. The plate was coated with 50 µL capture antibody overnight at 4 °C. After

washing, blocking was performed with reagent diluent at RT for 1 h. 50 μ L murine serum sample (for CXCL4: pre-diluted 1:1000; for CCL5: undiluted) or supernatant of stimulated platelets (for CXCL4: pre-diluted 1:1000) was added to the plate and incubated at RT for 2 h, followed by 2-hour incubation with 50 μ L biotinylated detection antibody. After washing, 50 μ L streptavidin-HRP was added and incubated for 20 min at RT. Afterwards the plate was washed again and 50 μ L of substrate solution was added followed by an incubation for 20 min in the dark. Subsequently 25 μ L stop solution was added and the OD at 450 nm (reference wavelength: 550 nm) was determined with a Tecan Infinite F200 PRO microplate reader. Sample values were interpolated in the standard curve generated by nonlinear regression (fourth order polynomial) curve fitting using GraphPad Prism 7.00.

4.2.3.3 Multiplex immunoassay

Multiple cytokine analysis in murine plasma was assessed using the ProcartaPlex ELISA-like immunoassay based on the Luminex xMAP technology (eBioscience). This procedure enabled the simultaneous measurement of the following 26 cytokines in plasma: IFN γ , IL12p70, IL13, IL1 β , IL2, IL4, IL5, IL6, TNF α , GM-CSF, IL18, IL10, IL17A, IL22, IL23, IL27, IL9, CXCL1, CXCL2, CXCL10, CCL2, CCL3, CCL4, CCL5, CCL7, CCL11. The assay was performed according to the manufacturer's protocol with slight modifications. Briefly, 25 μ L analyte-specific magnetic capture beads coated with target-specific capture antibodies were pipetted to the 96-well plate provided by the kit and washed using a magnetic plate holder. 25 μ L plasma sample, which was recentrifuged at 10000 x g for 10 min at 4 °C to minimize lipids, was added to the plate together with 25 μ L universal buffer and incubated at 500 rpm for 120 min at RT. After washing, 12.5 μ L of the biotinylated analyte-specific detection antibody mix was added and incubated with shaking at 500 rpm for 30 min at RT, followed by washing and incubation with 25 μ L PE conjugated streptavidin at 500 rpm for 30 min at RT in the dark. Subsequently, 120 μ L reading buffer was added after washing and samples were measured with Luminex MAGPIX Instrument controlled by the xPonent Software. Data analysis was carried out with the ProcartaPlex Analyst software.

4.3 Histology and immunohistochemistry

After perfusion with PBS, hearts were kept in PBS on ice until freezing. The heart base including the valve level was collected by transverse sectioning and placed in a cryomold containing OCT. For freezing, the bottom part of the cryomold was exposed to 2-methylbutane, which was cooled by liquid nitrogen. Frozen blocks were stored in airtight closed bags at -20 °C until further processing. Using a Cryotome CM3050S, 5 μ m-thick serial sections were collected starting from the onset of the three aortic valves until they disappeared. Usually ten object slides containing eight serial sections were collected reflecting an area of 400 μ m. Half

of the sections were fixed in 4 % Roti-Histofix for 10 min and stored at RT, unfixed sections were kept at -20 °C.

4.3.1.1 Oil Red O staining

To analyze the size of the atherosclerotic plaque, serial sections of aortic roots were stained with Oil Red O (ORO). To remove OCT, fixed sections were incubated in PBS for 5 min. After 10-times dipping in 60 % 2-propanol, sections were stained for 15 min with freshly prepared ORO staining solution: 120 mL ORO stock solution (Table 7) diluted with 80 mL ddH₂O and filtered after 1 h stirring. To remove surplus ORO, slides were dipped 10-times in 60 % 2-propanol and rinsed for 5 min in tap water. Sections were counterstained with Hematoxylin solution for 3 min followed by rinsing for 5 min in tap water and subsequently embedding with Immu-Mount. Five sections per heart were utilized for plaque analysis using the LAS V4.3 software. Plaque size was normalized to the circumference of the internal elastic lamina (IEL).

4.3.1.2 Sirius Red staining

The collagen content in the plaque was determined via Sirius Red staining. Cryosections were incubated in PBS for 5 min, subsequently stained with 0.1 % Sirius Red solution (Table 7) at RT for 1 h, followed by differentiation in 0.01 M HCl for 2 min. After dehydration according to an ascending ethanol series (Table 24), sections were embedded with DPX Mountant.

Table 24: Dehydration protocol

Solution	Time
H ₂ O	4x dipping
70 % Ethanol	4x dipping
96 % Ethanol	4x dipping
100 % Ethanol	4x dipping
100 % Ethanol	4x dipping
Xylene	2 min
Xylene	2 min

Sirius Red positive area was detected based on a threshold and analyzed with the LAS V4.3 software as total collagen content or normalized to total plaque area.

4.3.1.3 Immunohistochemistry

4.3.1.3.1 Macrophage staining

To analyze the macrophage content within the plaque, aortic roots were stained with MAC2 (Table 16). Fixed sections were incubated in PBS for 5 min followed by antigen retrieval in citrate buffer (Table 7). The citrate buffer was heated until boiling using a microwave. Sections were added and the buffer was reheated for additional 10 min at 90 watts. Subsequently,

sections were washed two times with PBS for 5 min, followed by blocking with blocking buffer (Table 7) containing 10 % goat serum for 30 min. Sections were stained with the primary antibody MAC2 diluted in blocking buffer containing 1 % goat serum overnight at 4 °C in a moist chamber. As isotype control, sections were incubated with the same concentration of normal rat IgG (Table 17). The primary antibody binding was detected via alkaline phosphatase enzyme detection system using the VECTASTAIN ABC-AP staining kit (Vector Laboratories). Therefore, sections were washed three times with PBS for 5 min, followed by incubation with a biotinylated secondary anti-rat antibody (Table 18) for 45 min at RT in the dark. After washing, sections were incubated for 30 min with the ABC-AP working solution, which was prepared according to the manufacturer's instructions and pre-incubated for 30 min at RT before use. Sections were washed three times with PBS for 5 min, one drop of substrate solution, which was prepared according to the manufacturer's instructions of the VECTOR Red AP Substrate kit (Vector Laboratories), was added to each section, followed by incubation for 20 min in the dark. The reaction was stopped by washing with water for 5 min in the dark. After counterstaining with hematoxylin solution for 3 min, sections were rinsed with tap water and mounted with Immu-Mount. Macrophage content was quantified with the LAS V4.3 software based on a threshold analysis as total MAC2-positive content or normalized to total plaque size.

4.3.1.3.2 Smooth muscle cell staining

To analyze the content of SMCs in the plaque, aortic roots were stained with an antibody against α -SMA (Table 16). Therefore, antigen retrieval, blocking and primary antibody staining was carried out as described above (4.3.1.3.1). As control, normal IgG mouse (Table 17) was used. After washing, sections were incubated with the secondary anti-mouse AF594 (Table 18) for 45 min at RT in the dark. At the end of the incubation time one drop of hoechst (1:1500 diluted in PBS) was added for 2 min to stain the nuclei. After washing for three times with PBS, sections were mounted with Immu-Mount and stored in the dark at 4 °C. Images were recorded with the Leica DM6000 microscope. SMC content was analyzed with the LAS V4.3 software based on a threshold analysis and quantified as total α -SMA-positive area or normalized to total plaque area.

4.3.2 Flow cytometry

Flow cytometry analysis was applied for cell counting and protein expression analysis based on labeling with fluorescent antibodies (Table 13). Fc receptors on cells were blocked by resuspending cells in 50 μ L FACS buffer (Table 7) containing an anti-CD16/CD32 antibody and incubating for 5 min at RT. 50 μ L antibody master mix prepared in FACS buffer was added and incubated for 30 min at 4 °C in the dark. After washing, cells were resuspended in 300 μ L FACS buffer and acquired with the BD FACSDiva software on a BD FACS Canto II flow

cytometer. Data was analyzed using FlowJo v10.2 software. Protein expression was determined via geometric mean fluorescence intensity (MFI). For total cell counts, acquisition volumes were determined. To this end, a standard curve was generated by acquiring a solution of CountBright absolute counting beads for various time periods under low, medium and high flow rate at the BD FACS Canto II. The resuspension of samples in a defined volume and the acquisition with a certain flow rate and time enabled the calculation of total cell counts.

4.3.2.1 Determination of leukocyte counts in bone marrow and spleen

Total leukocyte counts of spleen and bone marrow were assessed by flow cytometry. To obtain splenic single cell suspensions, harvested spleens were meshed through a 70 µm cell strainer. For erythrocytes lysis, pellets were resuspended in 1 mL ACK buffer (Table 7) and incubated on ice for 5 min. Bone marrow cells were obtained from femurs, which were positioned in a cut 1 mL pipette tip placed in a 2 mL tube and centrifuged for 2 min at 9000 x g. Tips were discarded and pellets were resuspended in ACK buffer for lysis of erythrocytes. After washing and Fc-blocking, cells were stained with fluorochrome-conjugated anti-CD45.2-FITC, anti-CD11b-PerCP, anti-Ly6G-PE, anti-CD115-APC and anti-Ly6C-PE/Cy7 antibodies at 4 °C for 30 min. Myeloid cells were identified as CD45⁺ CD11b⁺, neutrophils as CD45⁺CD11b⁺Ly6G⁺ and classical monocytes as CD45⁺CD11b⁺CD115⁺Ly6C^{high}. Total cell counts were calculated using the CountBright absolute counting beads curve.

4.3.2.2 Protein expression on arterial endothelial cells and leukocytes

For staining of aortic endothelial cells, PBS-flushed aortas were digested with 500 µL aortic digestion cocktail (Table 7) containing collagenase IV and DNase I (Table 19) at 750 rpm for 40 min at 37 °C as previously described.¹⁶⁴ Digested aortic tissues were filtered through a 35 µm cell strainer. After washing, cells were incubated with Fc block followed by staining with anti-CD45-APCeFluor780 anti-CD31-PE/Cy7, anti-CD107a-BV421, anti-ICAM1-APC and anti-VCAM1-PerCP/Cy5.5 antibodies. Aortic endothelial cells were defined as CD45⁺CD31⁺CD107a⁺.

For measurement of adhesion molecule expression and lipid transporters on blood leukocytes, 50 µL blood was erythylsed for 10 min on ice followed by Fc-blocking. Subsequently adhesion molecules were stained with anti-CD11b-PerCP, anti-CD11a-PE/Cy7, anti-CD18-FITC, anti-CD49d-PE, anti-PSGL1-PerCP, anti-CD62L-FITC and anti-CD31-PE/Cy7 antibodies. Lipid transporters were stained with anti-CD36-PE, anti-SRI (+anti-rabbit BV421), anti-ABCA1-AF405, anti-ABCG1 (+anti-rabbit AF488) antibodies.

4.3.2.3 Assessment of platelet-leukocyte aggregates

For assessment of circulating PLAs in mice, blood was carefully taken via cardiac puncture using a 26 G needle and a syringe containing 100 µL ACD buffer (Table 7). 150 µL blood was

added to 1 mL RBC Lysis/Fixation Solution (BioLegend) and incubated for 15 min at RT. After washing, cells were resuspended in Fc block followed by staining with anti-CD45.2-FITC, anti-CD11b-PerCP, anti-Ly6G-APC/Cy7, anti-CD115-PE and anti-CD41-APC antibodies for 20 min at RT. After washing, cells were resuspended in 300 μ L FACS buffer (Table 7) and acquired for 5 min at low flow rate. Particular care was taken to use a low acquisition speed, since it was reported that a high flow rate leads to false-positive PLA counts.¹⁶⁵ PLAs were identified as leukocytes positive for the platelet marker CD41.

4.3.3 Murine cell isolation

4.3.3.1 Platelet isolation and *in vitro* stimulation

For murine platelet isolation, blood was carefully taken by heart puncture using a 26 G needle and a syringe containing 100 μ L ACD buffer (Table 7) and transferred into a citrate micro tube. Blood was centrifuged at 100 x g for 10 min at RT without break. The obtained platelet-rich plasma was diluted 1:2 with PBS and centrifuged again at 100 x g for 10 min at RT without break. After 1:2 dilution with pre-warmed ACD buffer, platelets were obtained by centrifugation at 2600 x g for 5 min at RT, resuspended in 300 μ L pre-warmed tyrode buffer (Table 7) and counted using a hematology analyzer.

For *in vitro* activation, 2×10^8 platelets/mL were stimulated with 0.5 U/mL thrombin (Table 19) for 20 min at 37 °C. After centrifugation at 2600 x g for 5 min at 4 °C, supernatants were collected for CXCL4 ELISA (4.2.3.2). Platelet activation was verified by anti-CD62P-PE antibody staining using flow cytometry analysis of geometric MFI.

4.3.3.2 Isolation of monocytes and neutrophils from bone marrow

To analyze messenger RNA (mRNA) levels of 5-HTRs in myeloid cells, neutrophils and monocytes were isolated from femurs of *ApoE*^{-/-} mice. Therefore, femurs were centrifuged for 2 min at 9000 x g, followed by erythrocyte lysis with ACK buffer (Table 7). After washing, bone marrow cells of three mice were pooled and filtered through a 70 μ m cell strainer to obtain single cell suspensions. Neutrophils and monocytes were isolated by negative selection using a mouse Neutrophil/Monocyte Isolation kit (Miltenyi Biotec GmbH) followed by the manufacturer's protocol. The obtained purity of neutrophils and monocytes was verified using FACS analysis (4.3.2). Isolated neutrophils and monocytes were pelleted and RNA was extracted (4.3.4.1).

4.3.4 Biomolecular methods

4.3.4.1 RNA isolation

Total RNA was extracted from murine tissues or isolated cells. If not directly processed, samples were snap-frozen in a 2 mL microcentrifuge tube and stored at -80 °C until RNA extraction. Lysis of isolated cells was performed by up- and down-pipetting in 500 μ L of

peqGOLD TriFast. For tissue lysis, Qiagen TissueLyser steel beads and 500 µL of peqGOLD TriFast were added to the frozen tissue and the lysis was accomplished using a TissueLyser (2 min; 50 Hz). Subsequently, lysates were centrifuged at maximal speed for 2 min and transferred to a new microcentrifuge tube. 100 µL of chloroform was added and the tube was shaken for 30 s followed by an incubation for 5 min at RT. Centrifugation at 12000 x g for 5 min at RT led to a separation into three phases: the lower red phenol-chloroform phase carrying proteins, the interphase reflecting the genomic DNA and the colorless upper aqueous phase bearing RNA. The latter was transferred into a new tube without touching the interphase to avoid contamination through genomic DNA. The RNA extraction was proceeded with the peqGOLD Total RNA Kit (Peqlab Biotechnologie) according to the manufacturer instructions. The RNA yield and purity was determined with a Nanodrop 100.

4.3.4.2 Reverse transcription

1 µg of the extracted RNA was transcribed into complementary DNA (cDNA) using the PrimeScript RT reagent kit (TaKaRa). The reverse transcription (RT) reaction mix was pipetted according to Table 25.

Table 25: RT reaction mix

Reagent	Amount
RNA	1 µg
5x PrimeScript Buffer	2 µL
PrimeScript RT Enzyme mix I	0,5 µL
Oligo dt Primer (50 µM)	0,5 µL
Random6mers (100 µM)	2 µL
RNase-free H ₂ O	ad 10 µL

RNase = Ribonuclease

The RT was carried out in a PCR Thermocycler using the program shown in Table 26. The transcribed cDNA was diluted with RNase-free H₂O to obtain a cDNA concentration of 5 ng/mL.

Table 26: RT program

Temperature	Time
37 °C	15 min
85 °C	5 s
4 °C	∞

4.3.4.3 Quantitative real-time PCR (TaqMan)

To analyze changes in gene expression in samples of different groups, a quantitative real-time PCR using the TaqMan technology was performed with the the KAPA PROBE FAST Universal qPCR kit (Peqlab Biotechnologie). For amplification of specific genes, primers and probes were either self-designed and purchased from MWG or bought as pre-designed primer-probe mixes from Life Technolgies (Table 9).

Table 27: Primer-probe mix

Self-designed 4x primer-probe mix		Pre-designed 4x primer-probe mix	
Primer fwd (100 μM)	4 μL	Primer-probe-Mix	0.5 μL
Primer rev (100 μM)	4 μL	Nuclease-free H ₂ O	Ad 5 μL
Probe (100 μM)	1 μL		
Nuclease-free H ₂ O	ad 250 μL		

After preparing a 4x primer-probe mix as shown in Table 27, the qPCR mix was pipetted according to Table 28.

Table 28: qPCR reaction mix

Reagent	Amount
Master mix 2x	10 μL
Primer-probe mix	5 μL
Reference dye high	0.4 μL
cDNA (5 ng/mL)	4.6 μL

As negative control, nuclease-free H₂O was used instead of cDNA. Samples were pipetted in duplicates on a semi-skirted 96-well qPCR plate and the qPCR was carried out on a 7900HT Sequence Detection System using the qPCR FAST program:

Table 29: qPCR FAST program

Temperature	Time	
95 °C	20 s	} 40 cycles
95 °C	1 s	
60 °C	20 s	

The analysis was accomplished via SDS2.4 Software. As endogenous control *Hypoxanthin-Guanin-Phosphoribosyltransferase (Hprt)* was utilized. For the comparison of gene expression in isolated monocytes and neutrophils a second housekeeping gene *Glycerinaldehyd-3-phosphat-Dehydrogenase (Gapdh)* was used. Target gene expression was normalized to the endogenous control and presented as fold change calculated according to the following equations:

$$dCt = Ct(\text{gene of interest}) - Ct(\text{endogenous control})$$

$$ddCt = dCt(\text{treated}) - \text{average } dCt(\text{untreated})$$

$$\text{fold change} = 2^{-ddCt}$$

4.3.5 Generation of a 5-HTR2a-overexpressing cell line

To investigate the signaling of 5-HTR2a, a Flp-In T-Rex-293 cell line overexpressing the receptor was generated. First, the coding sequence was cloned into a pcDNA5/FRT/TO expression vector, N-terminally flanked with the coding sequence for eYFP (Figure 13).

Second, Flp-In T-Rex 293 cells (Table 12) were transfected with the plasmid and stable clones were generated.

4.3.5.1 Restriction digest

The plasmid harboring the human coding sequence of *5-HTR2a* between BamHI (5') and XhoI (3') restriction sites was purchased from cDNA Resource Center. To clone the *5-HTR2a* sequence in the expression vector of interest, the purchased plasmid and the vector containing the backbone were digested with XhoI and BamHI-HF (Table 19) according to the protocol listed in Table 30. The digest was performed at 37 °C for 1 h:

Table 30: Digestion mix

Reagent	Amount
Plasmid/PCR product	10 µg/10 µL
CutSmart 10x buffer	2 µL
BamHI-HF	1 µL
XhoI	1 µL
H ₂ O	ad 20 µL

4.3.5.2 Agarose gel electrophoresis and gel extraction

To separate DNA fragments, digested plasmids were loaded on a 1 % agarose gel. Therefore, 1 g of agarose was dissolved in 100 mL 1x TAE buffer (Table 7) by heating. After cooling, 14 µL of ethidium bromide solution (Table 7) was added and directly poured into a tray. The polymerized gel was covered with TAE buffer and the digested plasmids supplemented with the corresponding amount of 6x loading dye were loaded next to a 1 kb DNA ladder. After running the gel with 180 V for 20 min using an electrophoresis power supply (Kyoritsu), it was visualized with the Gel imager INTAS. The DNA fragments of interest were cut out and purified via the QIAquick Gel Extraction kit (Qiagen) following the manufacturer's instructions.

4.3.5.3 Ligation

The ligation reaction mix was pipetted according to Table 31 and incubated at 16 °C for 1 h.

Table 31: Ligation reaction mix

Reagent	Amount
Digested vector DNA	1 µL
Digested insert DNA	5 µL
T4 Ligase 10x Buffer	1 µL
T4 Ligase	1 µL
H ₂ O	ad 10 µL

4.3.5.4 Bacterial transformation

For plasmid amplification a bacterial transformation was performed. Therefore, 50 μL JM109 competent bacteria cells (4.1.6) were thawed on ice, mixed with 5 μL ligation reaction mix and incubated on ice for 30 min. After performing a heat shock at 42 °C for 30 s, cells were incubated for another 1.5 min on ice. 110 μL of pre-warmed S.O.C. medium was added, the mixture was shaken at 37 °C for 1 h, plated on an LB agar plate (Table 7) and incubated at 37 °C overnight.

4.3.5.5 Colony PCR

Single cell colonies were screened for insert incorporation by performing a colony PCR. A single clone was picked with a tip and dipped into the reaction mix, which was pipetted according to Table 32.

Table 32: Colony PCR mix

Reagent	Amount
CoralLoad 10x	1.5 μL
Q-solution 5x	3.0 μL
CMV fwd (10 μM)	0.75 μL
5-HTR2a rev (10 μM)	0.75 μL
dNTPs (10 mM)	0.3 μL
Taq Polymerase	0.15 μL
H ₂ O	ad 15 μL

The PCR reaction was carried out with the colony PCR program (Table 33) in a PCR Thermocycler. The whole reaction mix was loaded on a 1 % agarose gel (4.3.5.2), to verify the size of the amplified DNA fragment.

Table 33: Colony PCR program

Temperature	Time	
94 °C	180 s	
94 °C	60 s	} 25 cycles
55 °C	30 s	
72 °C	90 s	
72 °C	10 min	
4 °C	∞	

4.3.5.6 Plasmid amplification and purification

Clones positively tested for insert incorporation via colony PCR (4.3.5.5) were used to inoculate 5 mL of LB medium (Table 7) supplemented with 10 μL ampicillin. The bacterial cultures were incubated at 37 °C overnight. After pelleting, plasmid DNA isolation and purification was

performed using the QIAprep Spin Miniprep Kit (Qiagen) according to the manufacturer's instructions. The DNA concentration was measured with a Nanodrop 100.

4.3.5.7 Sequencing

To verify the sequence of the inserted fragment, the plasmid was sent for sequencing of DNA to Eurofins MWG Operon (Ebersberg, Germany). The sequence was verified by alignment with the NCBI reference sequence using the software program ApE.

4.3.5.8 Cell transfection

For stable and inducible expression of the eYFP-5-HTR2a construct, Flp-In T-Rex 293 cells (Table 12) were transfected with the pcDNA5/FRT/TO plasmid harboring the gene of interest downstream of a hybrid human CMV/TetO2 promoter (Table 11, Figure 13). The Flp-In T-Rex 293 cell line comprises a FRT site, which allows site directed construct integration. Co-transfection of the pOG44 plasmid (Table 11) carrying the Flp recombinase and the pcDNA5/FTR/TO vector containing the gene of interest, results in homologous recombination between the FRT sites in pcDNA5/FRT/TO and on the Flp-In T-Rex 293 cells chromosome. Only correct insertion into the FRT sites brings the ATG initiation codon and the SV40 promoter into frame leading to expression of the hygromycin resistance gene. Thus, cells containing a correctly integrated *eYFP-5-HTR2a* construct can be selected by hygromycin.

Flp-In T-Rex 293 cells were seeded in a 12-well plate. Upon reaching 90 % confluence, 0.4 µg vector DNA and 1.6 µg pOG44 plasmid DNA were added to 50 µL DMEM without FBS. The plasmid solution was mixed with 50 µL DMEM supplemented with 4 µL EcoTransFect and incubated at RT for 15 min to allow complex formation. Directly before cell transfection, the old medium was replaced by 1 mL fresh culturing medium. Then, the transfection solution was carefully added to the medium. After 24 h, cells were transferred into a 10-cm dish using trypsin/EDTA solution. Upon reaching 70 % to 80 % confluence, culture medium was changed and supplemented with hygromycin (0.25 mg/mL) for selection. After 2 to 3 days, medium was changed to discard dead cells. Once single cell colonies were formed, at least three different clones were transferred to a 12-well plate and further cultured with culture medium supplemented with hygromycin. Clones of the newly established cell line were verified for 5-*HTR2a* expression after tetracycline induction by measuring eYFP levels using flow cytometry and microscopy.

4.3.6 Cell-based *in vitro* assays

4.3.6.1 Calcium assay

Changes in intracellular calcium concentrations upon stimulation of 5-HTR2a overexpressing HEK-293 cells were assessed with the FLPR Calcium 5 Assay kit (Molecular Devices) following the manufacturer's protocol. Cells were seeded in a black 96-well microplate with a clear

bottom with 100 μ L DMEM supplemented with 10 % FBS, 100 U/mL penicillin/streptomycin and 2 % poly-D-lysine. *5-HTR2a* expression was induced by adding 100 μ L culture medium containing tetracycline (final concentration in the well: 0.5 μ g/mL) and cells were incubated at 37 °C for 48 h (80 % confluence). After washing with HBSS, 100 μ L of HBSS was added to each well together with 100 μ L loading buffer and incubated for 1 h at 37 °C. Fluorescence of the calcium sensitive dye (excitation: 485 nm, emission 525 nm) was measured at 37 °C with a Tecan Infinite F200 PRO microplate reader. First, basal levels were determined followed by measurement after ligand stimulation. Relative light units were normalized to basal level and displayed as x-fold over basal level.

4.3.6.2 GloSensor cAMP assay

To assess the signaling of $G\alpha_{i/o}$ coupled receptors, cAMP was measured using the GloSensor cAMP assay from Promega. This technology enables a luciferase-based biosensors for real-time detection of intracellular cAMP changes. The GloSensor luciferase has a binding site for cAMP. Upon cAMP binding a conformational change in the luciferase occurs, leading to an increase in luminescence activity directly proportional to the amount of cAMP. The signaling of the two G protein $G\alpha_{i/o}$ -coupled receptors CCR1 and CCR5 upon CCL5 stimulation was assessed by the observed reduction of a cAMP signal generated by forskolin, a direct activator of adenylyl cyclases.

F20 Flp-In T-Rex 293 cells (Table 12), expressing CCR1 or CCR5 in addition to the GloSensor luciferase, were seeded in white 96-well microplate with a clear bottom with 100 μ L culture medium supplemented with 4 % poly-D-lysine. To induce the receptor expression, 1 μ g/mL tetracycline (final concentration in the well: 0.5 μ g/mL) was added in 100 μ L culture medium and the cells were incubated at 37 °C for at least 48 h until reaching 100 % confluence. Cells were washed with HBSS/HEPES buffer (Table 7) and 2.5 % (v/v) of Luciferin-EF (Promega) was added in 67.5 μ L HBSS/HEPES buffer followed by incubation in the dark for 1.5 h at RT. The clear bottom was covered with a white adhesive bottom seal and the basal glow luminescence was measured with a Tecan Infinite F200 PRO microplate reader at 25 °C for 19 cycles. Afterwards, 7.5 μ L FLX was added per well and possible changes in intracellular cAMP levels were assessed for 7 cycles (15 min) followed by addition of CCL5 and measurement for additional 19 cycles. 1 μ M forskolin was added to each well and the increasing cAMP levels were followed for 15 cycles. Relative light units were normalized to basal level.

4.3.6.3 Stimulation of SVEC4-10 cells

ICAM1 and VCAM1 protein levels on endothelial cells upon stimulation were assessed by flow cytometry (4.3.2) using the murine endothelial cell line SVEC4-10 (Table 12). Therefore, cells were seeded in RPMI-1640 supplemented with 10 % FBS and 100 U/mL penicillin/strepto-

mycin in a 12-well microplate and grown until reaching confluence. Cells were stimulated with different concentrations of 5-HT or FLX in serum-free medium for 15 min, followed by activation with TNF α (10 ng/mL) for 6 h. After washing with PBS, cells were stained with anti-ICAM1-APC and anti-VCAM1-PerCP/Cy5.5 antibodies (Table 13) in FACS buffer (Table 7) at 4 °C in the dark for 15 min. After washing, cells were resuspended in 300 μ L FACS buffer and acquired at a BD FACS Canto II. Protein expression levels were calculation via geometric MFI.

4.3.6.4 Integrin activation assay

4.3.6.4.1 Murine ICAM1/VCAM1 binding assay

Integrin activity was assessed in the murine system by measuring ICAM1 and VCAM1 binding to blood leukocytes.¹⁶¹ Therefore, murine blood was taken carefully by cardiac puncture. All incubation and centrifugation steps were performed at RT. 50 μ L blood was added to 3 mL ACK buffer (Table 7) for lysis of erythrocytes and incubated for 15 min. After addition of 1 mL integrin assay buffer (Table 7), cells were centrifuged at 300 x g for 5 min, followed by an additional washing step. Cells were resuspended in 100 μ L recombinant ICAM1/Fc chimera or VCAM1/Fc chimera (Table 20), which were pre-labeled with an anti-human IgG1-PE antibody (Table 18) by 5 min incubation. 5-HT (1 μ M), FLX (1 μ M) or escitalopram (0.1 μ M) was added and cells were treated for 15 min at 37 °C, followed by stimulation with murine CCL5 (5 μ g/mL; Table 20) for additional 5 min. After washing, cells were stained with anti-CD45-APC, anti-CD11b-PerCP, anti-Ly6G-FITC and anti-Gr1-APCeFluor780 antibodies (Table 13) for 15 min at RT. After washing, cells were resuspended in 200 μ L assay buffer and measured by flow cytometry. Neutrophils were determined as CD45⁺CD11b⁺Gr1⁺Ly6G⁺ and classical monocytes as CD45⁺CD11b⁺Gr1^{high}Ly6G⁻. ICAM1 or VCAM1 binding was assessed via geometric MFI of PE-stained cells.

4.3.6.4.2 Assessment of human high-affinity β 2-integrin conformation

In the human system, integrin activation was measured by assessing the high affinity conformation of LFA1, representing β 2-integrin activation. As a cell culture model, human promyelocytic leukemia HL-60 cells (Table 12) were differentiated into neutrophil-like cells. Therefore, 1x10⁶ HL-60 cells were seeded in 10 mL RPMI-1640 supplemented with 10 % FBS and 100 U/mL penicillin/streptomycin and incubated with 1.3 % DMSO for 6 days.^{166,167} After counting, cells were resuspended in adhesion medium (2x10⁶ cells/mL; Table 7). 50 μ L of the cell suspension was added to 50 μ L adhesion medium containing FLX (1 μ M) or 5-HT (1 μ M) and the mAb24 antibody (Table 14), which only binds to the high affinity β 2-integrin conformation.¹⁶⁸ Simultaneously, cells were stimulated with human CCL5 (5 μ g/mL; Table 20) or left unstimulated for 20 min at 37 °C. Cells were washed twice with PBS, stained with the AF488-conjugated (Fab')₂ antibody (Table 18) for 20 min on ice and fixated for 10 min on ice. After washing, cells were resuspended in 50 μ L PBS and acquired with the FACS BD

LSRFortessa 5L. The high-affinity β 2-integrin conformation was determined via MFI of Alexa Fluor 488-stained cells.

4.3.7 Statistics

Statistical analysis was performed using GraphPad Prism 7 software (Table 23). All data are shown as a mean \pm standard error of the mean (SEM). Gaussian distribution was tested with D'Agostino Pearson omnibus or Shapiro Wilk normality test. If normally test failed, Mann Whitney *U* test was applied. In case of Gaussian Distribution, Student's *t*-test was used for normally distributed data with equal variances after comparing variances via F test. If variances were significantly different Welch's *t*-test was applied. For highly skewed datasets, log transformation was performed prior to statistical calculations. For multiple comparisons, depending on the distribution, either one-way analysis of variance (ANOVA) followed by Bonferroni post hoc test or Kruskal-Wallis test followed by Dunn's post hoc test was applied. For two independent factors, two-way ANOVA followed by Bonferroni post hoc test was applied. Outliers were determined by Tukey's method. *P* values <0.05 were considered as statistical significant.

5 RESULTS

5.1 Atherogenesis modulates the serotonergic system

To investigate the influence of atherosclerosis on the components of the serotonergic system, the expression pattern of the proteins involved were analyzed in diverse tissues of *ApoE*^{-/-} mice at different stages of the disease. Apart from aorta, bone marrow and spleen were analyzed because of their function as a cell reservoir during atherogenesis. *ApoE*^{-/-} mice were euthanized for tissue harvest (0 weeks) or fed a HFD for 4 or 16 weeks prior to organ harvest and gene expression of *5-Htr2a*, *5-Htr1b*, *5-Htr2b* and *Sert* was measured.

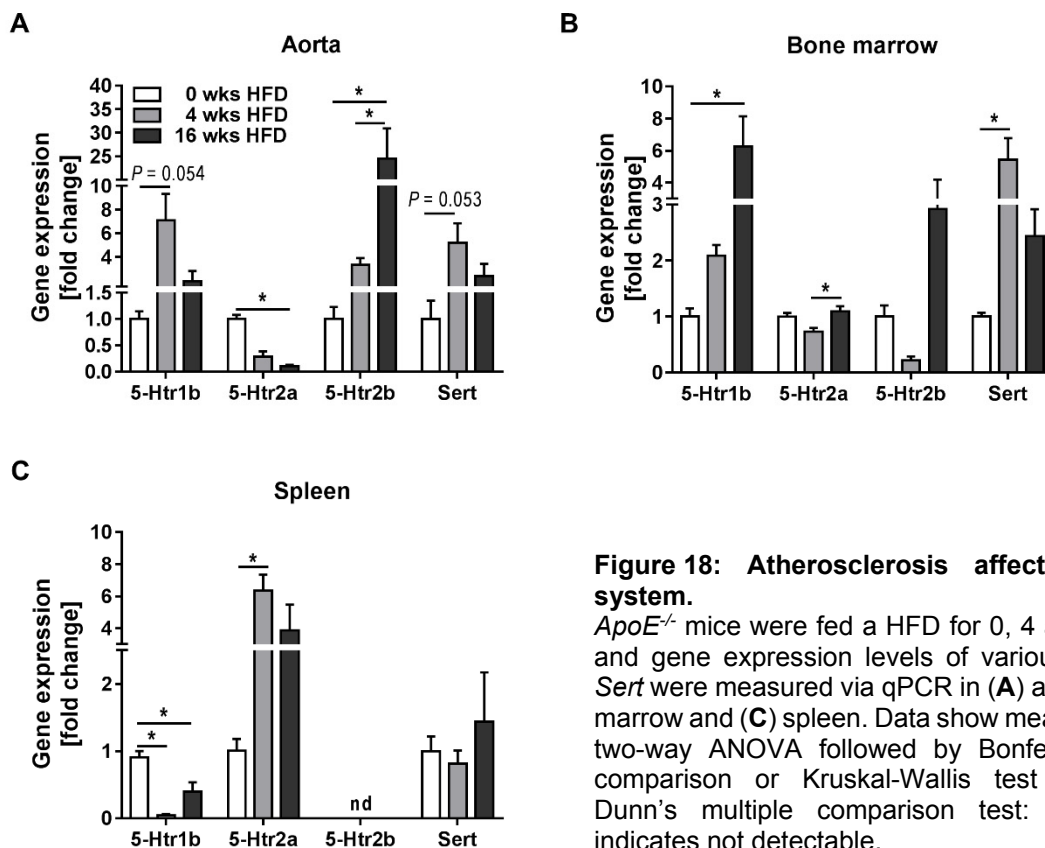


Figure 18: Atherosclerosis affects the 5-HT system.

ApoE^{-/-} mice were fed a HFD for 0, 4 and 16 weeks and gene expression levels of various *5-Htrs* and *Sert* were measured via qPCR in (A) aorta, (B) bone marrow and (C) spleen. Data show mean±SEM, n=5, two-way ANOVA followed by Bonferroni multiple comparison or Kruskal-Wallis test followed by Dunn's multiple comparison test: **P*<0.05, nd indicates not detectable.

The transition from normal chow diet to HFD caused a decline in the *5-Htr2a* expression in the aorta, while the expression of the other two receptors and *Sert* increased, at least at the onset of HFD (Figure 18A). The most important upregulation was observed for *5-Htr2b*. In bone marrow (Figure 18B), the expression of *5-Htr2a* also initially dropped, returning to baseline level with progressed atherosclerosis. Similar to the expression levels in aorta, *5-Htr1b*, *-2b* and *Sert* expression increased during atherogenesis. A different expression pattern was observed in spleen (Figure 18C). Here, *5-Htr2a* expression increased in association with HFD, while *5-Htr1b* expression decreased. The mRNA level of *Sert* was unaffected and *5-Htr2b* was not detectable. Moreover, 5-HT serum levels, reflecting the 5-HT platelet storage, progressively decreased with HFD feeding, possibly caused by enhanced platelet activation

during atherosclerosis (Figure 19). Taken together, the progression of atherosclerosis affects several components of the 5-HT system including platelet 5-HT storage as well as the gene expression of *Sert* and several *5-Htrs*.

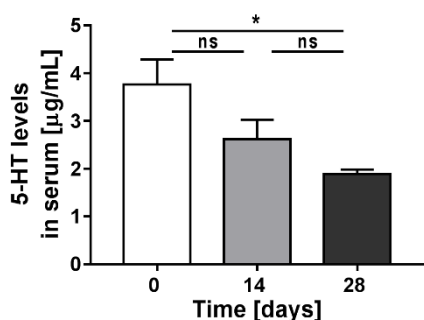


Figure 19: Atherosclerosis leads to reduced 5-HT levels in serum.

ApoE^{-/-} mice were fed a HFD for 0, 14 and 28 days and 5-HT levels were measured in serum via ELISA. Data show mean±SEM, n=3-4, Kruskal-Wallis test followed by Dunn's multiple comparison test: **P*<0.05, ns indicates not significant. (Modified from Rami *et al.*)¹⁶⁹

5.2 Chronic FLX treatment leads to platelet 5-HT depletion without affecting 5-HT plasma levels

In order to verify the efficiency of chronic FLX treatment, a time course experiment was performed. Therefore, *ApoE*^{-/-} mice were treated for 0, 3, 7, 14 days with FLX, while feeding a HFD. FLX was administered orally with a dose of 160 mg/L via the drinking water as previously reported.⁷³ Taking into account the daily drinking volume of 3-5 mL per mouse, the calculated oral intake of FLX in this experimental setting is approximately 18 mg/kg/day. In mouse, this was reported to result in FLX plasma concentrations equivalent to those determined in patients taking 20 to 80 mg FLX per day.¹⁷⁰

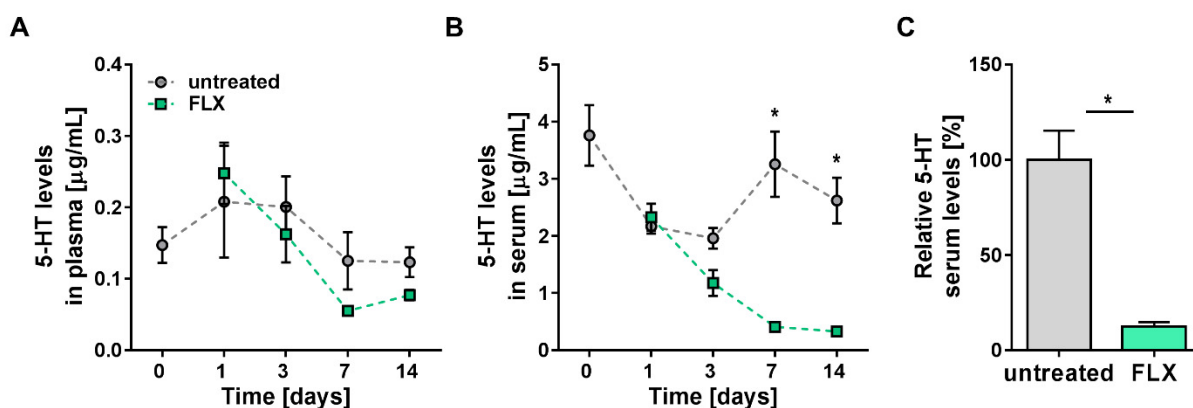


Figure 20: FLX treatment leads to platelet 5-HT depletion.

ApoE^{-/-} mice were fed a HFD for 0, 1, 3, 7 and 14 days and in parallel treated +/- FLX via the drinking water. 5-HT levels in (A) plasma and (B) serum were measured via ELISA. Data show mean±SEM, n=3, two-way ANOVA followed by Bonferroni multiple comparison test: **P*<0.05. (C) 5-HT depletion efficiency after 2 weeks of FLX treatment was quantified as a percentage of 5-HT serum levels of FLX-treated to control mice. Data show mean±SEM, n=3, Welch's *t*-test: **P*<0.05. (Modified from Rami *et al.*)¹⁶⁹

Plasma 5-HT levels representing the free circulating 5-HT, which is generally low, were not affected by chronic FLX treatment (Figure 20A). Serum 5-HT levels, reflecting the platelet 5-HT storage, decreased with chronic FLX treatment with a significant reduction after 7 days of treatment (Figure 20B). After 2 weeks of treatment the achieved platelet 5-HT storage depletion, which reflects the drug efficiency was 88 % (Figure 20C).

5.3 FLX leads to reduced leukocyte extravasation in wild type mice

Duerschmied and co-workers showed that during inflammation platelet serotonin promotes leukocyte recruitment and adhesion to mesenteric venous endothelium in mice. Moreover, they demonstrated that neutrophil extravasation in mice deficient for the enzyme TPH1, which are lacking non-neuronal 5-HT, is reduced in an acute peritonitis model.¹¹⁵ To investigate if the effect on extravasation can also be observed upon 5-HT depletion by FLX, we treated wild type C57Bl/6 mice for 2 weeks with FLX. Two hours after induction of an acute peritonitis by injection of 4 % thioglycolate the number of leukocytes obtained from the abdominal cavity lavage was significantly decreased in the FLX-treated group, mainly due to less neutrophil extravasation (Figure 21). Since leukocyte extravasation plays a crucial role in atherosclerosis, it was hypothesized that platelet 5-HT depletion via chronic FLX treatment reduces vascular inflammation leading to attenuated atherosclerosis.

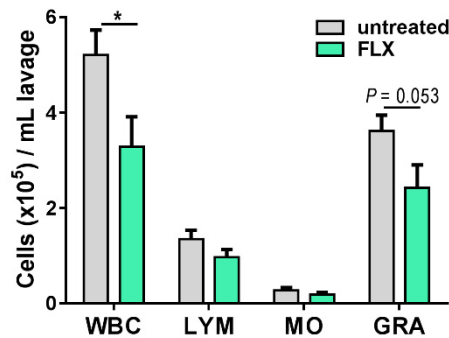


Figure 21: FLX impairs leukocyte extravasation in wild type mice.

Male C57Bl/6 mice were treated with FLX for 2 weeks. Two hours after the induction of an acute peritonitis by 4 % thioglycolate solution, the number of white blood cells (WBC), lymphocytes (LYM), monocytes (MO) and granulocytes (GRA) in the peritoneal lavage was determined with a hematology analyzer. Data show mean±SEM, n=9-10, Student's *t*-test: **P*<0.05.

5.4 Chronic FLX treatment aggravates atherosclerosis

To investigate the effect of chronic FLX treatment on atherosclerosis, male *ApoE*^{-/-} mice were treated for 2, 4 and 16 weeks with FLX accompanied by feeding a HFD. As expected, mice fed with a HFD had increased body weights and cholesterol levels, but both parameters were not affected by FLX treatment (Figure 22A,B).

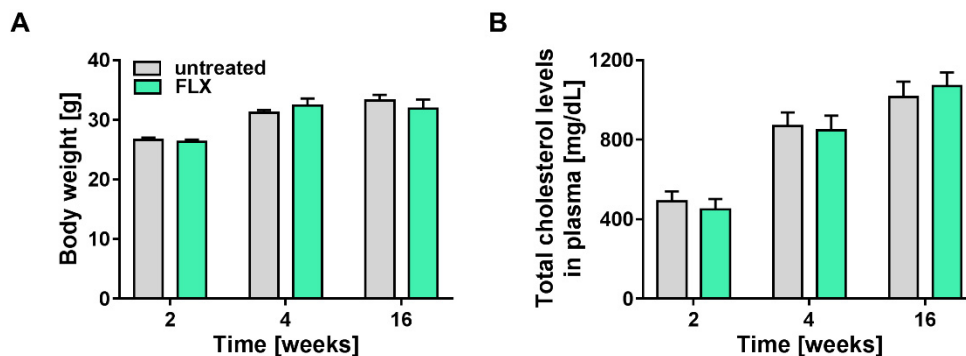


Figure 22: FLX does not affect body weight and cholesterol levels.

ApoE^{-/-} mice were treated for indicated periods of time with FLX while feeding a HFD. (A) Body weight was measured at the endpoint of the experiment. Data show mean±SEM, n=10-11 (2 weeks) n=10 (4 weeks) n=8-10 (16 weeks), Mann-Whitney *U* test. (B) Total plasma cholesterol was measured with a colorimetric assay. Data show mean±SEM, n=5 (2 weeks), n=10 (4 weeks) and n=8-10 (16 weeks), Student's *t*-test was performed to compare untreated vs FLX for each time point.

RESULTS

Atherogenesis was determined as lesion size in the aortic roots measured by ORO staining of cryosections. Unexpectedly, FLX treatment resulted in significantly increased lesion areas in all stages of atherosclerosis as evidenced by elevated absolute and normalized plaque size in the aortic root of FLX-treated mice compared to untreated control group (Figure 23). Of note, the strongest effect was observed at very early lesion formation (2 weeks) with a 1.7-fold increase, while at advanced atherosclerosis (16 weeks) the difference was only 1.3-fold.

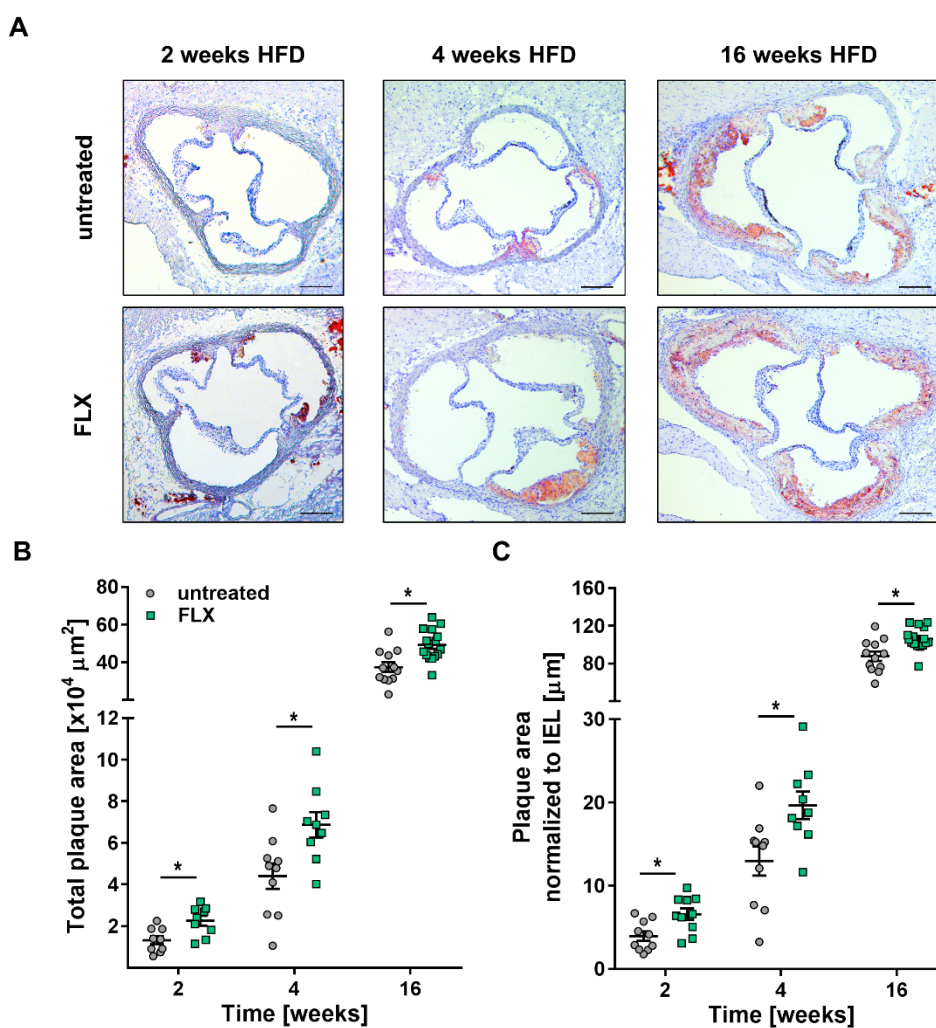


Figure 23: FLX treatment enhances atherosclerosis.

ApoE^{-/-} mice were fed a HFD for 2, 4 and 16 weeks accompanied by FLX treatment via the drinking water, while control mice received normal drinking water. **(A)** Representative images of ORO staining of frozen sections of aortic roots for plaque quantification. Scale bar=200 μm . Quantitative analysis of ORO staining as **(B)** absolute lesion area or **(C)** normalized to IEL as measure of the vessel size. Data show mean \pm SEM. Student's *t*-test: **P*<0.05. (Modified from Rami *et al.*)¹⁶⁹

It has been reported that in hypercholesterolemia blood monocytes may contribute to the pathogenesis of atherosclerosis by accumulating lipids in the circulation and subsequently transporting them into atherosclerotic lesions.^{53,171,172} To clarify if chronic SSRI treatment affects lipid content in circulating leukocytes independent of total plasma cholesterol, free and esterified cellular lipid content was assessed after 2 weeks of treatment. However, the ratio of esterified cholesterol to total cholesterol was similar in FLX-treated and control mice

RESULTS

(Figure 24A). Similar, protein levels of cholesterol transporters ABCA1, ABCG1, CD36 and SR1 on circulating myeloid cells, of which non-classical monocytes showed the highest expression, did not differ between the two groups (Figure 24B). Thus, these results argue against the possibility that FLX may affect cholesterol efflux in circulating leukocytes.

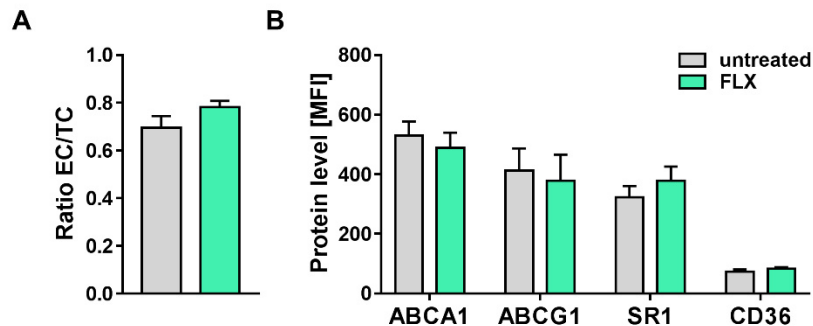


Figure 24: FLX has no effect on lipid loading in circulating leukocytes.

ApoE^{-/-} mice were fed a HFD for 2 weeks +/- FLX and lipid loading of circulating leukocytes was assessed. (A) Neutral lipid content of circulating leukocytes was measured with the Amplex Red Cholesterol Assay kit as ratio of esterified cholesterol (EC) to total cholesterol (TC). (B) Protein levels of cholesterol transporters ABCA1, ABCG1, CD36 and SR1 were analyzed on circulating non-classical monocytes (CD45⁺/CD11b⁺/CD115⁺/Ly6C^{low}) by flow cytometry via geometric MFI. Data show mean±SEM, n=5-6, Student's *t*-test: **P*<0.05. (Modified from Rami *et al.*)¹⁶⁹

To evaluate the effect of FLX on already established plaques, *ApoE*^{-/-} mice were fed a HFD for 16 weeks while FLX was administered in parallel only during the last 4 weeks. Interestingly, as seen in Figure 25, no differences were observed in total as well as in normalized plaque size of aortic roots between FLX-treated and control mice, suggesting that FLX rather affects lesion initiation than progression.

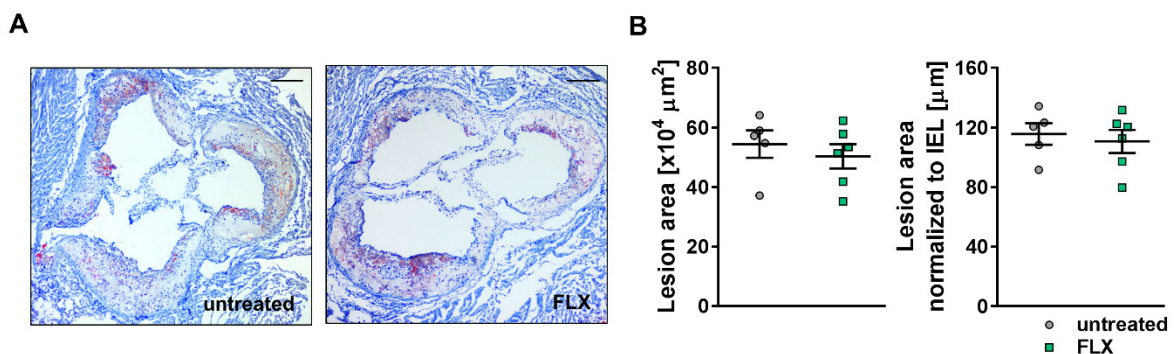


Figure 25: FLX does no effect the progression of already established plaques.

ApoE^{-/-} mice were fed a HFD for 12 weeks before starting in parallel FLX administration for additional 4 weeks. Lesion area was quantified in aortic roots via ORO staining. (A) Representative images. Scale bar=200 μm. (B) Quantitative analysis of ORO staining as absolute lesion area (left) or normalized to IEL (right). Data show mean±SEM. n = 5-6. Student's *t*-test: **P*<0.05.

Remarkably, it was reported that an acute FLX treatment leads to temporary elevated plasma 5-HT concentrations and promotes leukocyte endothelial interaction, as shown after 2 h of FLX treatment onset.¹¹⁶ To validate if transiently increased plasma 5-HT may cause the observed pro-atherogenic effect, mice were pre-treated with FLX for 2 weeks before starting HFD feeding with continuous FLX treatment for 2 weeks. Thereby, may occurring transiently

RESULTS

elevated plasma 5-HT levels at the onset of FLX treatment do not exhibit a possible confounding effect. However, the observed plaque phenotype in the pre-treatment experiment (Figure 26) was comparable with the one in the standard experimental setup (Figure 23). This excludes the possibility that the FLX-mediated pro-atherogenic effect is only due to potentially elevated 5-HT plasma levels at the beginning of the FLX treatment.

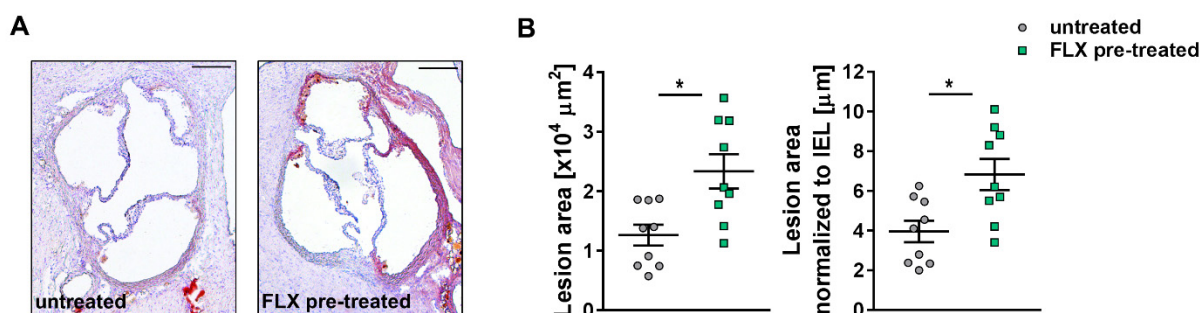


Figure 26: Pre-treatment with FLX reveals similar results to standard experimental setup.

ApoE^{-/-} mice were pre-treated with FLX for 2 weeks before starting HFD feeding in parallel for 2 weeks. (A) Representative images of ORO staining of aortic roots of untreated and pre-treated FLX-mice. Scale bar=200 μm . (B) Quantitative analysis of total lesion area (left) or normalized to IEL (right). Data show mean \pm SEM, n=9, Student's *t*-test: **P*<0.05. (Modified from Rami *et al.*)¹⁶⁹

To investigate systemic inflammatory parameters upon FLX treatment, the impact of FLX on the plasma cytokine profile was assessed. Interestingly, plasma levels of IL22 were significantly decreased in the FLX-treated group (Figure 27A). The abundance of other tested cytokines was not affected by the treatment, except for a mild increase of IFN γ and CXCL1 (Figure 27B).

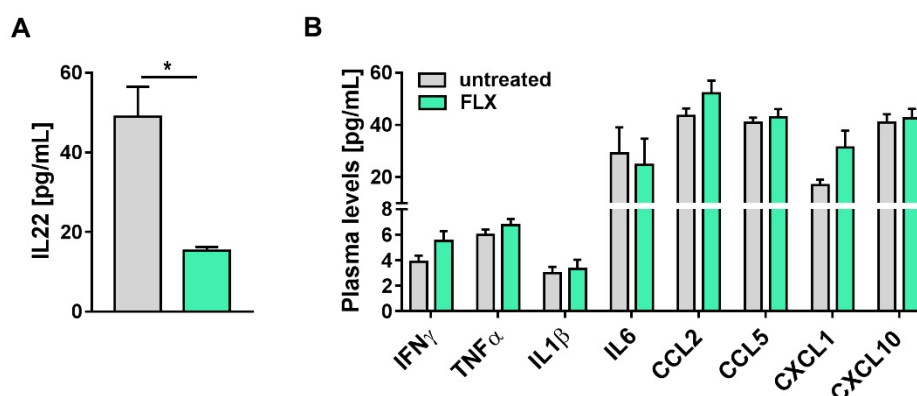


Figure 27: IL22 plasma levels were elevated by FLX treatment while the abundance of other cytokines was not affected.

Plasma cytokine levels were measured in untreated and FLX-treated *ApoE*^{-/-} mice after feeding a HFD for 4 weeks. (A) Plasma concentrations of IL22 and (B) a variety of other cytokines were assessed by multiplex immunoanalysis. Data show mean \pm SEM, n=8-9, Welch's *t* test: **P*<0.05.

The early phase of atherosclerosis is mainly characterized by the recruitment of myeloid cells. Looking closer at aortic plaques after 4 weeks of treatment, FLX-treated mice showed an elevated neointimal macrophage content compared to the untreated control group, as evidenced by an augmented amount of MAC2-positive cells in the plaque (Figure 28). The

RESULTS

relative macrophage content was not changed, suggesting that the detected increase in plaque size in FLX-treated mice was mainly caused by macrophage accumulation.

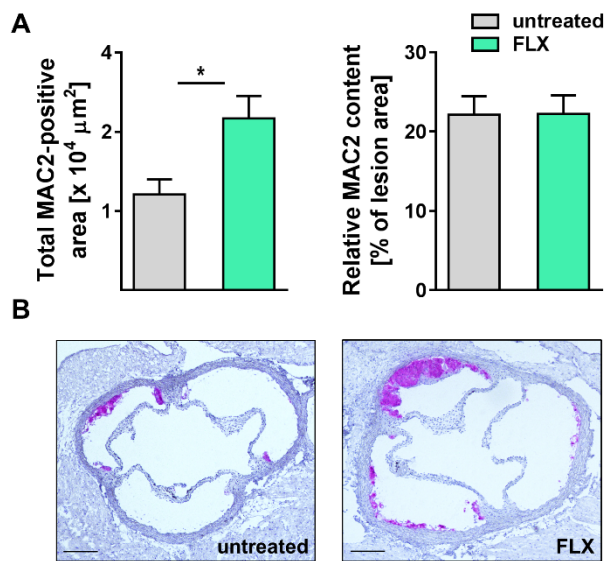


Figure 28: FLX treatment leads to elevated macrophage content in aortic lesions.

Macrophage content in aortic plaques of control and FLX treated *ApoE*^{-/-} mice after feeding a HFD for 4 weeks was determined by immunohistochemistry. **(A)** Quantitative analysis of macrophage plaque content as total MAC2-positive area (left) or normalized to plaque area (right). **(B)** Representative images. Scale bar=200 μm . Data show mean \pm SEM, n=14-18, Student's *t*-test: **P*<0.05. (Modified from Rami *et al.*)¹⁶⁹

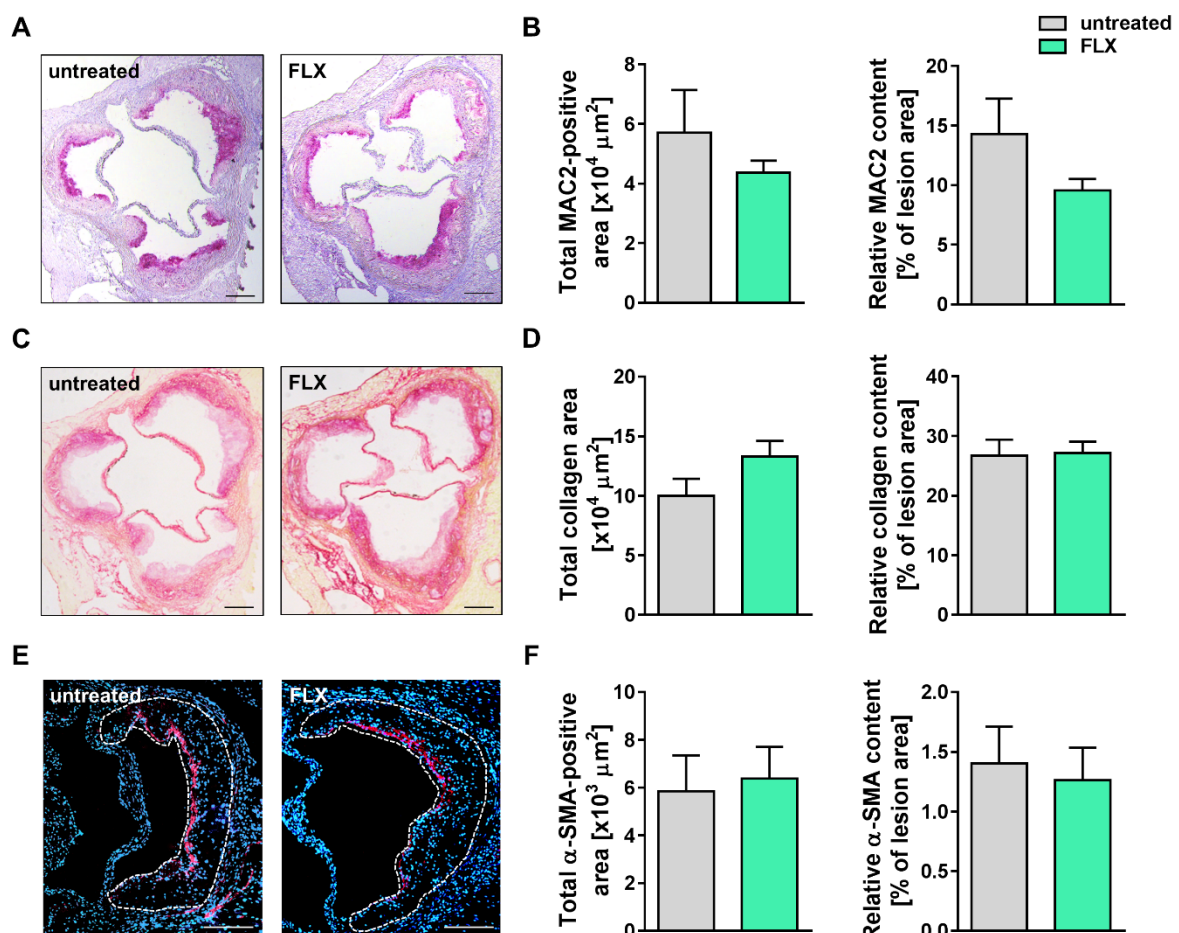


Figure 29: FLX does not affect composition of advanced plaques.

Plaque content of untreated and FLX treated *ApoE*^{-/-} mice was examined after 16 weeks of feeding a HFD. Representative images of **(A)** staining with the macrophage marker MAC2, **(C)** Sirius red staining for total collagen and **(E)** α -SMA immunofluorescence staining for SMC content (dotted line delineates the plaque area). Scale bar=200 μm . Quantitative analysis of **(B)** macrophage, **(D)** collagen and **(F)** SMC content as total area (left) or normalized to plaque size (right). Data show mean \pm SEM, n=12-16, Student's *t*-test. (Modified from Rami *et al.*)¹⁶⁹

Interestingly, differences in macrophage content were no longer detectable at advanced atherogenesis (Figure 29A,B). Furthermore, the plaque content of collagen and SMC was not changed by FLX treatment (Figure 29C-F), indicating that FLX is not affecting plaque stability.

5.5 FLX transiently lowers circulating leukocyte and platelet counts

To verify the reason for elevated neointimal macrophage content in FLX-treated mice in early atherogenesis, leukocyte blood counts were measured.

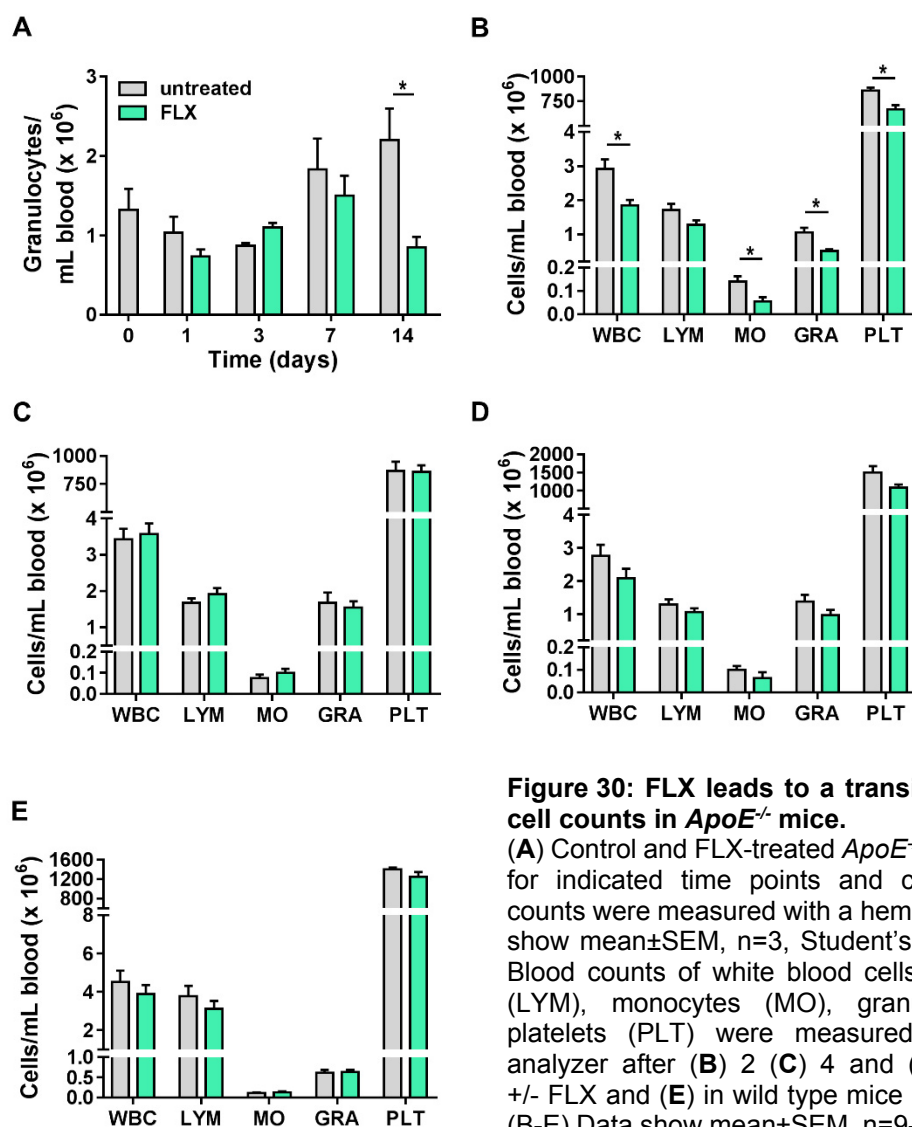


Figure 30: FLX leads to a transient decline in blood cell counts in *ApoE*^{-/-} mice.

(A) Control and FLX-treated *ApoE*^{-/-} mice were fed a HFD for indicated time points and circulating granulocyte counts were measured with a hematology analyzer. Data show mean \pm SEM, n=3, Student's *t*-test: **P*<0.05. (B-E) Blood counts of white blood cells (WBC), lymphocytes (LYM), monocytes (MO), granulocytes (GRA) and platelets (PLT) were measured with a hematology analyzer after (B) 2 (C) 4 and (D) 16 weeks of HFD +/- FLX and (E) in wild type mice after 2 weeks +/- FLX. (B-E) Data show mean \pm SEM, n=9-10 (B), n=8 (C), n=8-9 (D) and n=7-8 (E), Student's *t*-test or Mann-Whitney *U* test: **P*<0.05. (Modified from Rami *et al.*)¹⁶⁹

The investigation of blood leukocyte counts from the initial time course experiment (Figure 20) revealed a significant decline in granulocyte numbers after 14 days of treatment (Figure 30A). A more detailed analysis of this time point identified an overall drop in circulating white blood cell counts, which was mainly due to a decreased number of granulocytes and accompanied by a decline in platelet numbers (Figure 30B). However, this effect was no longer visible after 4 and 16 weeks of treatment (Figure 30C,D) and was not present in wild type mice without

atherogenic background (Figure 30E). Thus, the transient reduction of circulating myeloid cells might reflect augmented platelet and neutrophil recruitment to the arterial wall, which is most pronounced in early lesion formation.

5.6 FLX does not affect myelopoiesis and mobilization from bone marrow and spleen

To subsequently verify potential changes in leukocyte production and mobilization from the bone marrow and spleen upon FLX treatment, cell counts were assessed in both organs by flow cytometric analysis. Absolute numbers of neutrophils and classical monocytes in spleen as well as in bone marrow were comparable between FLX and control group (Figure 31A-D). This indicates that FLX has no impact on myelopoiesis and mobilization of myeloid cells.

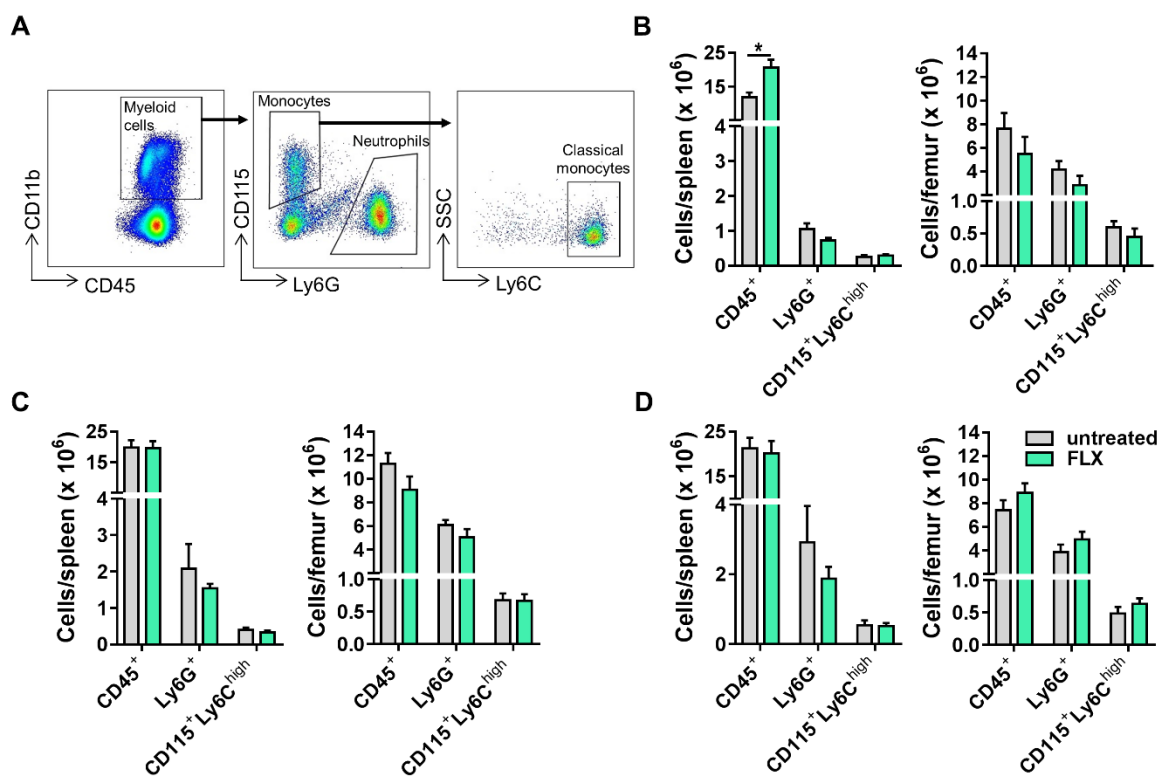


Figure 31: FLX treatment has no impact on myelopoiesis and mobilization from bone marrow and spleen.

(A) Representative gating strategy to identify neutrophils (CD45⁺/CD11b⁺/Ly6G⁺) and classical monocytes (CD45⁺/CD11b⁺/CD115⁺/Ly6C^{high}) by flow cytometry. (B-D) Leukocyte counts of spleen (left) and femur (right) were measured in untreated and FLX-treated *ApoE*^{-/-} mice after feeding a HFD for (B) 2, (C) 4 and (D) 16 weeks. Data show mean \pm SEM, n=4-6 (B), n=9-11 (C) and n=8-10 (D), Student's *t*-test or Mann-Whitney *U* test: **P*<0.05. (Modified from Rami *et al.*)¹⁶⁹

5.7 Arterial adhesion of myeloid cells is enhanced by FLX

Given that circulating leukocyte counts were transiently decreased at the onset of FLX treatment, which was not explained by changes in myelopoiesis or recruitment from bone marrow or spleen, FLX might enhance leukocyte adhesion to the inflamed endothelium in aortas of atherosclerosis-prone mice. To investigate arterial adhesion *in vivo* as well as rolling of myeloid cells on the endothelium intravital microscopy was performed at the carotid artery bifurcation, known as a predilection site for atherosclerotic plaque development. Myeloid cells were visualized by injecting fluorescent antibodies against CD11b and Ly6G in control and FLX-treated mice which had received a HFD for 4 weeks. Live imaging showed a 2.5-fold increase in the number of adhering CD11b-stained myeloid cells of FLX-treated mice compared to control (Figure 32A,B). This effect was even more striking when specifically analyzing neutrophils, identified as Ly6G-labeled cells, with a 3.4-fold higher count of adherent cells in the FLX-treated group. In contrast, rolling on the endothelium was not affected by FLX (Figure 32C).

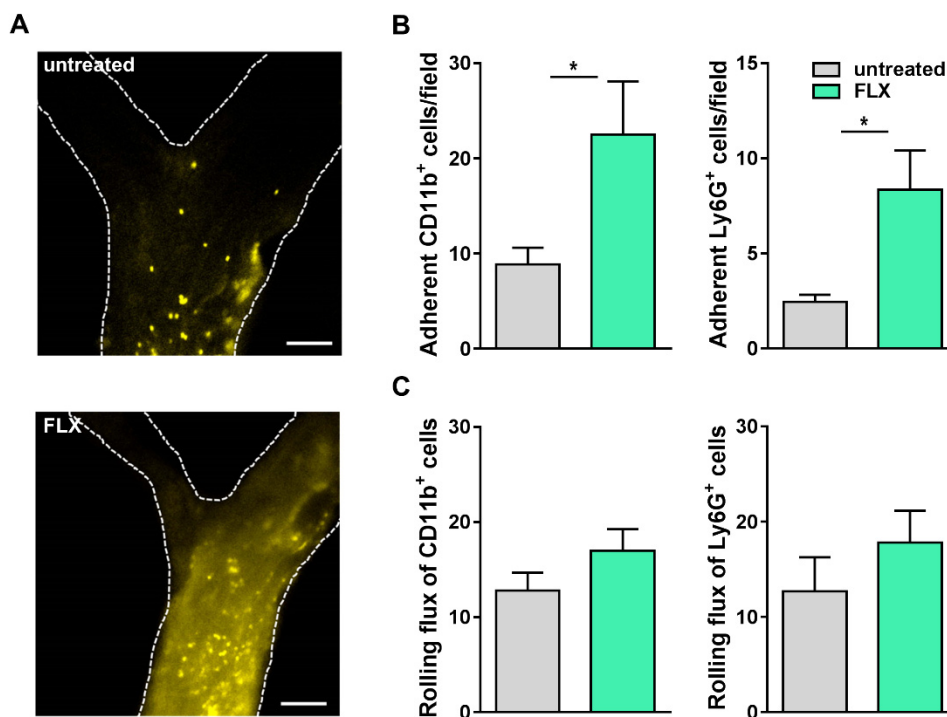


Figure 32: FLX enhances arterial adhesion of myeloid cells.

Intravital microscopy of the left carotid artery was performed in *ApoE*^{-/-} mice, which were fed a HFD for 4 weeks +/- FLX. To track myeloid cells or neutrophils antibodies against CD11b or Ly6G were injected intravenously 10 min before measurement. (A) Representative images of adherent myeloid cells. Scale bar=100 μ m. (B) Number of counted adherent CD11b⁺ (left) and Ly6G⁺ (right) cells per field. (C) Number of counted rolling CD11b⁺ (left) and Ly6G⁺ (right) cells. Data show mean \pm SEM, n=9-10, * P <0.05, Welch's t test or Mann-Whitney U test. (Modified from Rami *et al.*)¹⁶⁹

5.8 5-HTR1b antagonism has no influence on atherogenesis

It was shown that stimulation of 5-HTR1b receptor expressed on the endothelium leads to an increase in NO production via the Akt/eNOS pathway.⁹¹ Since an increase in NO is well known to block the expression of adhesion molecules, we aimed to investigate the influence of 5-HTR1b signaling in atherogenesis. Based on the fact that a loss of NO results in an upregulation of adhesion molecules,⁷ antagonism of 5-HTR1b was hypothesized to enhance atherosclerosis. To examine this hypothesis, *ApoE*^{-/-} mice were injected every second day with a selective antagonist for 5-HTR1b for 2 weeks accompanied by HFD feeding. However, mice administered with the antagonist showed similar plaque sizes (Figure 33A,B) and blood cell counts (Figure 33C) compared to vehicle group. This suggests that the observed FLX-mediated increase in atherosclerosis is not caused by the loss of 5-HTR1b signaling through the depletion of peripheral 5-HT.

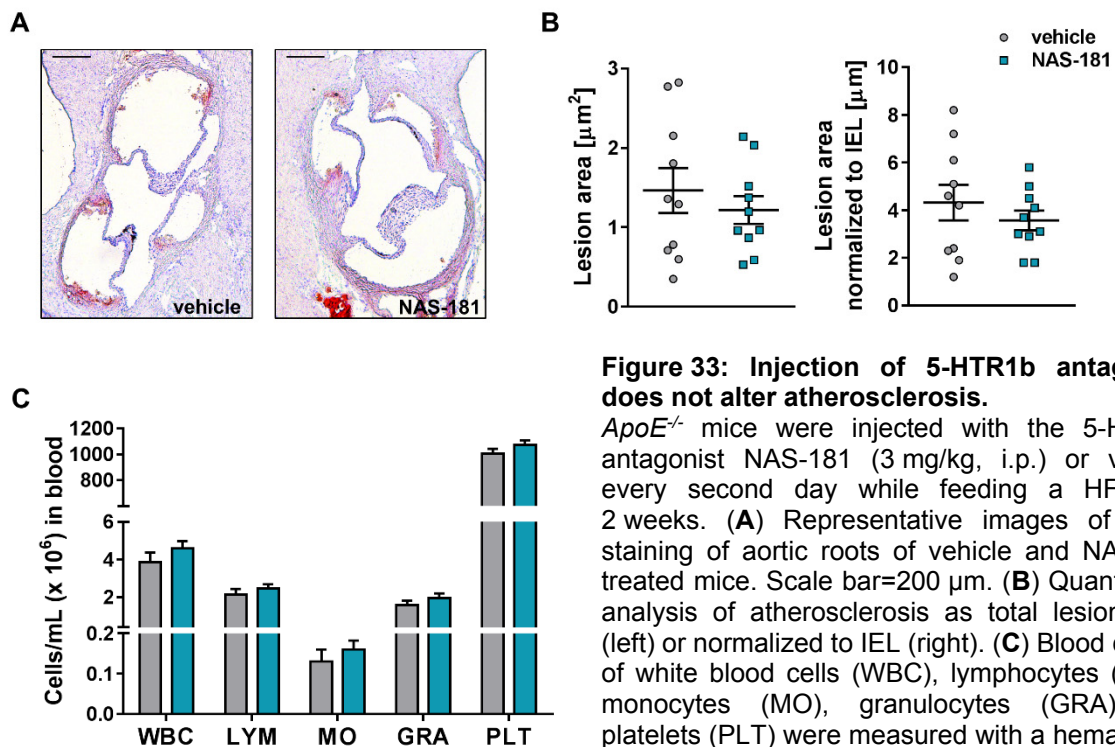


Figure 33: Injection of 5-HTR1b antagonist does not alter atherosclerosis.

ApoE^{-/-} mice were injected with the 5-HTR1b antagonist NAS-181 (3 mg/kg, i.p.) or vehicle every second day while feeding a HFD for 2 weeks. (A) Representative images of ORO staining of aortic roots of vehicle and NAS-181 treated mice. Scale bar=200 μm . (B) Quantitative analysis of atherosclerosis as total lesion area (left) or normalized to IEL (right). (C) Blood counts of white blood cells (WBC), lymphocytes (LYM), monocytes (MO), granulocytes (GRA) and platelets (PLT) were measured with a hematology analyzer. Data show mean \pm SEM, n=10, Student's *t*-test: **P*<0.05.

5.9 FLX does not alter platelet characteristics

Circulating activated platelets are known to interact with leukocytes to form PLAs. This leads to enhanced leukocyte adhesiveness to inflamed endothelium by depositing CCL5 and CXCL4 on the monocyte and endothelial surface, which in turn promotes formation of atherosclerotic lesions.⁶¹ The depletion of platelet 5-HT storage might crucially affect these pro-atherogenic properties. However, CCL5 and CXCL4 serum levels were not affected by FLX (Figure 34A,B). Moreover, *in vitro* activation of isolated platelets after 2 weeks treatment did not reveal any differences in CXCL4 release between control and FLX-treated group (Figure 34C). The MPV is a marker for platelet activity and the increase is associated with larger and more active platelets. For instance, patients with acute myocardial infarction or stable coronary artery disease exhibit a significantly higher MPV.¹⁷³ However, MPVs of control and FLX-treated mice were comparable (Figure 34D).

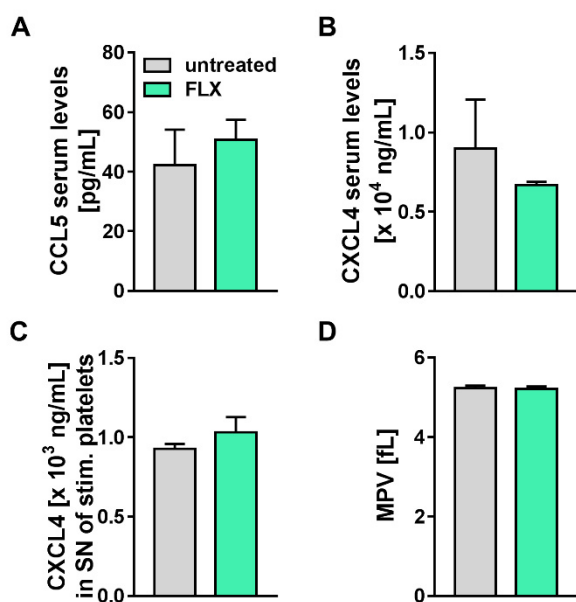
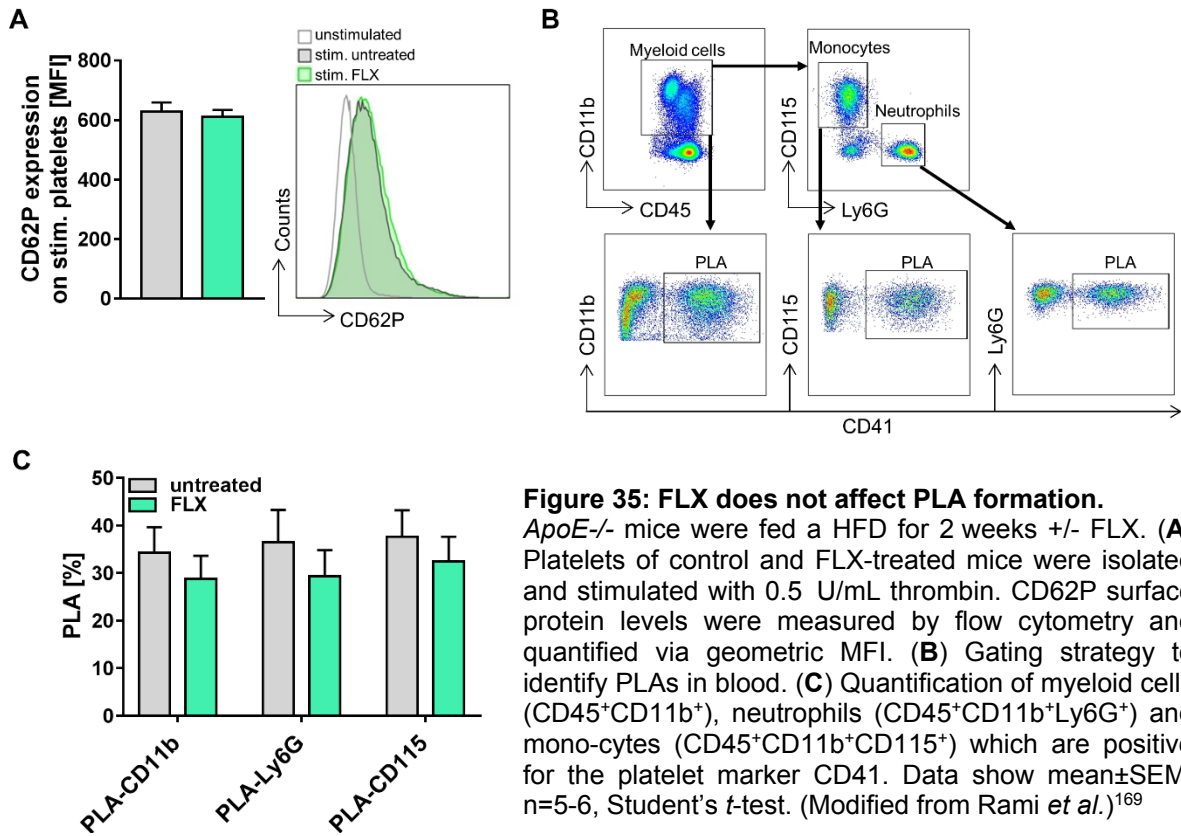


Figure 34: FLX does not affect platelet characteristics.

ApoE^{-/-} mice were fed a HFD for 2 weeks +/- FLX. (A) CCL5 and (B) CXCL4 serum levels were determined via ELISA. (C) CXCL4 content of isolated and with 0.5 U/mL thrombin stimulated platelets was analyzed via ELISA. (D) MPV was assessed with a hematology analyzer. Data show mean \pm SEM, n=3 (A, B), n=5-6 (C) and n=10 (D), Student's *t*-test: **P*<0.05. (Modified from Rami *et al.*)¹⁶⁹

The common platelet activation marker CD62P (P-selectin), is essential for PLA formation, since it mediates platelet-leukocyte binding. Upon activation, CD62P is rapidly translocated from the α -granules to the platelet surface making it an ideal marker to assess platelet activation with flow cytometry.⁵⁷ However, CD62P surface levels of *in vitro* activated and isolated platelets of mice after 2 weeks of treatment were similar in the two groups (Figure 35A). In line with this result, no differences were detected in circulating platelet-leukocyte aggregates (Figure 35B,C). Of note, flow cytometry analysis was performed with low acquisition speed since Mauler *et al.* noted false-positive PLA counts when measuring with increasing flow rate.¹⁶⁵ These results suggest that the observed enhanced leukocyte adhesion and the transient reduction in circulating platelet counts in FLX-treated mice were not caused by augmented binding of activated platelets to leukocytes in circulation.

RESULTS



5.10 FLX enhances vascular permeability

In atherosclerosis, endothelial function is disturbed leading to destabilized vascular integrity and consequently enhanced permeability. The disrupted endothelial barrier facilitates transendothelial migration of leukocytes to the arterial intima.⁶ To investigate whether increased macrophage accumulation in FLX-treated lesions occurred due to changes in vascular integrity, vessel leakage was measured by an *in vivo* permeability assay using Evans blue.

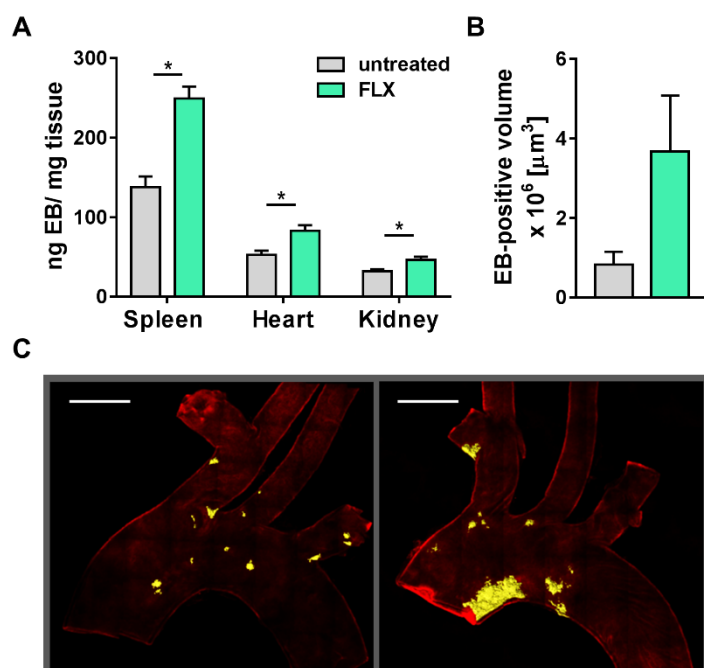


Figure 36: FLX aggravates vascular permeability.

ApoE^{-/-} mice fed a HFD for 2 weeks +/- FLX were injected with Evans blue (EB; 40 mg/kg, i.v.) and vascular permeability was assessed in different tissues by measuring the extravasation of EB. (A) Quantification of EB-extravasation in spleen, heart and kidney by OD620 measurement in supernatants. (B) Quantification of EB-positive volume in aortic arches assessed by confocal laser scanning microscopy. (C) Representative tilescan 3D reconstructions of aortic arches acquired with confocal microscopy. EB-positive regions are shown in yellow. Red represents autofluorescence of the adventitia. Scale bars=1 mm. Data show mean±SEM, n=7-8, Student's *t*-test or Welch's *t*-test: **P*<0.05. (Modified from Rami *et al.*)¹⁶⁹

FLX-treated mice showed aggravated vascular leakage compared to control mice, as evidenced by an increased Evans blue extravasation in spleen, kidney and heart (Figure 36A). In line with these findings, confocal imaging of aortic arches revealed Evans blue-positive area tend to be larger in FLX-treated mice (Figure 36B,C).

5.11 FLX does not affect adhesion molecule expression

Since FLX did not alter platelet properties, the *in vivo* detected enhanced cell adhesion to the arterial endothelium might be provoked by increased expression of proteins involved in leukocyte recruitment on the endothelium itself or on circulating leukocytes. At first, mRNA expression of the adhesion molecules *Icam1* and *Vcam1* as well as of several chemokines and chemokine receptors was assessed in aortas of control and FLX-treated mice after 4 weeks of treatment. However, no modification in mRNA expression was detected which would corroborate enhanced leukocyte recruitment (Figure 37A).

RESULTS

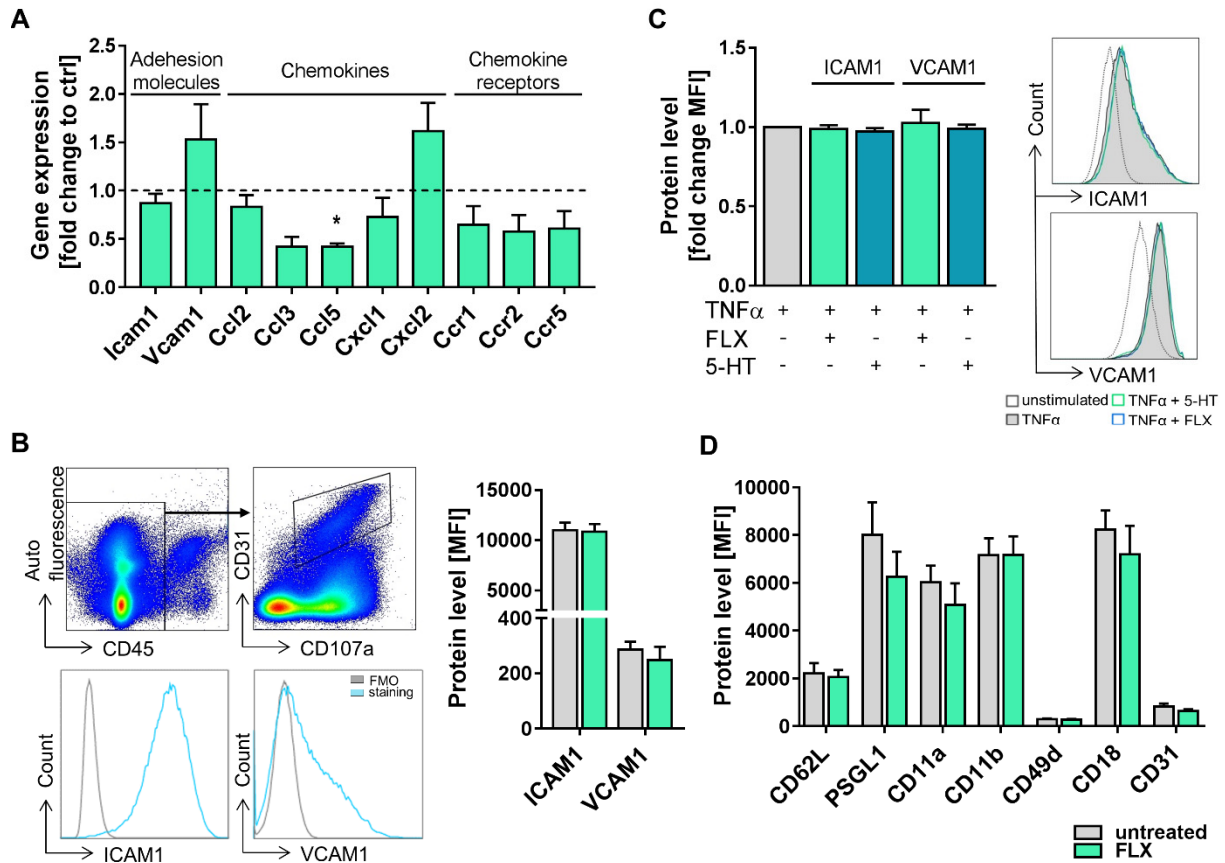


Figure 37: FLX does not induce expression of molecules involved in adhesion.

(A) *ApoE*^{-/-} mice were fed a HFD for 4 weeks +/- FLX and mRNA expression of adhesion molecules, chemokines and chemokine receptors was determined in aortas using qPCR. (B) The expression of adhesion molecules on aortic endothelial cells (CD45⁺CD31⁺CD107a⁺), identified with the indicated gating strategy, was assessed from *ApoE*^{-/-} mice fed a HFD for 2 weeks +/- FLX via flow cytometry. Data show mean \pm SEM, n=9-10 (A) and n=7 (B), Student's *t*-test or Mann-Whitney *U* test. (C) Murine endothelial cells (SVEC4-10) were treated with FLX (1 μ M) or 5-HT (1 μ M) before TNF α -stimulation and VCAM1 and ICAM1 surface protein levels was measured by flow cytometry and normalized to control (TNF α). Data show mean \pm SEM, at least 4 independent experiments were performed, Student's *t*-test. (D) The surface protein levels of adhesion molecules on blood neutrophils of *ApoE*^{-/-} mice fed a HFD for 2 weeks +/- FLX were determined via flow cytometry. Data show mean \pm SEM, n=7, Student's *t*-test. **P*<0.05. (Modified from Rami *et al.*)¹⁶⁹

Since changes in surface levels can also be caused by post-transcriptional regulations, measurement of mRNA expression might not be sufficient. Therefore, surface protein levels of ICAM1 and VCAM1 on aortic endothelial cells were determined using a new protocol for enzymatic digestion of aortas followed by flow cytometric analysis.¹⁶⁴ However, no elevated proteins levels of endothelial adhesion molecules were identified in FLX-treated mice (Figure 37B). In line with these results, *in vitro* treatment of TNF α -stimulated murine SVEC4-10 endothelial cells with FLX did not show an elevated amount of ICAM1 or VCAM1 on the cell surface (Figure 37C). Additionally, 5-HT stimulation did also not influence adhesion molecule levels. Given that no changes on the endothelium were observed, the surface levels of adhesion molecules and integrins on blood neutrophils were measured (Figure 37D). Again, no significant differences were identified.

5.12 FLX amplifies chemokine-mediated integrin activation on myeloid cells

In the process of leukocyte recruitment, adhesion and transmigration, it is well documented that selectins mediate the rolling, while integrins are more involved in adhesion of leukocytes. Given that intravital microscopy analysis (Figure 32) revealed an effect of FLX on myeloid cell adhesion but not rolling suggests that the treatment alters integrin- rather than selectin-mediated binding. Integrins are mostly regulated by activation through conformational modifications instead of changes in their expression levels.⁴⁰ Consequently, integrin activation of circulating leukocytes was studied after stimulation with CCL5, a chemotactic molecule which is considered to be important in arterial myeloid cell recruitment.^{61,64,65} Activation of β 1- and β 2-integrins of blood leukocytes of control and FLX-treated mice receiving a HFD for 2 weeks was assessed by binding to their natural ligands ICAM1 and VCAM1. To this end, blood cells were incubated with recombinant mouse ICAM1 and VCAM1 chimeras, which were fused to a human Fc domain. The use of an anti-human IgG1-PE antibody enabled the measurement of integrin binding via flow cytometry. Interestingly, circulating monocytes and neutrophils of *in vivo* FLX-treated mice revealed an enhanced ligand binding capability of β 1- and β 2-integrins (Figure 38) compared to untreated control group.

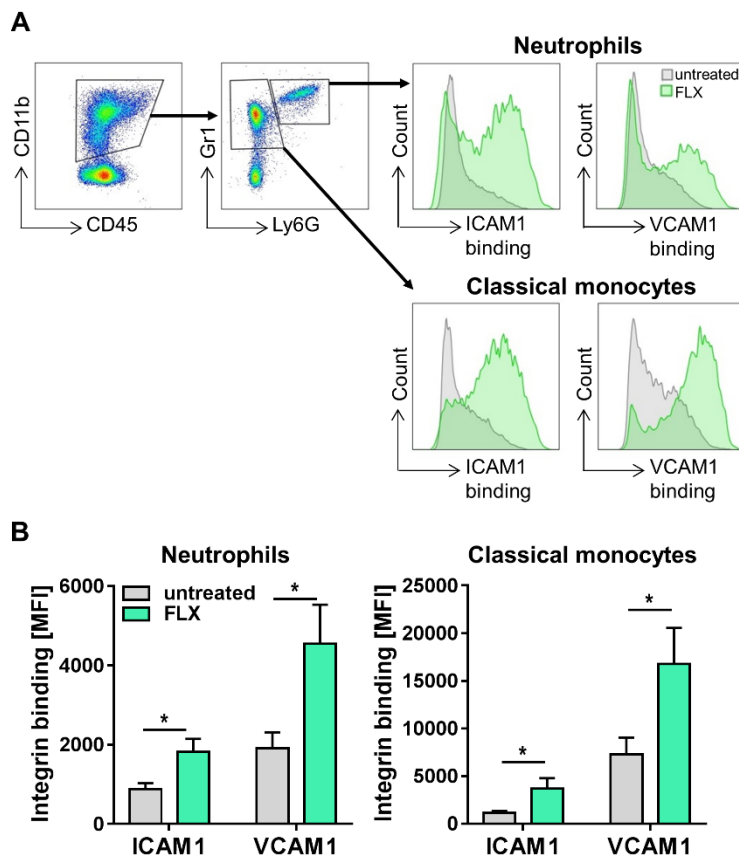


Figure 38: FLX-treated mice show enhanced CCL5-mediated integrin activation.

CCL5-mediated integrin binding to ICAM1 and VCAM1 by blood leukocytes of control and FLX-treated *ApoE*^{-/-} mice fed a HFD for 2 weeks was measured via flow cytometry. (A) Gating strategy to identify integrin activity by ICAM1 and VCAM1 binding of neutrophils (CD45⁺CD11b⁺Gr1⁺Ly6G⁺) and classical monocytes (CD45⁺CD11b⁺Gr1^{high}Ly6G⁻) expressed as geometric MFI. Data show mean \pm SEM, n=8-9, Welch's *t*-test: **P*<0.05. (Modified from Rami *et al.*)¹⁶⁹

To elucidate whether the elevated integrin binding activity in chronically FLX-treated mice is caused by the lack of peripheral 5-HT or by the drug FLX itself, blood cells of wild type C57Bl/6J mice were pre-stimulated *in vitro* with FLX or 5-HT to determine CCL5-evoked integrin binding

RESULTS

capability to ICAM1 and VCAM1. Based on literature, a working concentration of 1 μM FLX was used, similar to the one observed in serum of mice treated with 18 mg/kg FLX per day.¹⁷⁰

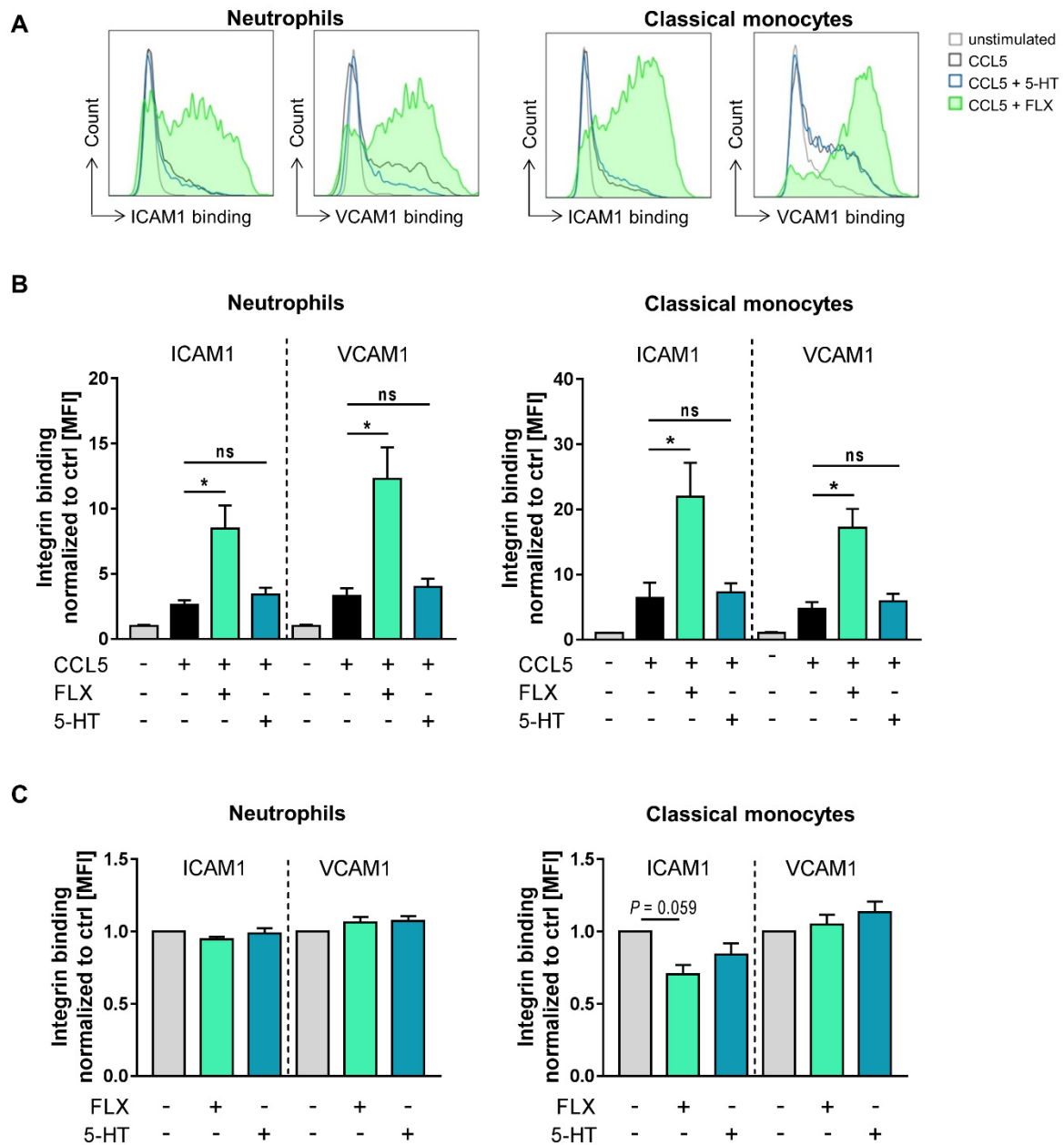


Figure 39: *In vitro* stimulation with FLX, but not 5-HT promotes CCL5-mediated integrin binding activity of murine blood leukocytes.

Integrin binding activity of blood leukocytes of C57Bl/6J wild type mice was analyzed after *in vitro* stimulation with FLX (1 μM) or 5-HT (1 μM) in the presence or absence of CCL5 via flow cytometry. **(A)** Histogram overlays of integrin activity by neutrophils ($\text{CD45}^+\text{CD11b}^+\text{Gr1}^+\text{Ly6G}^+$) or classical monocytes ($\text{CD45}^+\text{CD11b}^+\text{Gr1}^{\text{high}}\text{Ly6G}^-$) binding to recombinant ICAM1/Fc chimera or VCAM1/Fc chimera. Quantitative analysis of the effect of FLX or 5-HT on integrin activation **(B)** in the presence or **(C)** absence of CCL5. Data show mean \pm SEM, $n=9$ (B) and $n=7-8$ (C), one-way ANOVA followed by Bonferroni multiple comparison test or Kruskal-Wallis test followed by Dunn's multiple comparison test: * $P<0.05$. (Modified from Rami *et al.*)¹⁶⁹

Surprisingly, pre-treatment with FLX strongly enhanced the CCL5-induced activation of $\beta 1$ - and $\beta 2$ -integrins on neutrophils and classical monocytes, whereas the presence of 5-HT did not alter the binding to ICAM1 and VCAM1 (Figure 39A, B). However, in the absence of CCL5,

FLX did not trigger integrin activation, but rather reduced ICAM1 binding of classical monocytes (Figure 39C). These findings suggest that FLX directly alters leukocyte adhesion properties in an inflammatory setting in presence of enhanced chemokine levels, which is independent of 5-HT platelet depletion.

To examine whether the FLX-mediated effect on murine myeloid cells also occurs in human cells, integrin activation was assessed in neutrophil-like HL-60 cells. In human cells, activated β 2-integrins can be monitored by the antibody mAb24, which recognizes an epitope only existing in the fully extended conformation state.¹⁶⁸ As shown in Figure 40, CCL5 induced the switch of β 2-integrins to the activated state, which was further amplified in the presence of FLX as evidenced by enhanced mAb24 binding. This effect was not observed upon 5-HT treatment, supporting the results obtained in murine myeloid cells. Moreover, FLX alone did not promote mAb24 binding.

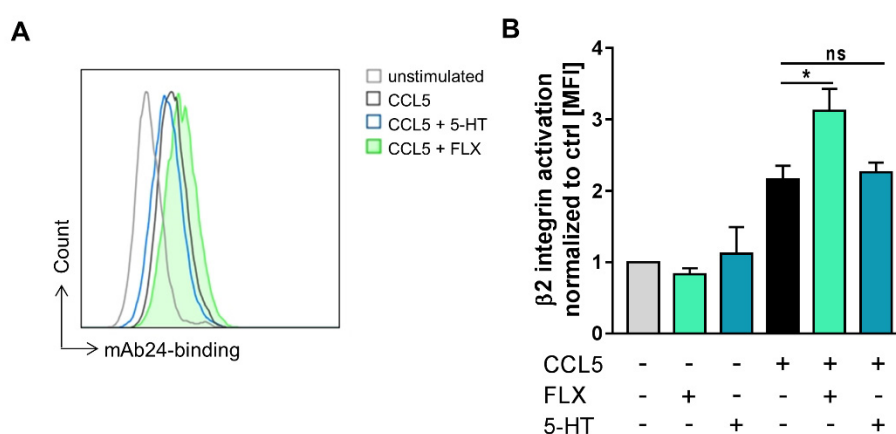


Figure 40: FLX triggers CCL5-mediated integrin activation in human neutrophil-like cells.

Human HL-60 cells, which were differentiated into neutrophil-like cells, were stimulated with CCL5 in the presence of FLX (1 μ M) or 5-HT (1 μ M). CCL5-mediated β 2-integrin activation was quantified as binding to mAb24, which was measured by MFI using flow cytometry. Data show mean \pm SEM, n=9 (A), n=5 (B), one-way ANOVA followed by Bonferroni multiple comparison test: * P <0.05. (Modified from Rami *et al.*)¹⁶⁹

To elucidate whether the CCL5-dependent induction of integrin activation is solely triggered by FLX or is possibly also evoked by other SSRIs, additional murine integrin activation assays were performed using the newest generation SSRI escitalopram. This drug blocks SERT not only by orthosterically binding in the central cavity, but additionally by binding at an allosteric site, leading to a prolonged SERT blocking activity. Thus, escitalopram shows higher efficiency compared to other SSRIs explaining the lower standard dose of \leq 20 mg/day.¹²⁷ Based on the reported therapeutically used range of 0.05-0.2 μ M in plasma of patients,¹²⁹ a concentration of 0.1 μ M escitalopram was utilized for the *in vitro* experiments. Interestingly, escitalopram strongly augmented CCL5-triggered β 1-integrin binding capability of murine myeloid cells as evidenced by enhanced binding to VCAM1 (Figure 41). However, ICAM1 binding reflecting β 2-integrin activation was less affected. Similar to FLX, escitalopram alone had no effect on

ICAM1 or VCAM1 binding in the absence of CCL5. These findings suggest that SSRIs might more generally influence leukocyte activation.

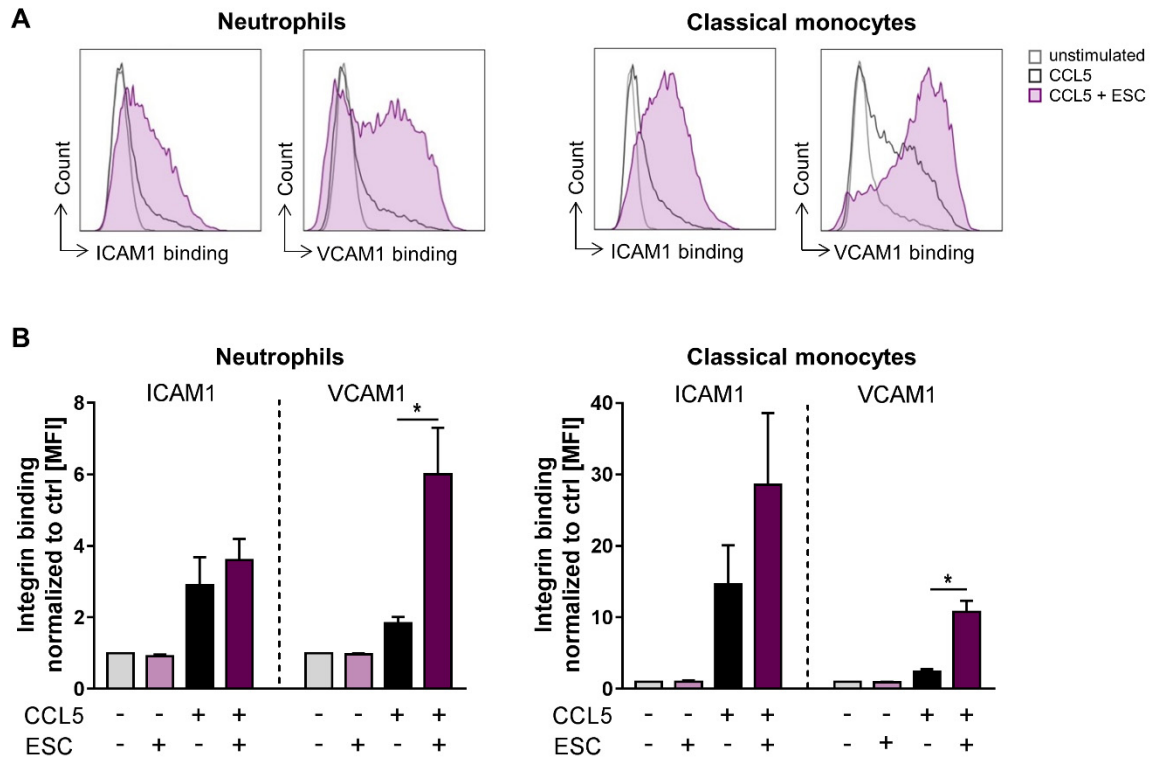


Figure 41: Escitalopram induces CCL5-evoked β 1-integrin activation on mouse blood leukocytes after *in vitro* stimulation.

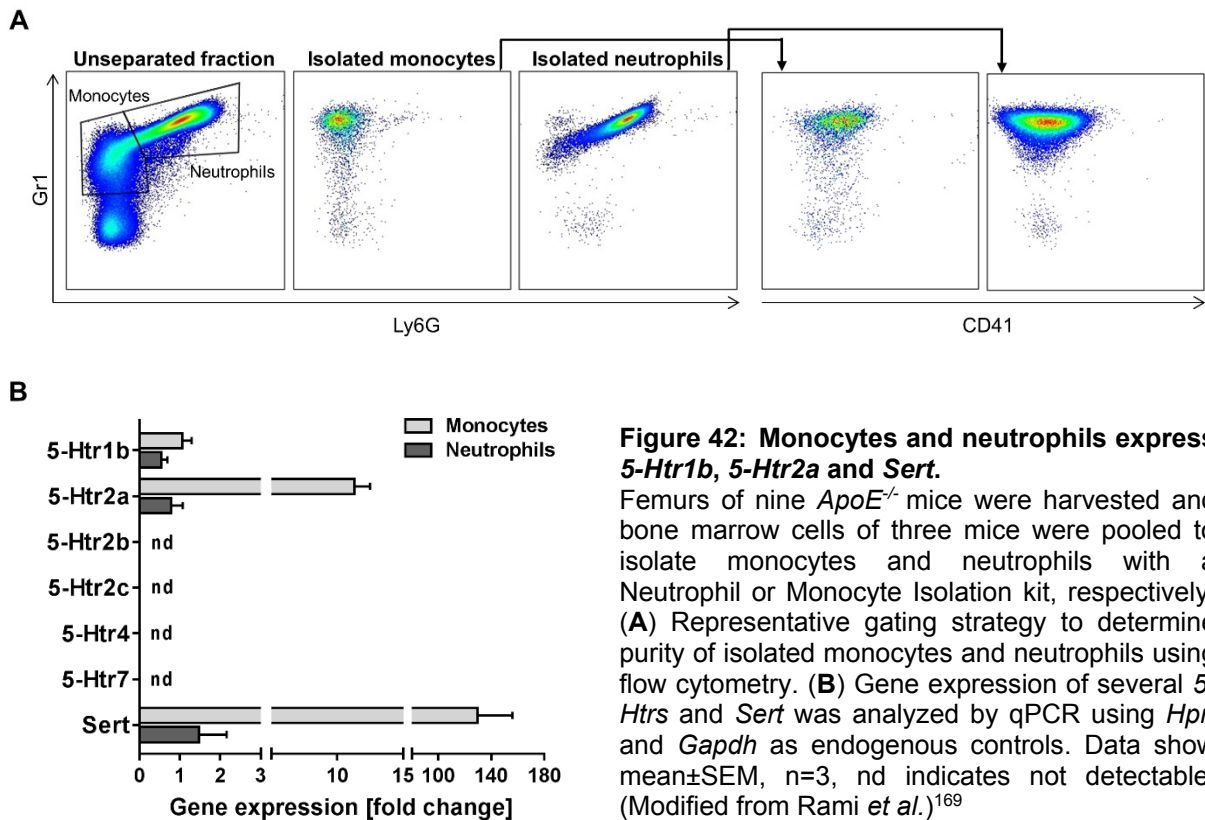
Integrin binding activity by blood leukocytes of C57Bl/6J wild type mice was evaluated after *in vitro* stimulation with escitalopram (ESC; 0.1 μ M) in the presence or absence of CCL5 via leukocyte binding to recombinant ICAM1/Fc or VCAM1/Fc chimera measured by flow cytometry. (A) Representative histogram overlays of ICAM1 and VCAM1 binding of neutrophils (CD45⁺CD11b⁺Gr1⁺Ly6G⁺) and classical monocytes (CD45⁺CD11b⁺Gr1^{high}Ly6G⁻). (B) Quantitative analysis of integrin binding activity of neutrophils and classical monocytes via geometric MFI. Data show mean \pm SEM, n=8-9, one-way ANOVA followed by Bonferroni multiple comparison test: * P <0.05. (Modified from Rami *et al.*)¹⁶⁹

5.13 FLX does not induce a calcium response via 5-HTR2a

Although it is generally assumed that FLX is highly specific for SERT, it was previously reported that it also binds to several 5-HTRs even though with a lower affinity.¹⁷⁴ To further understand the mechanism behind the FLX-evoked enhanced integrin activation, the presence of 5-HTRs and SERT in myeloid cells was analyzed. Therefore, murine monocytes and neutrophils were isolated from pooled bone marrow cells and purity was verified by flow cytometric analysis. The average of the obtained purity of the three pools of monocytes and neutrophils was 85 % and 98 %, respectively (Figure 42A). Since staining for platelet marker CD41 was negative a contamination with platelets was excluded. Gene expression analysis was performed in the three pools of isolated neutrophils and monocytes via qPCR. While mRNA levels of *5-Htr2b*, *5-Htr2c*, *5-Htr4* and *5-Htr7* were below the limit of detection, expression of *5-Htr1b*, *5-Htr2a* and *Sert* was verified in both monocytes and neutrophils (Figure 42B). Of note, the mRNA

RESULTS

levels of *5-Htr1b*, *5-Htr2a* and *Sert* in monocytes compared to neutrophils were higher by 2-fold, 14-fold and 88-fold respectively.



Additionally, possible FLX-mediated effects on gene expression of *5-Htrs* and *Sert* were investigated in aortas of mice fed a HFD for 2 or 4 weeks. After 2 weeks treatment, *Sert* and receptor expression only tended to be changed by FLX (Figure 43A). After 4 weeks, *5-Htr2a* expression was induced whereas *5-Htr2b* and *Sert* expression was decreased in FLX-treated mice compared to untreated control group (Figure 43B). *5-Htr2c* and *5-Htr4* and *5-Htr7* mRNA levels were below the limit of detection.

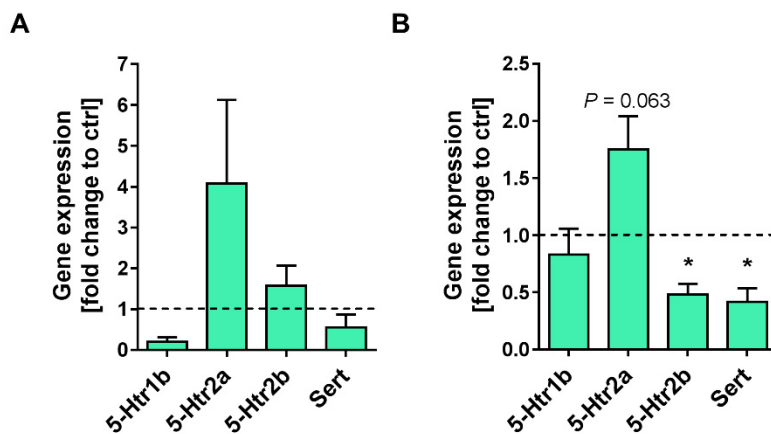


Figure 43: FLX treatment alters expression of *5-Htrs* and *Sert* in aorta.

Gene expression of *5-Htrs* and *Sert* was determined via qPCR in *ApoE*^{-/-} mice treated for (A) 2 or (B) 4 weeks with FLX while feeding a HFD. mRNA levels were analyzed via fold change of treated versus untreated mice. n=4-5 (A) and n=8-10 (B), Student's *t*-test or Mann-Whitney *U* test: **P*<0.05.

RESULTS

Literature reports of binding assays identified 5-HTR2a, 5-HTR2b and 5-HTR2c with the highest affinity for FLX of all tested 5-HTRs.¹⁷⁴ Given that *5-Htr2c* was neither detectable in aortas nor in murine myeloid cells and *5-Htr2b* expression was below the detection limit in myeloid cells (Figure 42B), further experiments focused on the receptor 5-HTR2a. Similar to most other 5-HTRs, 5-HTR2a is a GPCR. It is coupled to G $\alpha_{q/11}$ ¹⁷⁵ and activation leads to an increase of calcium flux, which is described to be essential for integrin activation.^{44,176,177} To elucidate the possibility that FLX might provoke an induction in intracellular calcium levels via 5-HTR2a binding, calcium assays based on human HEK-293 cells were carried out. Therefore, 5-HTR2a-overexpressing Flp-In T-Rex 293 cells were generated. To obtain the expression vector, a restriction digest was performed with a commercially available plasmid coding for the human *5-HTR2a* sequence and with a pcDNA5/FRT/TO plasmid containing N-terminally the coding sequence for the marker gene *eYFP* (Figure 44A). The digest of the plasmid containing the human *5-HTR2a* sequence (line 1) resulted in a band located between 1000 bp and 1650 bp which matches the expected size of 1420 bp for the 5-HTR2a fragment. This band as well as the digested pcDNA5/FRT/TO backbone (line 2) were cut out, purified and ligated followed by bacterial transformation. Several clones were picked and verified for incorporation of *5-HTR2a* via colony PCR (Figure 44B). All tested clones showed the expected size (1420 bp+720 bp) for the fusion protein eYFP-5-HTR2a. The DNA sequence of the plasmid of one of the positively tested clones was verified by sequencing and used for transfection of the inducible Flp-In T-Rex 293 cells. After selection with hygromycin, the expression of the eYFP-5-HTR2a fusion protein of a single cell clone was induced by tetracycline and verified by flow cytometry (Figure 44C) and microscopy (Figure 44D).

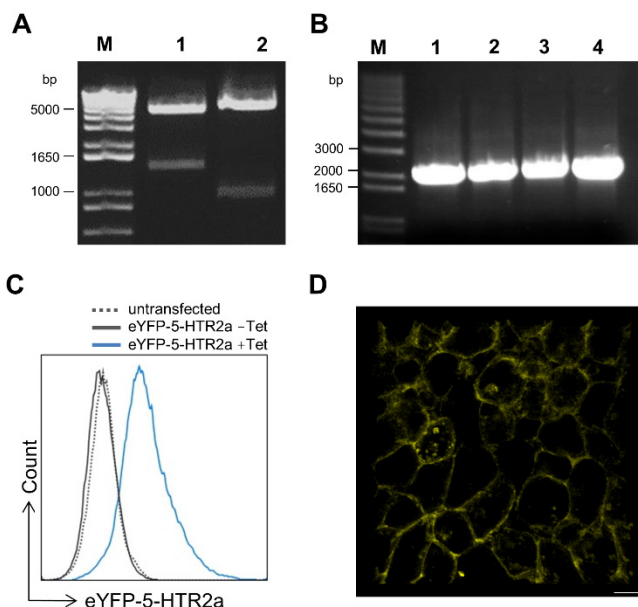


Figure 44: Generation of a 5-HTR2a-overexpressing HEK-293 cell line.

5-HTR2a-overexpressing HEK-293 cell line was generating by first, cloning the cDNA into a pcDNA5/FRT/TO expression vector, N-terminally flanked with the coding sequence for *eYFP* and second, transfection of Flp-In T-Rex 293 cells. (A) Agarose gel of restriction digest with XhoI and BamHI. M = marker, 1 = digested commercially purchased plasmid carrying the coding sequence for human *5-HTR2a*, 2 = digested pcDNA5/FRT/TO expression vector. (B) Colony PCR to verify incorporation of *5-HTR2a* sequence. M = marker, 1-4 = different clones. (C) Representative histogram of eYFP-5-HTR2a-overexpressing HEK-293 cells after induction with tetracycline (Tet). (D) Image of eYFP-5-HTR2a-overexpressing HEK-293 cells recorded with confocal microscopy. Scale bar=8 μ m.

The functionality of the 5-HTR2a-overexpressing cell line was tested by measuring the calcium response upon 5-HT stimulation. 5-HT stimulation led to a concentration-dependent increase in intracellular calcium efflux (Figure 45A). However, FLX, did not induce a calcium response in stably 5-HTR2a-overexpressing HEK-293 cells (Figure 45B), suggesting that FLX does not act via 5-HTR2a.

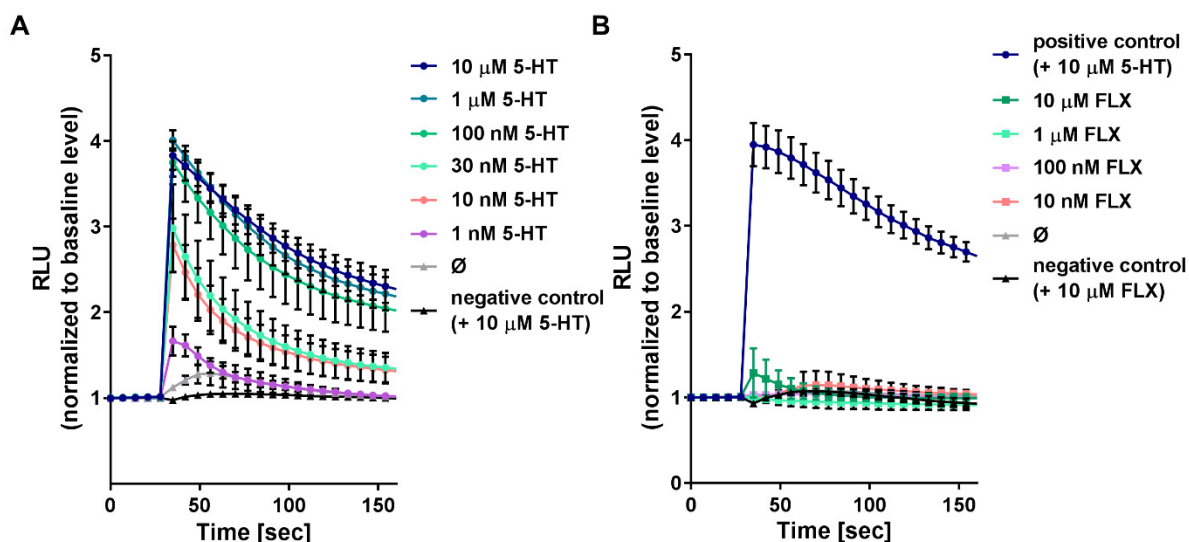


Figure 45: FLX does not trigger a calcium response via 5-HTR2a.

Intracellular calcium was measured in 5-HTR2a-overexpressing HEK-293 cells in response to stimulation with (A) 5-HT or (B) FLX using the FLPR Calcium 5 Assay kit. Non-transfected cells served as negative control. Data show mean \pm SEM, $n=4$ (A) and $n=3$ (B). (Modified from Rami *et al.*)¹⁶⁹

5.14 FLX co-stimulation of chemokine receptors reveals inconclusive findings

Since FLX-mediated integrin activation only occurred in the presence of CCL5, it is possible that FLX affects integrin activity through signaling via acting directly on CCL5 chemokine receptors CCR1 and/or CCR5. In view of this possibility further *in vitro* experiments with HEK-293 cells stably expressing CCR1 or CCR5, respectively, were performed. These cells express in addition to the receptor a luciferase fused to a cAMP binding site. Binding of cAMP to this fusion protein induces luciferase activation, leading to an enhanced luminescence activity in the presence of the appropriate substrate. The signaling of the two G protein $G\alpha_i$ -coupled receptors upon CCL5 stimulation was assessed by the observed reduction of a cAMP signal generated by forskolin, a direct activator of adenylyl cyclases. An additive effect of FLX on CCL5-induced CCR1 and CCR5 signaling would be monitored by a further reduction in cAMP levels. Although dose-dependent CCL5-induced inhibition of cAMP responses in CCR1 and CCR5 expressing cell clones was reproducible (Figure 46A and B), the co-treatment with FLX did not reveal conclusive findings (Figure 46C and D). Therefore, a conclusion on synergistic effects of FLX on CCL5-induced CCR1 and/or CCR5 signaling cannot be drawn.

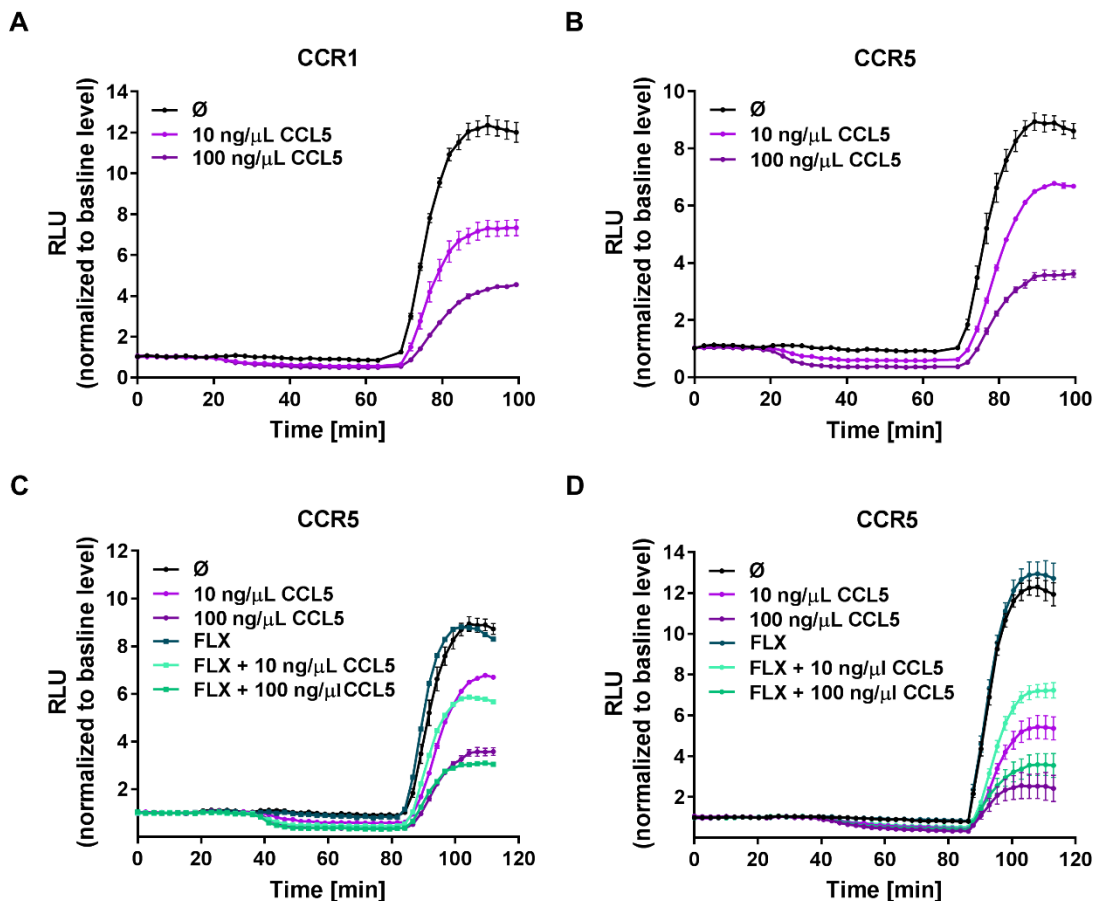


Figure 46: Measurement of CCR1 and CCR5 signaling.

Concentration-response curves for cAMP levels in (A) CCR1- and (B) CCR5-overexpressing HEK-293 cells after stimulation with CCL5 prior to forskolin (1 μ M) treatment using the GloSensor Technology. (C-D) Examples for inconclusive co-stimulation with FLX (1 μ M), 15 min prior to CCL5 treatment followed by forskolin in CCR5-overexpressing HEK-293 cells. Representative results of 2 experiments are shown, obtained with the same clone.

5.15 Pharmacologic TPH1 inhibition does not enhance atherogenesis

To further investigate the hypothesis that the pro-atherogenic effect mediated by FLX was not a consequence of platelet 5-HT depletion but solely caused by the drug, a final *in vivo* experiment with a different approach for peripheral 5-HT depletion was performed. To this end, LP-533401, an inhibitor of the peripheral 5-HT synthesizing enzyme TPH1, was daily administered to *ApoE*^{-/-} mice for 2 or 4 weeks, respectively, in parallel to HFD feeding. First, inhibition efficiency was verified by measuring serum 5-HT levels. At both time points, 5-HT serum levels were significantly decreased upon treatment confirming effective TPH1 inhibition (Figure 47A). Of note, after 2 weeks of injection, overall 5-HT serum levels were very low. More precisely, vehicle mice had with 0.295 μ g/mL much lower 5-HT levels compared to normal serum concentration (> 2 μ g/mL) in *ApoE*^{-/-} mice (Figure 19). At this time point the depletion efficiency was 91 %. After 4 weeks of treatment, vehicle 5-HT serum concentrations were comparable with normal levels of *ApoE*^{-/-} mice, while the 5-HT depletion efficiency was only

RESULTS

36 %. At both time points, neither body weight nor total plasma cholesterol levels were affected by the treatment (Figure 47B,C). Interestingly, in contrast to FLX treatment, TPH1 inhibition did not promote atherosclerosis. In fact, 2 weeks treatment revealed smaller plaque size in aortic roots, which was no longer observed after 4 weeks of treatment (Figure 47D-E).

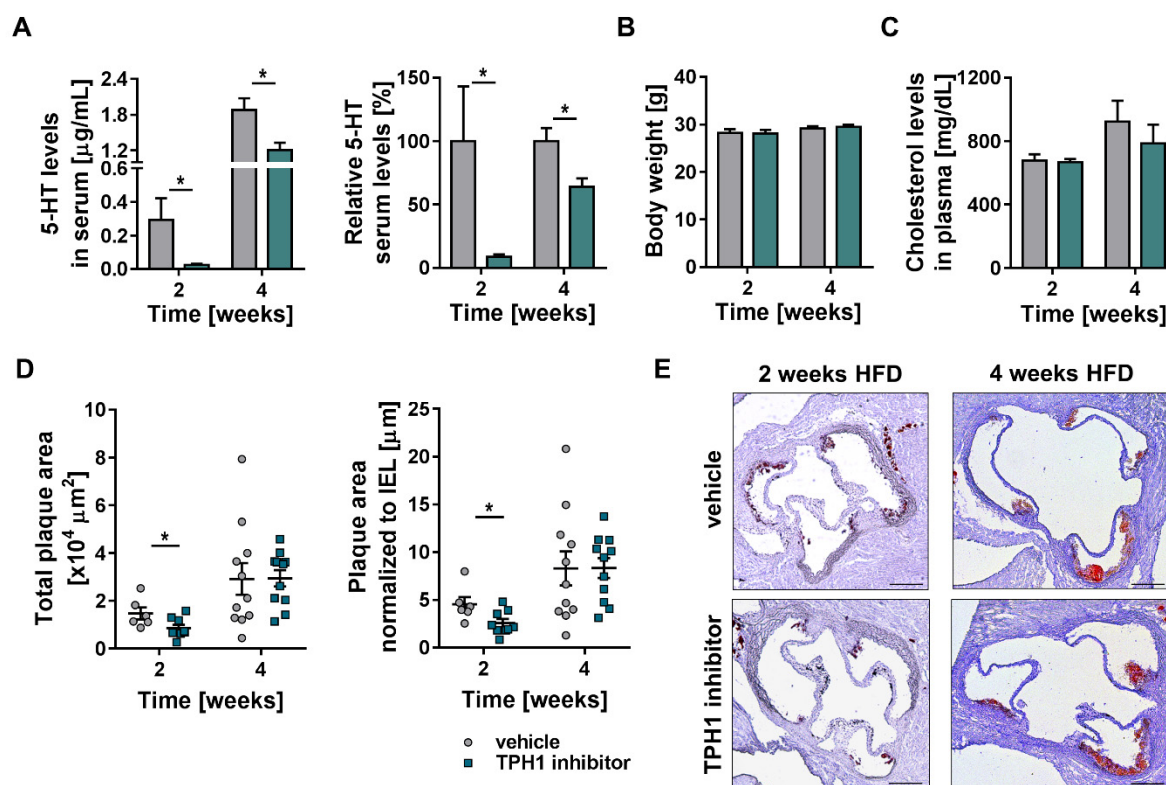


Figure 47: TPH1 inhibition does not promote atherosclerosis.

TPH1 inhibitor LP-533401 (25 mg/kg, i.p.) or vehicle was daily administered to *ApoE*^{-/-} mice parallel to feeding a HFD for 2 weeks or 4 weeks, respectively. (A) TPH1 inhibition was verified by measurement of serum 5-HT levels by ELISA (left) and 5-HT depletion efficiency was determined as reduction of 5-HT serum levels upon treatment (right). (B) Body weight and (C) total plasma cholesterol levels of mice after 2 and 4 weeks treatment. (D) Quantitative analysis of atherosclerosis as total plaque size (left) or normalized to IEL (right) after 2 (n=6-9) and 4 (n=11) weeks of treatment. (E) Representative images of ORO staining of aortic roots. Scale bar=200 μm . Data show mean \pm SEM, Student's *t*-test: **P*<0.05. (Modified from Rami *et al.*)¹⁶⁹

Contrary to FLX treatment, TPH1 inhibition did not transiently decrease leukocyte or platelet counts (Figure 48A). Also, MPV was not affected by pharmacological 5-HT depletion (Figure 48B). Similarly, the surface protein levels of ICAM1 and VCAM1 on aortic endothelial were comparable between groups (Figure 48C). Focusing on the analysis of adhesion molecule on blood neutrophils revealed that protein levels of L-selectin (CD62L) tend to be decreased and PSGL1 increased, while the amount of integrins and CD31 was not affected by LP-53340 treatment (Figure 48D).

RESULTS

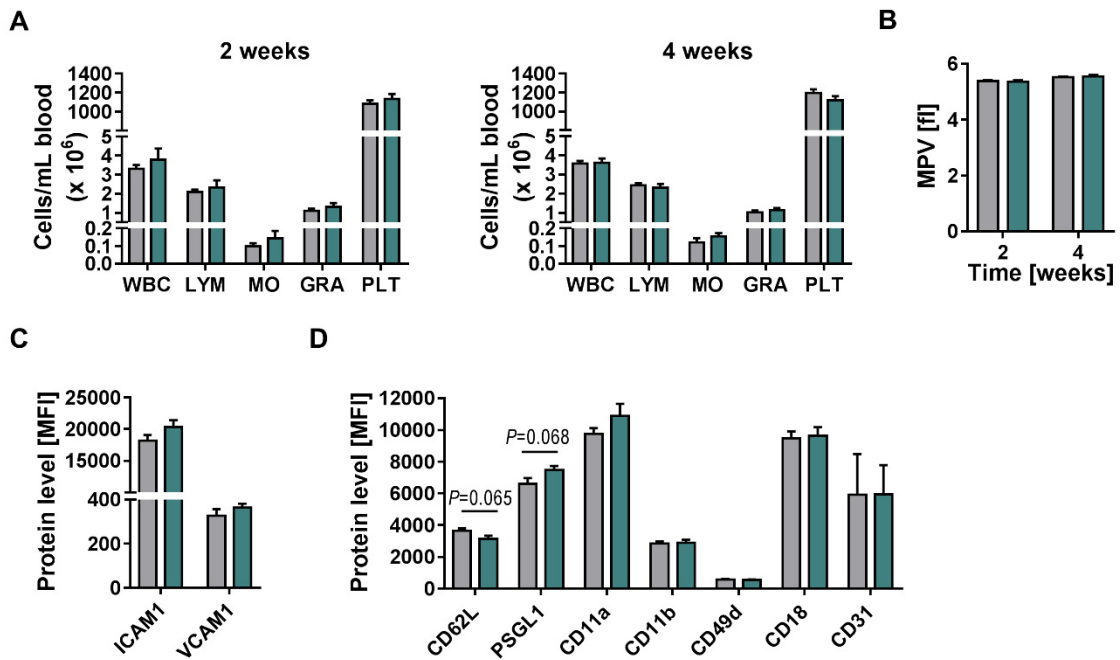


Figure 48: Effect of TPH1 inhibition on blood cell counts and adhesion molecule levels.

ApoE^{-/-} mice were injected daily with TPH1 inhibitor LP-533401 (25 mg/kg, i.p.) or vehicle parallel to HFD feeding. (A) blood counts of white blood cells (WBC), lymphocytes (LYM), monocytes (MO), granulocytes (GRA) and platelets (PLT) were measured with a hematology analyzer after 2 (left) or 4 (right) weeks treatment. (B) MPV was measured using a hematology analyzer. The protein levels of adhesion molecules were assessed on (C) aortic endothelial cells (CD45⁺CD31⁺CD107a⁺) after 2 weeks treatment and on (D) blood neutrophils after 4 weeks treatment by flow cytometry. Data show mean \pm SEM, n=8-9 (A-C) and n=10-11 (D), Student's *t*-test or Mann-Whitney *U* test: **P*<0.05.

6 DISCUSSION

CVD and depression are among the most frequent health problems of our society.^{1,118} It is widely accepted that there is a link between both diseases. This is evident not just by the high prevalence of depression among CVD patients, but also by the finding that depression poses an independent cardiovascular risk factor.^{119,120} However, it is not merely a risk factor, but depression was also reported to worsen the outcome of CVDs.^{178,179} The underlying mechanism of this association, however, remains poorly understood. One aspect might be the behavior and lifestyle of people suffering from depression.¹⁸⁰ The question thus arises if antidepressant treatment may reduce the incidence of CVDs. So far, several studies investigated the potential effect of SSRIs, the most prescribed antidepressants, on the incidence of cardiovascular events. However, the findings are inconclusive.^{135,136,145–154,137,155,138–144} In this thesis, the impact of the common SSRI FLX on the onset and progression of atherosclerosis was investigated in a mouse model. The rationale of this experimental setting was to minimize confounding effects by depression and behavioral risk factors.

6.1 FLX treatment enhances atherogenesis by promoting leukocyte recruitment

The effect of FLX intake on the different stages of atherosclerosis was studied in *ApoE*^{-/-} mice which were fed with a Western diet. Unexpectedly, FLX exhibited a pro-atherogenic effect already observed after 2 weeks of treatment, which was preserved up to 16 weeks. This observed pro-atherogenic effect can be explained by increased vascular leakage and enhanced myeloid cell recruitment due to amplified CCL5-induced integrin activation upon FLX treatment. An alternative approach for peripheral 5-HT depletion by pharmacological TPH1 inhibition did not phenocopy the FLX-mediated pro-atherogenic effect, indicating that FLX enhances plaque formation despite 5-HT platelet depletion.

Although FLX therapy was described to be associated with a reduction of body weights and cholesterol levels in patients,^{181,182} both parameters were similar in control and FLX-treated mice at any end point of the treatment. The weight loss in patients was assigned to only occur temporarily due to an impact on appetite, since chronic treatment revealed no differences.¹⁸¹ In mice, transient changes in body weight at the onset of the treatment might be blunted when changing from normal chow to Western diet. As to the opposing findings in cholesterol levels, these may rely on the different lipid profiles between humans and mice. The reduction of cholesterol levels in patients was caused by a decrease in LDL levels. In wild type mice, however, the main subfraction is HDL while *ApoE*^{-/-} mice have a massive increase in the VLDL fraction.¹² However, given that total cholesterol levels were not affected by FLX treatment, a detailed analysis of cholesterol subfractions was not performed.

Chronic FLX administration is known to deplete intra-platelet 5-HT, which reflects the major peripheral 5-HT storage site. This has been reported in depressed patients treated with SSRIs as well as in mice receiving the same drug.^{115,131} Indeed, after seven days of FLX administration, mice possessed a significant decrease in serum 5-HT. Because several studies associate platelet 5-HT with a pro-inflammatory role in diseases such as colitis,⁸² asthma⁸³, inflammatory bowel disease,⁸² and obesity,⁸⁴ the pro-atherogenic effect of FLX in atherogenesis was surprising. Herr *et al.* described that an acute FLX treatment leads to transiently elevated plasma 5-HT levels within the first hours, thereby promoting leukocyte-endothelial interactions.¹¹⁶ However, the same pro-atherogenic effect of FLX was observed irrespective of the time point of FLX onset, with or without FLX pretreatment for 2 weeks before starting the atherogenic diet. Thus, temporary increased 5-HT concentrations were excluded as underlying cause for the observed increase in plaque formation. FLX administration neither altered the plaque composition in advanced lesions, nor the progression of already established plaques. Remarkably, the FLX-mediated increase in lesion size was most pronounced during the early phase of atherogenesis. These findings suggest that FLX may affect the processes involved in plaque formation such as myeloid cell recruitment, enhanced platelet activity and endothelial activation. Indeed, FLX-treated mice exhibited an increased neointimal macrophage accumulation. This might be caused by enhanced transendothelial migration, since FLX-treated mice revealed an augmented vascular permeability and increased arterial adhesion of myeloid cells.

As already mentioned above, myeloid cell recruitment to the arterial wall is a crucial step in plaque formation. The interaction of circulating leukocytes with the endothelium involves a coordinated interplay of endothelial adhesion molecules with their counterparts on leukocytes.²⁴ On the part of the endothelium, an FLX-induced modulation of the adhesion molecules was excluded. This contradicts previously published *in vitro* data, which reported that FLX decreased TNF α -induced ICAM-1 and VCAM-1 protein levels in human aortic endothelial cells.¹⁸³ However, apart from direct *in vitro* stimulation of murine immortalized endothelial cells, the observation that FLX does not affect endothelial adhesion molecules was confirmed by mRNA and protein measurement in aortas of FLX-treated mice. This provides evidence that FLX is not altering protein levels of adhesion molecules in these settings. Cell transmigration is also dependent on the vascular integrity, which can be regulated and maintained by platelets.⁵⁶ 5-HT is known to provoke platelet activity by a positive feedback mechanism leading to amplified platelet activation.¹⁰⁶ One may speculate that the detected increase in vascular permeability upon FLX-treatment is caused by reduced platelet activation. However, platelet characteristics were similar between control and FLX-treated mice. Thus, the aggravated endothelial permeability might be rather a secondary consequence of FLX-mediated leukocyte recruitment. The barrier function of the endothelium is not only maintained

by platelets but also by multiple proteins regulating the intercellular junctions between endothelial cells. By altering the strength of the endothelial cell-cell interactions, the organism can adjust vascular permeability to adapt to particular needs. In addition, endothelial permeability is increased by inflammatory stimulation. Several proteins are involved in the regulation of permeability of which claudins, occludins and JAMs are the best known.⁶ It is conceivable that FLX affects endothelial intercellular junctions, which was not further investigated in this study.

Lesional leukocytes originate from bone marrow and spleen, from where they are recruited into the circulation and subsequently to the vessel wall. An effect of FLX on these organs was excluded, based on the observation that similar myeloid cell counts in these organs were determined in FLX treated mice compared to the control group. The observed transient decrease in circulating leukocyte and platelet counts might be a consequence of enhanced arterial adhesion. In humans and mice, the increased frequency of circulating PLAs is associated with more severe inflammation.^{61,63} However, FLX-treated mice did not reveal a higher incidence of PLAs, which could be one explanation for decreased platelet number and amplified adhesion. The detected neutropenia and enhanced endothelial recruitment is somehow in conflict with previously published data obtained in mice lacking peripheral 5-HT.¹¹⁵ Duerschmied and colleagues observed a mild neutrophilia and less neutrophil adhesion to mesenteric post-capillary venules in mice deficient for TPH1 as well as in wild type mice treated with FLX.¹¹⁵ The opposing findings might arise from the different vascular beds examined by Duerschmied *et al.* and the present study. While Duerschmied *et al.* assessed leukocyte adhesion in the microvasculature, the present study performed intravital microscopy of atherosclerosis-prone carotid arteries, which refers to macrovasculature. In large arteries under high blood pressure, leukocyte recruitment to the endothelium may require other mechanisms than those described in post-capillary venules to facilitate adhesion.³³ Indeed, dissimilarities in leukocyte adhesion between micro- and macrovasculature were observed before.^{17,18} Drechsler *et al.* found that recruitment of neutrophils to large arteries is dependent on the chemokine receptors CCR1, CCR2, CCR5, and CXCR2, whereas recruitment to peripheral veins is independent of CCR1 and CCR5 and only requires CCR2 and CXCR2. They propose that this is ascribed to the deposition of the CCR1 and CCR5 ligand CCL5 on the endothelium by platelets, which occurs in arteries but not in veins.¹⁷ Similarly, Ortega-Gomez *et al.* demonstrated that neutrophil-derived cathepsin G preferentially binds to arterial rather than venular endothelium in a CCL5-dependent manner, thereby inducing integrin clustering, which in turn results in arterial-specific myeloid cell adhesion.¹⁸ They speculate that differences in the composition of surface molecules on the arterial endothelium are causing these observations.¹⁸ In fact, shear forces are much higher in macrocirculation compared to microcirculation. As a consequence, the endothelium and the mechanisms involved in

leukocyte adhesion are adapted to withstand those high flow rates. Scott *et al.* highlighted the heterogeneity that exists on the endothelium from different vascular beds. For example, ICAM1 and VCAM1 expression patterns upon inflammatory stimulation differ between endothelial cells from different origins. Furthermore, they also found that N-glycan profiles on the cell surfaces are vascular bed-specific,¹⁸⁴ which may explain the vessel-dependent dissimilarities in CCL5 binding.¹⁸ Thus, site-specific differences in this study (macrovasculature) compared to the one from Duerschmied *et al.* (microvasculature) may explain the opposing findings. Another important aspect is the underlying hypercholesterolemia in *ApoE*^{-/-} mice receiving a HFD. These mice display a chronic inflammation including endothelial dysfunction. The relevance of the inflammatory setting and the site-specificity is corroborated by the findings that non-atherogenic wild type mice treated with FLX did not exhibit the transient reduction in blood counts and showed less neutrophil extravasation in an acute peritonitis model.

The recruitment of leukocyte to the site of inflammation is not only dependent on alterations of the endothelium but also on the activation of leukocytes.²⁴ The leukocyte-endothelial binding is mediated by the interaction of selectins and integrins with their corresponding ligands. FLX treatment neither altered the surface levels of adhesion molecules such as PSGL1 and CD62L nor the protein levels of several integrins on circulating neutrophils. The *in vivo* imaging of leukocyte adhesion revealed that FLX affects adhesion but not rolling. The main adhesion proteins involved in this process are the integrins. These molecules are rather regulated by activation than changes in expression. Several studies described that integrin activation and clustering are important events in atherogenesis.^{18,161} Indeed, neutrophils and monocytes of FLX-treated mice revealed an increased CCL5-induced integrin activity, which was observed in both β 1- and β 2-integrins. Remarkably, *in vitro* stimulation of blood leukocytes of wild type mice and human neutrophils-like cells with FLX amplified CCL5-induced integrin binding capacity. However, this effect only occurred in the presence of CCL5. This positively supports the hypothesis that the observed FLX-mediated pro-atherogenic effect is site-specific and dependent on the presence of enhanced chemokine levels, as in the case of chronic hypercholesterolemia. The fact that 5-HT *in vitro* stimulation of mouse and human cells did not affect integrin capability provides evidence that the *in vivo* detected pro-atherogenic phenotype of FLX is independent of 5-HT platelet depletion.

6.2 Atherosclerosis affects the serotonergic system

Several components of the serotonergic system are present in cells which are involved in atherogenesis. While *5-Htr1b* is highly expressed by endothelial cells and *5-Htr2a* by vascular SMCs,¹⁰⁴ immune cells express several *5-Htrs*.^{75,81,85,105} In this study, *5-Htr1b* and *5-Htr2a* as well as *Sert* were detectable in murine monocytes and neutrophils isolated from the bone marrow. Apart from *5-Htr2a* and *Sert*, which are known to be expressed by monocytes, *5-Htr1b*

was also found to be present, which was not reported before. However, transcripts for *5-Htr4* and *5-Htr7*, which were measured in other studies, were under the detection limit. Less is known about the existence of *5-Htrs* and *Sert* in neutrophils.⁷⁵ To my knowledge, this is the first study showing a clear signal for *Sert* in murine neutrophils, even though it is much weaker than the transcript level in monocytes. Inconsistencies between different studies may arise from methodical issues, such as qPCR sensitivity, or the activation status of the examined cells. For example, in naïve T cells the expression of *5-Htr1b* and *5-Htr2a* was reported to be undetectable, while T cell activation led to a substantial increase of mRNA and protein levels.¹⁸⁵ In the current study, cells were isolated from the bone marrow instead of blood to avoid a contamination by leukocyte-bound platelets. The purity of monocytes and neutrophils was 85 % and 98 %, respectively. Therefore, minor contaminations cannot be fully excluded. Novel technologies such as single-cell RNA sequencing would be helpful to unravel in-depth the *5-Htr* expression profiles of immune cells. Nevertheless, it is undoubtful that monocytes as well as neutrophils comprise several components of the serotonergic system. Interestingly, atherosclerosis affected the serotonergic system, as evidenced by the analysis of *Sert* and *5-Htr* expression patterns in aorta, bone marrow and spleen. Given that *5-Htrs* and *Sert* are differentially expressed in many leukocytes as well as in endothelial cells and vascular SMC, a shift in the cell-composition within the measured organs with progressing atherosclerosis might be a possible explanation for the observed changes in relative expression levels of *Sert* and *5-Htrs*. In addition, cell activation during atherosclerosis might alter the expression pattern within the different cell types. Apart from the receptors, 5-HT serum levels decreased with advanced atherosclerosis, possibly linked to augmented platelet activity. This is in line with a publication showing that plasma 5-HT levels are elevated during atherosclerosis as a consequence of an enhanced release of 5-HT by activated platelets in patients with atherosclerosis.¹⁸⁶

6.3 The underlying molecular mechanism of FLX-mediated integrin activation requires further investigation

A limitation of this study is that the exact mechanism how FLX enhances CCL5-induced integrin activity in myeloid cells was not elucidated. One possible mechanistic explanation might reside in an interaction between SERT and integrin signaling. Indeed, there seems to be a link between SERT and integrins. In platelets, a physical interaction between $\alpha\text{IIb}\beta\text{3}$ integrin and SERT has been described to influence SERT trafficking and activity.¹⁸⁷ Potentially there is a mutual interaction between these two membrane-bound proteins, hence, SERT stimulation might also affect integrin function. Another conceivable explanation might be that FLX mediates integrin activity independent of SERT signaling via binding to one of the 5-HTRs. There are publications revealing that SSRIs are able to act through pathways different from their canonical mode of action. Citalopram, for instance, was recently reported to inhibit platelet

function at high concentrations *in vitro* by a yet unknown mechanism, which is independent of SERT-mediated 5-HT transport.¹⁸⁸ Furthermore, FLX causes bone resorption by interfering with calcium–calmodulin signaling in osteoclasts in a 5-HT-reuptake-independent pathway.¹⁸⁹ Although SSRIs are considered to be highly selective for SERT, a binding study, however, revealed that FLX displays affinity for some 5-HTR-subtypes, even though much lower than for SERT. FLX had a K_i value of 119 nM for 5-HTR2a, 118 nM for 5-HTR2c and 2514 nM for 5-HTR2b, respectively, while the affinity mainly arises from the (*R*)-enantiomer.¹⁷⁴ Whereas 5-*Htr2c* was neither detectable in aortas nor in murine myeloid cells and 5-*Htr2b* was below the detection limit in myeloid cells, 5-*Htr2a* was present in myeloid cells and regulated upon FLX treatment in aortas. Thus, one may speculate that the action of FLX is mediated by 5-HTR2a. This receptor is GPCR coupled to $G\alpha_{q/11}$, thus stimulation leads to a PLC-mediated release of calcium from the intracellular storages.⁸⁶ The exact mechanism of integrin inside-out signaling is not well defined. It is believed that chemokine-induced GPCR stimulation triggers PLC-mediated Rap1 GTPase activation. Downstream signaling leads to integrin extension to their high affinity conformation, consequently resulting in integrin activation and thereby enabling ICAM1/VCAM1 binding.^{33,39} Interestingly, FLX was shown to provoke intracellular calcium release in a lymphoma and bladder carcinoma cell line.^{190,191} However, the possibility that FLX induces a calcium response by 5-HTR2a stimulation was excluded by *in vitro* assays with 5-HTR2a-overexpressing HEK-293 cells. In contrast to FLX, 5-HT stimulation caused a strong calcium signal. Thus the question arises why 5-HT *in vitro* did not enhance integrin activity in myeloid cells. The two detected 5-HTRs on myeloid cells, 5-HTR2a and 5-HTR1b, are coupling to different G proteins, since 5-HTR1b signals via $G\alpha_{i/o}$.⁸⁷ While FLX was found to bind to 5-HTR2a, the reported K_i value for 5-HTR1b was >5000 nM, indicating that FLX has no affinity for this receptor.¹⁷⁴ As a result, FLX- and 5-HT-induced 5-HTR signaling may differ depending on the receptor affinities, which in turn results in alternative responses.

Given that the FLX-mediated increase in integrin activation only occurred in the presence of CCL5, another likely cause may reside in a synergistic effect of FLX and CCL5 on the CCL5 chemokine receptors CCR1 and CCR5. However, *in vitro* assays investigating a possible additive effect on CCR1 or CCR5 revealed inconclusive findings, although dose-dependent CCL5-induced signaling was reproducible. Thus, at this time point a clear statement on this issue cannot be made. Apart from that, the transfected HEK-293 only presents signaling responses of individual overexpressed receptors. Therefore, co-activation and interaction between different chemokine receptors and 5-HTRs cannot be excluded as a potential mechanism affecting integrin binding capability. Furthermore, it is also probable that FLX is not directly amplifying integrin activation but prevents integrin inactivation and thereby prolongs the activity. Thus, the exact underlying molecular mechanism by which FLX promotes the binding of integrin to ICAM1 and VCAM1 still remains to be clarified.

6.4 TPH1 inhibition as therapeutic target

The notion that the FLX-mediated pro-atherogenic phenotype is independent of platelet 5-HT depletion was further supported by the finding that pharmacological depletion of peripheral 5-HT did not enhance atherosclerosis. The TPH1 inhibition was accomplished by using LP-533401, a peripheral TPH1 inhibitor, which has already been patented for treating diabetes and obesity.^{192,193} However, so far there are no clinical studies using this drug for the treatment of both diseases.¹⁹⁴ Remarkably, the TPH1 inhibition by LP-533401 even mitigated lesion plaque formation after 2 weeks of treatment. In the FLX experiments, the pro-inflammatory phenotype of FLX might override the anti-inflammatory effect caused by platelet 5-HT depletion. In fact, FLX-treated mice also displayed some anti-inflammatory markers as shown by a significant reduction of *Ccl5* expression in aortas. To confirm this statement further analyses of mice treated with the TPH1 inhibitor are needed. Interestingly, the anti-atherogenic phenotype of LP-533401 observed after 2 weeks was no longer present at the later time point. One possible reason could be the lower inhibition efficiency detected after 4 weeks of treatment compared to 2 weeks. Notably, at the early time point both treated and vehicle group revealed very low 5-HT serum levels compared to those of *ApoE*^{-/-} mice without injections. This might be a stress-related phenomenon due to daily injections at the beginning of the experiment. Another conceivable explanation is that the pharmacological peripheral 5-HT depletion affects only the very early lesion formation. A previous study demonstrated that mice deficient for JAM-A in platelets exhibit accelerated plaque formation in aortic roots at the very early stage after 2 weeks, which was no longer present at a later time point. The authors claim that this effect is caused by platelet hyper-reactivity, most profoundly on events involved in the onset of atherogenesis.¹⁹⁵ Thus, TPH1 inhibition might alter platelet reactivity, which is particularly relevant at lesion initiation. To confirm this hypothesis, the analysis of the platelet function in LP-533401-treated mice is an interesting part of future studies. Furthermore, generation of genomic *Tph1* knockout in mice with an atherogenic background would help to further understand the role of peripheral 5-HT in atherosclerosis.

Consistent with findings of Duerschmied *et al.* obtained in *Tph1*^{-/-} mice, pharmacological TPH1 inhibition by LP-533401 revealed an almost significant reduction of L-selectin in circulating neutrophils.¹¹⁵ The authors postulated that the decreased L-selectin density on the cell surface of neutrophils is a consequence of enhanced shedding, which results in diminished neutrophil-endothelium interactions. While they observed that PSGL-1 levels are not affected, LP-533401 treatment showed a mild induction. Whether chronic LP-533401 administration also affects leukocyte adhesion to the arterial wall will be an important issue of future experiments.

A previous study by Crane and colleagues showed that LP-533401 treatment protects mice from HFD-induced obesity via activation of brown adipose tissue thermogenesis.¹⁵⁹ The reduction in body weight was significant after 6 weeks of treatment. Thus, no effect on body

weights in *ApoE*^{-/-} mice after 2 and 4 weeks of LP-533401 injection are in line with the observations of Crane *et al.* Whether the use of LP-533401 may not only be a beneficial treatment for obesity¹⁵⁹ and other related diseases such as type 2 diabetes,¹⁵⁹ but also for atherosclerosis deserves further investigation.

6.5 FLX-mediated aggravation of atherosclerosis – a drug class specific effect?

FLX mediated a pro-atherogenic effect caused by enhanced leukocyte adhesion due to amplified integrin activation. Given that the SSRI escitalopram also triggered integrin binding capability, this effect is probably not unique for the drug FLX but SSRI class specific. This is further supported by a previous published study with primates, which showed that diet-induced coronary artery atherosclerosis was aggravated in cynomolgus macaques treated with the SSRI sertraline.¹⁹⁶

SSRIs are small molecules with diverse chemical structures, which differ not only in the binding affinity to SERT but also in the structural basis of binding.^{100,128} For example, escitalopram is described to occupy, in addition to the central binding cavity, a second so-called allosteric binding site.¹⁰⁰ This likely accounts for the slight dissimilarity in integrin activation between FLX and escitalopram with the latter preferentially activating β 1-integrins over β 2-integrin. Future studies have to address the question if the treatment with other SSRIs also leads to a pro-atherogenic phenotype.

6.6 Conclusion and future perspectives

Given the increasing incidence of depression and CVDs, it is of crucial importance to clarify a possible influence of SSRIs, the first line antidepressant medication, on cardiovascular risk. The results from this thesis make an important contribution to that issue by providing the first experimental proof that FLX induces atherogenesis in a mouse model. While this study found an unexpected effect of FLX on integrin activation in myeloid cells, further experiments are required to understand additional mechanistic details. At this stage, it can only be concluded that the integrin activation is a direct effect of the drug itself, but not a consequence of its pharmacological effect in lowering 5-HT serum levels. First, it would be interesting to elucidate how exactly FLX induces integrin activation. Therefore, the question should be addressed if the SSRI-mediated effect on integrin activation is dependent on interference with the serotonergic system or with other proteins such as chemokine receptors. Further *in vitro* and *in vivo* experiments using specific antagonists for 5-HTRs and mice deficient for SERT, CCR5 and CCR1 would be needed to assign the function to a specific molecule. Moreover, the analysis of integrin clustering (based on confocal or atomic force microscopy), a process of high importance to achieve effective adherence under high-shear flow in large arteries,¹⁸ would also provide further insight into the impact of SSRIs on integrin regulation.

Patients with major depression possessed decreased lymphocyte blood counts after intake of escitalopram for 8 weeks, while monocyte and neutrophil counts were not affected.¹⁹⁷ Since the observed reduction in the mouse model was only transient, it would be interesting to assess blood count changes in patients after the onset of SSRI treatment in a time course experiment. It should be noted that the time point of blood sampling is crucial, because the number of circulating leukocytes in the blood oscillates due to the circadian rhythm.¹⁹⁸ Although FLX affected human neutrophil-like cells similar to murine cells, additional studies are needed to corroborate the relevance for humans. Besides, the metabolite of FLX, norfluoxetine, plays an important role for the therapeutic effect in patients,¹⁹⁹ which was not taken into account in the *in vitro* assays. Therefore, integrin activation should be assessed in leukocytes from depressed patients with and without hypercholesterolemia before and after the onset of SSRI treatment.

In summary, the present study is the first report of a pro-atherogenic effect of the SSRI FLX, which is provoked by enhanced CCL5-induced integrin activation in a 5-HT-independent manner (Figure 49). These novel mechanistic insights are of broad scientific interest, as they suggest that FLX potentially increases the risk for acute cardiovascular events such as myocardial infarction. Due to possible pro-atherogenic effects of SSRIs, the use of these drugs should be carefully reconsidered especially in cardiovascular risk patients or at least these patients should be carefully monitored.

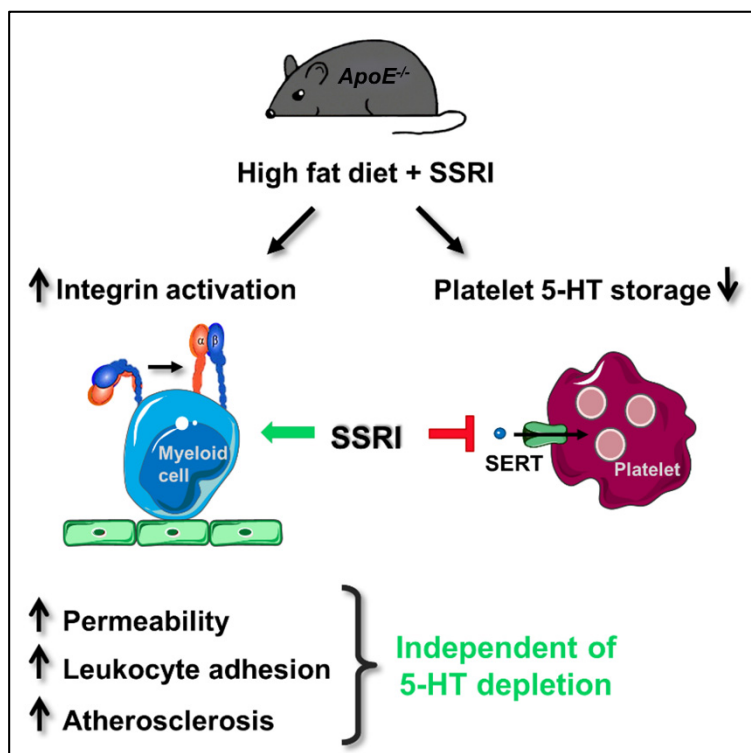


Figure 49: Summary of the effect of chronic SSRI intake on atherosclerosis in a mouse model.

ApoE^{-/-} mice were treated with the SSRI FLX in parallel to HFD feeding. Aside from the expected depletion in platelet 5-HT, FLX treatment leads to enhanced integrin activation on myeloid cells. This was accompanied by augmented vascular permeability and increased leukocyte adhesion, which in turn leads to aggravated atherosclerosis. These findings were independent of 5-HT, but dependent on an inflammatory milieu. (Adapted from Rami *et al.*)¹⁶⁹

7 REFERENCES

1. WHO | Cardiovascular diseases (CVDs). WHO. <http://www.who.int/mediacentre/factsheets/fs317/en/>. Published 2017. Accessed January 8, 2018.
2. Global atlas on cardiovascular disease prevention and control. *WHO*. 2011;105:3A-9A.
3. Dahlöf B. Cardiovascular Disease Risk Factors: Epidemiology and Risk Assessment. *AJC*. 105:3A-9A.
4. Gisterå A, Hansson GK. The immunology of atherosclerosis. *Nat Rev Nephrol*. 2017;13:368-380.
5. Libby P, Ridker PM, Hansson GK. Progress and challenges in translating the biology of atherosclerosis. *Nature*. 2011;473:317-325.
6. Patrick L, Lehoux S, Gros R, Bobryshev Y V, Chistiakov DA, Orekhov AN. Endothelial Barrier and Its Abnormalities in Cardiovascular Disease. *Front Physiol*. 2015;6:365.
7. Zhou J, Li Y-S, Chien S. Shear stress-initiated signaling and its regulation of endothelial function. *Arterioscler Thromb Vasc Biol*. 2014;34:2191-2198.
8. Ference BA, Ginsberg HN, Graham I, et al. Low-density lipoproteins cause atherosclerotic cardiovascular disease. 1. Evidence from genetic, epidemiologic, and clinical studies. A consensus statement from the European Atherosclerosis Society Consensus Panel. *Eur Heart J*. 2017;38:2459-2472.
9. Woollard KJ. Immunological aspects of atherosclerosis. *Clin Sci (Lond)*. 2013;125:221-235.
10. Bobik A. Transforming growth factor-betas and vascular disorders. *Arterioscler Thromb Vasc Biol*. 2006;26:1712-1720.
11. Hansson GK, Libby P, Tabas I. Inflammation and plaque vulnerability. *J Intern Med*. 2015;278:483-493.
12. Emini Veseli B, Perrotta P, De Meyer GRA, Roth L, Van der Donckt C, Martinet W, De Meyer GRY. Animal models of atherosclerosis. *Eur J Pharmacol*. 2017;816:3-13.
13. Albert PR, Benkelfat C. The neurobiology of depression--revisiting the serotonin hypothesis. II. Genetic, epigenetic and clinical studies. *Philos Trans R Soc Lond B Biol Sci*. 2013;368:20120535.
14. Silvestre-Roig C, de Winther MP, Weber C, Daemen MJ, Lutgens E, Soehnlein O. Atherosclerotic Plaque Destabilization. *Circ Res*. 2014;114:214-226.

REFERENCES

15. Swirski FK, Nahrendorf M. Leukocyte behavior in atherosclerosis, myocardial infarction, and heart failure. *Science*. 2013;339:161-166.
16. Soehnlein O, Swirski FK. Hypercholesterolemia links hematopoiesis with atherosclerosis. *Trends Endocrinol Metab*. 2013;24:129-136.
17. Drechsler M, Megens RTA, Van Zandvoort M, Weber C, Soehnlein O. Hyperlipidemia-triggered neutrophilia promotes early atherosclerosis. *Circulation*. 2010;122:1837-1845.
18. Ortega-Gomez A, Salvermoser M, Rossaint J, et al. Cathepsin G Controls Arterial But Not Venular Myeloid Cell Recruitment. *Circulation*. 2016;134:1176-1188.
19. Döring Y, Drechsler M, Wantha S, Kemmerich K, Lievens D, Vijayan S, Gallo RL, Weber C, Soehnlein O. Lack of Neutrophil-Derived CRAMP Reduces Atherosclerosis in Mice. *Circ Res*. 2012;110:1052-1056.
20. Lessner SM, Prado HL, Waller EK, Galis ZS. Atherosclerotic lesions grow through recruitment and proliferation of circulating monocytes in a murine model. *Am J Pathol*. 2002;160:2145-2155.
21. Swirski FK, Pittet MJ, Kircher MF, Aikawa E, Jaffer FA, Libby P, Weissleder R. Monocyte accumulation in mouse atherogenesis is progressive and proportional to extent of disease. *Proc Natl Acad Sci U S A*. 2006;103:10340-10345.
22. Swirski FK, Libby P, Aikawa E, Alcaide P, Luscinskas FW, Weissleder R, Pittet MJ. Ly-6Chi monocytes dominate hypercholesterolemia-associated monocytosis and give rise to macrophages in atheromata. *J Clin Invest*. 2007;117:195-205.
23. Marcovecchio PM, Thomas GD, Mikulski Z, Ehinger E, Mueller KAL, Blatchley A, Wu R, Miller YI, Nguyen AT, Taylor AM, McNamara CA, Ley K, Hedrick CC. Scavenger Receptor CD36 Directs Nonclassical Monocyte Patrolling Along the Endothelium During Early Atherogenesis. *Arterioscler Thromb Vasc Biol*. 2017;37:2043-2052.
24. Vestweber D. How leukocytes cross the vascular endothelium. *Nat Rev Immunol*. 2015;15:692-704.
25. Chèvre R, González-Granado JM, Megens RTA, Sreeramkumar V, Silvestre-Roig C, Molina-Sánchez P, Weber C, Soehnlein O, Hidalgo A, Andrés V. High-Resolution Imaging of Intravascular Atherogenic Inflammation in Live Mice. *Circ Res*. 2014;114:770-779.
26. Jones DP, True HD, Patel J. Leukocyte Trafficking in Cardiovascular Disease: Insights from Experimental Models. *Mediators Inflamm*. 2017;2017:9746169.
27. Gerhardt T, Ley K. Monocyte trafficking across the vessel wall. *Cardiovasc Res*. 2015;107:321-330.

REFERENCES

28. Ley K, Laudanna C, Cybulsky MI, Nourshargh S. Getting to the site of inflammation: the leukocyte adhesion cascade updated. *Nat Rev Immunol.* 2007;7:678-689.
29. Ulbrich H, Eriksson EE, Lindbom L. Leukocyte and endothelial cell adhesion molecules as targets for therapeutic interventions in inflammatory disease. *Trends Pharmacol Sci.* 2003;24:640-647.
30. Yang J, Hirata T, Croce K, Merrill-Skoloff G, Tchernychev B, Williams E, Flaumenhaft R, Furie BC, Furie B. Targeted gene disruption demonstrates that P-selectin glycoprotein ligand 1 (PSGL-1) is required for P-selectin-mediated but not E-selectin-mediated neutrophil rolling and migration. *J Exp Med.* 1999;190:1769-1782.
31. Eriksson EE, Xie X, Werr J, Thoren P, Lindbom L. Importance of primary capture and L-selectin-dependent secondary capture in leukocyte accumulation in inflammation and atherosclerosis in vivo. *J Exp Med.* 2001;194:205-218.
32. An G, Wang H, Tang R, Yago T, McDaniel JM, McGee S, Huo Y, Xia L. P-selectin glycoprotein ligand-1 is highly expressed on Ly-6Chi monocytes and a major determinant for Ly-6Chi monocyte recruitment to sites of atherosclerosis in mice. *Circulation.* 2008;117:3227-3237.
33. Finney AC, Stokes KY, Pattillo CB, Orr AW. Integrin signaling in atherosclerosis. *Cell Mol Life Sci.* 2017;74:2263-2282.
34. Schramm R, Menger MD, Schaeffers H-J, Thorlacius H. Leukocyte adhesion in aorta and femoral artery in vivo is mediated by LFA-1. *Inflamm Res.* 2004;53:523-527.
35. Dong ZM, Brown AA, Wagner DD. Prominent Role of P-Selectin in the Development of Advanced Atherosclerosis in ApoE-Deficient Mice. *Circulation.* 2000;101:2290-2295.
36. Gjurich B, Taghavi-Moghadam P, Ley K, Galkina E. L-selectin deficiency decreases aortic B1a and Breg subsets and promotes atherosclerosis. *Thromb Haemost.* 2014;112:803-811.
37. Collins RG, Velji R, Guevara N V, Hicks MJ, Chan L, Beaudet AL. P-Selectin or intercellular adhesion molecule (ICAM)-1 deficiency substantially protects against atherosclerosis in apolipoprotein E-deficient mice. *J Exp Med.* 2000;191:189-194.
38. McArdle S, Mikulski Z, Ley K. Live cell imaging to understand monocyte, macrophage, and dendritic cell function in atherosclerosis. *J Exp Med.* 2016;213:1117-1131.
39. Montresor A, Toffali L, Constantin G, Laudanna C. Chemokines and the Signaling Modules Regulating Integrin Affinity. *Front Immunol.* 2012;3:127.
40. Ley K, Rivera-Nieves J, Sandborn WJ, Shattil S. Integrin-based therapeutics: biological basis, clinical use and new drugs. *Nat Rev Drug Discov.* 2016;15:173-183.

REFERENCES

41. Schittenhelm L, Hilkens CM, Morrison VL. β 2Integrins As Regulators of Dendritic Cell, Monocyte, and Macrophage Function. *Front Immunol*. 2017;8:1866.
42. Iwamoto D V, Calderwood DA. Regulation of integrin-mediated adhesions. *Curr Opin Cell Biol*. 2015;36:41-47.
43. Hyun Y-M, Lefort CT, Kim M. Leukocyte integrins and their ligand interactions. *Immunol Res*. 2009;45:195-208.
44. Herter J, Zarbock A. Integrin Regulation during Leukocyte Recruitment. *J Immunol*. 2013;190:4451-4457.
45. Yang JT, Rayburn H, Hynes RO. Cell adhesion events mediated by alpha 4 integrins are essential in placental and cardiac development. *Development*. 1995;121:549-560.
46. Barringhaus KG, Phillips JW, Thatte JS, Sanders JM, Czarnik AC, Bennett DK, Ley KF, Sarembock IJ. Alpha4beta1 integrin (VLA-4) blockade attenuates both early and late leukocyte recruitment and neointimal growth following carotid injury in apolipoprotein E (-/-) mice. *J Vasc Res*. 2004;41:252-260.
47. Shih PT, Brennan ML, Vora DK, Territo MC, Strahl D, Elices MJ, Lusis AJ, Berliner JA. Blocking very late antigen-4 integrin decreases leukocyte entry and fatty streak formation in mice fed an atherogenic diet. *Circ Res*. 1999;84:345-351.
48. Huo Y, Hafezi-Moghadam A, Ley K. Role of Vascular Cell Adhesion Molecule-1 and Fibronectin Connecting Segment-1 in Monocyte Rolling and Adhesion on Early Atherosclerotic Lesions. *Circ Res*. 2000;87:153-159.
49. Nie Q, Fan J, Haraoka S, Shimokama T, Watanabe T. Inhibition of mononuclear cell recruitment in aortic intima by treatment with anti-ICAM-1 and anti-LFA-1 monoclonal antibodies in hypercholesterolemic rats: implications of the ICAM-1 and LFA-1 pathway in atherogenesis. *Lab Invest*. 1997;77:469-482.
50. Watanabe T, Fan J. Atherosclerosis and inflammation mononuclear cell recruitment and adhesion molecules with reference to the implication of ICAM-1/LFA-1 pathway in atherogenesis. *Int J Cardiol*. 1998;66 Suppl 1:S45-53.
51. Merched A, Tollefson K, Chan L. Beta2 integrins modulate the initiation and progression of atherosclerosis in low-density lipoprotein receptor knockout mice. *Cardiovasc Res*. 2010;85:853-863.
52. Gower RM, Wu H, Foster GA, Devaraj S, Jialal I, Ballantyne CM, Knowlton AA, Simon SI. CD11c/CD18 expression is upregulated on blood monocytes during hypertriglyceridemia and enhances adhesion to vascular cell adhesion molecule-1. *Arterioscler Thromb Vasc Biol*. 2011;31:160-166.

REFERENCES

53. Wu H, Gower RM, Wang H, Perrard X-YD, Ma R, Bullard DC, Burns AR, Paul A, Smith CW, Simon SI, Ballantyne CM. Functional role of CD11c+ monocytes in atherogenesis associated with hypercholesterolemia. *Circulation*. 2009;119:2708-2717.
54. Cybulsky MI, Iiyama K, Li H, Zhu S, Chen M, Iiyama M, Davis V, Gutierrez-Ramos J-C, Connelly PW, Milstone DS. A major role for VCAM-1, but not ICAM-1, in early atherosclerosis. *J Clin Invest*. 2001;107:1255-1262.
55. Fitch-Tewfik JL, Flaumenhaft R. Platelet Granule Exocytosis: A Comparison with Chromaffin Cells. *Front Endocrinol (Lausanne)*. 2013;4:77.
56. Sharda A, Flaumenhaft R. The life cycle of platelet granules. *F1000Research*. 2018;7:236.
57. Yun S-H, Sim E-H, Goh R-Y, Park J-I, Han J-Y. Platelet Activation: The Mechanisms and Potential Biomarkers. *Biomed Res Int*. 2016;2016:9060143.
58. Semple JW, Italiano JE, Freedman J. Platelets and the immune continuum. *Nat Rev Immunol*. 2011;11:264-274.
59. NIESWANDT B, PLEINES I, BENDER M. Platelet adhesion and activation mechanisms in arterial thrombosis and ischaemic stroke. *J Thromb Haemost*. 2011;9:92-104.
60. Blair P, Flaumenhaft R. Platelet alpha-granules: basic biology and clinical correlates. *Blood Rev*. 2009;23:177-189.
61. Huo Y, Schober A, Forlow SB, Smith DF, Hyman MC, Jung S, Littman DR, Weber C, Ley K. Circulating activated platelets exacerbate atherosclerosis in mice deficient in apolipoprotein E. *Nat Med*. 2002;9:61-67.
62. Burger PC, Wagner DD, Nollert MU, Ault K, Smith B, Hoylaerts M. Platelet P-selectin facilitates atherosclerotic lesion development. *Blood*. 2003;101:2661-2666.
63. Ed Rainger G, Chimen M, Harrison MJ, Yates CM, Harrison P, Watson SP, Lordkipanidzé M, Nash GB. The role of platelets in the recruitment of leukocytes during vascular disease. *Platelets*. 2015;26:507-520.
64. von Hundelshausen P, Weber KS, Huo Y, Proudfoot AE, Nelson PJ, Ley K, Weber C. RANTES deposition by platelets triggers monocyte arrest on inflamed and atherosclerotic endothelium. *Circulation*. 2001;103:1772-1777.
65. Schober A, Manka D, von Hundelshausen P, Huo Y, Hanrath P, Sarembock IJ, Ley K, Weber C. Deposition of platelet RANTES triggering monocyte recruitment requires P-selectin and is involved in neointima formation after arterial injury. *Circulation*. 2002;106:1523-1529.

REFERENCES

66. Sachais BS, Turrentine T, Dawicki McKenna JM, Rux AH, Rader D, Kowalska MA. Elimination of platelet factor 4 (PF4) from platelets reduces atherosclerosis in C57Bl/6 and apoE^{-/-} mice. *Thromb Haemost.* 2007;98:1108-1113.
67. von Hundelshausen P, Koenen RR, Sack M, Mause SF, Adriaens W, Proudfoot AEI, Hackeng TM, Weber C. Heterophilic interactions of platelet factor 4 and RANTES promote monocyte arrest on endothelium. *Blood.* 2005;105:924-930.
68. von Hundelshausen P, Agten SM, Eckardt V, et al. Chemokine interactome mapping enables tailored intervention in acute and chronic inflammation. *Sci Transl Med.* 2017;9:eaah6650.
69. Koenen RR, von Hundelshausen P, Nesmelova I V, Zerneck A, Liehn EA, Sarabi A, Kramp BK, Piccinini AM, Paludan SR, Kowalska MA, Kungl AJ, Hackeng TM, Mayo KH, Weber C. Disrupting functional interactions between platelet chemokines inhibits atherosclerosis in hyperlipidemic mice. *Nat Med.* 2009;15:97-103.
70. Rapport MM, Green AA, Page IH. Crystalline Serotonin. *Science (80-).* 1948;108:329-330.
71. Van Nueten JM, Janssens WJ, Vanhoutte PM. Serotonin and vascular reactivity. *Pharmacol Res Commun.* 1985;17:585-608.
72. Lopez-Vilchez I, Diaz-Ricart M, White JG, Escolar G, Galan AM. Serotonin enhances platelet procoagulant properties and their activation induced during platelet tissue factor uptake. *Cardiovasc Res.* 2009;84:309-316.
73. Cloutier N, Paré A, Farndale RW, Schumacher HR, Nigrovic PA, Lacroix S, Boilard E. Platelets can enhance vascular permeability. *Blood.* 2012;120:1334-1343.
74. Hendrix TR, Atkinson M, Clifton JA, Ingelfinger FJ, Govier WM, Swoap OF, Brook MJ Vander. The effect of 5-hydroxytryptamine on intestinal motor function in man. *Am J Med.* 1957;23:886-893.
75. Herr N, Bode C, Duerschmied D. The Effects of Serotonin in Immune Cells. *Front Cardiovasc Med.* 2017;4:48.
76. Fidalgo S, Ivanov DK, Wood SH. Serotonin: From top to bottom. *Biogerontology.* 2013;14:21-45.
77. Walther DJ, Peter J-U, Bashammakh S, Hörtnagl H, Voits M, Fink H, Bader M. Synthesis of Serotonin by a Second Tryptophan Hydroxylase Isoform. *Science (80-).* 2003;299:76.
78. Berger M, Gray JA, Roth BL. The expanded biology of serotonin. *Annu Rev Med.* 2009;60:355-366.

REFERENCES

79. Mercado CP, Kilic F. Molecular mechanisms of SERT in platelets: regulation of plasma serotonin levels. *Mol Interv.* 2010;10:231-241.
80. Walther DJ, Peter J-U, Winter S, Höltje M, Paulmann N, Grohmann M, Vowinkel J, Alamo-Bethencourt V, Wilhelm CS, Ahnert-Hilger G, Bader M. Serotonylation of small GTPases is a signal transduction pathway that triggers platelet alpha-granule release. *Cell.* 2003;115:851-862.
81. Arreola R, Becerril-Villanueva E, Cruz-Fuentes C, Velasco-Velázquez MA, Garces-Alvarez ME, Hurtado-Alvarado G, Quintero-Fabian S, Pavon L. Immunomodulatory effects mediated by serotonin. *J Immunol Res.* 2015;2015:354957.
82. Coates MD, Mahoney CR, Linden DR, Sampson JE, Chen J, Blaszyk H, Crowell MD, Sharkey KA, Gershon MD, Mawe GM, Moses PL. Molecular defects in mucosal serotonin content and decreased serotonin reuptake transporter in ulcerative colitis and irritable bowel syndrome. *Gastroenterology.* 2004;126:1657-1664.
83. Lechin F, van der Dijs B, Orozco B, Lechin M, Lechin AE. Increased Levels of Free Serotonin in Plasma of Symptomatic Asthmatic Patients. *Ann Allergy, Asthma Immunol.* 1996;77:245-253.
84. Kim H-J, Kim JH, Noh S, Hur HJ, Sung MJ, Hwang J-T, Park JH, Yang HJ, Kim M-S, Kwon DY, Yoon SH. Metabolomic Analysis of Livers and Serum from High-Fat Diet Induced Obese Mice. *J Proteome Res.* 2011;10:722-731.
85. Shajib MS, Khan WI. The role of serotonin and its receptors in activation of immune responses and inflammation. *Acta Physiol.* 2015;213:561-574.
86. Filip M, Bader M. Overview on 5-HT receptors and their role in physiology and pathology of the central nervous system. *Acta Physiol (Oxf).* 2009;61:761-777.
87. Mccorvy JD, Roth BL. Structure and Function of Serotonin G protein Coupled Receptors. *Pharmacol Ther.* 2015;150:129-142.
88. Ito T, Ikeda U, Shimpo M, Yamamoto K, Shimada K. Serotonin increases interleukin-6 synthesis in human vascular smooth muscle cells. *Circulation.* 2000;102:2522-2527.
89. Marconi A, Darquenne S, Boulmerka A, Mosnier M, D'Alessio P. Naftidrofuryl-driven regulation of endothelial ICAM-1 involves nitric oxide. *Free Radic Biol Med.* 2003;34:616-625.
90. Yu B, Becnel J, Zerfaoui M, Rohatgi R, Boulares AH, Nichols CD. Serotonin 5-Hydroxytryptamine_{2A} Receptor Activation Suppresses Tumor Necrosis Factor- α -Induced Inflammation with Extraordinary Potency. *J Pharmacol Exp Ther.* 2008;327:316-323.

REFERENCES

91. Role of serotonin in angiogenesis: Induction of angiogenesis by sarpogrelate via endothelial 5-HT_{1B}/Akt/eNOS pathway in diabetic mice. *Atherosclerosis*. 2012;220:337-342.
92. Ahern GP. 5-HT and the Immune System. *Curr Opin Pharmacol*. 2011;11:29-33.
93. Barnes NM, Neumaier JF. Neuronal 5-HT Receptors and SERT. *Tocris Biosci Sci Rev Ser*. 2011;34:1-15.
94. Wang C, Jiang Y, Ma J, et al. Structural basis for molecular recognition at serotonin receptors. *Science*. 2013;340:610-614.
95. Wacker D, Wang C, Katritch V, et al. Structural features for functional selectivity at serotonin receptors. *Science*. 2013;340:615-619.
96. Frood A. Serotonin receptors offer clues to new antidepressants: Shapes of binding sites could help drug discovery and the study of consciousness. *Nature*. 2013;doi:10.1038/nature.2013.12659.
97. Baganz NL, Blakely RD. A dialogue between the immune system and brain, spoken in the language of serotonin. *ACS Chem Neurosci*. 2013;4:48-63.
98. Mauler M, Bode C, Duerschmied D. Platelet serotonin modulates immune functions. *Hamostaseologie*. 2015;36:11-16.
99. Murphy DL, Lesch K-P. Targeting the murine serotonin transporter: insights into human neurobiology. *Nat Rev Neurosci*. 2008;9:85-96.
100. Coleman JA, Green EM, Gouaux E. X-ray structures and mechanism of the human serotonin transporter. *Nature*. 2016;532:334-339.
101. Caron MG, Gether U. Structural biology: Antidepressants at work. *Nature*. 2016;532:320-321.
102. Davis RB, Meeker WR, McQuarrie DG. Immediate effects of intravenous endotoxin on serotonin concentrations and blood platelets. *Circ Res*. 1960;8:234-239.
103. Baskar K, Sur S, Selvaraj V, Agrawal DK. Functional constituents of a local serotonergic system, intrinsic to the human coronary artery smooth muscle cells. *Mol Biol Rep*. 2015;42:1295-1307.
104. Ullmer C, Schmuck K, Kalkman HO, Lübbert H. Expression of serotonin receptor mRNAs in blood vessels. *FEBS Lett*. 1995;370:215-221.
105. Dürk T, Panther E, Müller T, Sorichter S, Ferrari D, Pizzirani C, Di Virgilio F, Myrtek D, Norgauer J, Idzko M. 5-Hydroxytryptamine modulates cytokine and chemokine

REFERENCES

- production in LPS-primed human monocytes via stimulation of different 5-HTR subtypes. *Int Immunol.* 2005;17:599-606.
106. Mammadova-Bach E, Mauler M, Braun A, Duerschmied D. Immuno-Thrombotic Effects of Platelet Serotonin. In: *Serotonin - A Chemical Messenger Between All Types of Living Cells*. InTech; 2017.
107. Duerschmied D, Canault M, Lievens D, Brill A, Cifuni SM, Bader M, Wagner DD. Serotonin stimulates platelet receptor shedding by tumor necrosis factor-alpha-converting enzyme (ADAM17). *J Thromb Haemost.* 2009;7:1163–1171.
108. Iken K, Chheng S, Fargin A, Goulet A-C, Kouassi E. Serotonin Upregulates Mitogen-Stimulated B Lymphocyte Proliferation through 5-HT1A Receptors. *Cell Immunol.* 1995;163:1-9.
109. Freire-Garabal M, Núñez MJ, Balboa J, López-Delgado P, Gallego R, García-Caballero T, Fernández-Roel MD, Brenlla J, Rey-Méndez M. Serotonin upregulates the activity of phagocytosis through 5-HT1A receptors. *Br J Pharmacol.* 2003;139:457-463.
110. de las Casas-Engel M, Domínguez-Soto A, Sierra-Filardi E, Bragado R, Nieto C, Puig-Kroger A, Samaniego R, Loza M, Corcuera MT, Gómez-Aguado F, Bustos M, Sánchez-Mateos P, Corbí AL. Serotonin skews human macrophage polarization through HTR2B and HTR7. *J Immunol.* 2013;190:2301-2310.
111. Sternberg EM, Trial J, Parker CW. Effect of serotonin on murine macrophages: suppression of Ia expression by serotonin and its reversal by 5-HT2 serotonergic receptor antagonists. *J Immunol.* 1986;137:276-282.
112. Sternberg EM, Wedner HJ, Leung MK, Parker CW. Effect of serotonin (5-HT) and other monoamines on murine macrophages: modulation of interferon-gamma induced phagocytosis. *J Immunol.* 1987;138:4360-4365.
113. Palmer DS, Aye M, Ganz PR, Halpenny MR, Hashemi SJ. Adenosine nucleotides and serotonin stimulate von Willebrand factor release from cultured human endothelial cells. *Thromb Haemost.* 1994;72:132-139.
114. Schlüter T, Bohnensack R. Serotonin-induced secretion of von Willebrand factor from human umbilical vein endothelial cells via the cyclic AMP-signaling systems independent of increased cytoplasmic calcium concentration. *Biochem Pharmacol.* 1999;57:1191-1197.
115. Duerschmied D, Suidan GL, Demers M, Herr N, Carbo C, Brill A, Cifuni SM, Mauler M, Cicko S, Bader M, Idzko M, Bode C, Wagner DD. Platelet serotonin promotes the

REFERENCES

- recruitment of neutrophils to sites of acute inflammation in mice. *Blood*. 2013;121:1008-1015.
116. Herr N, Mauler M, Witsch T, Stallmann D, Schmitt S, Mezger J, Bode C, Duerschmied D. Acute fluoxetine treatment induces slow rolling of leukocytes on endothelium in mice. *PLoS One*. 2014;9:e88316.
117. Gershon MD. Review article: roles played by 5-hydroxytryptamine in the physiology of the bowel. *Aliment Pharmacol Ther*. 1999;13 Suppl 2:15-30.
118. WHO. Depression. <http://www.who.int>. Accessed April 21, 2017.
119. Hare DL, Toukhsati SR, Johansson P, Jaarsma T. Depression and cardiovascular disease: a clinical review. *Eur Heart J*. 2014;35:1365-1372.
120. Ladwig KH, Baumert J, Marten-Mittag B, Lukaschek K, Johar H, Fang X, Ronel J, Meisinger C, Peters A. Room for depressed and exhausted mood as a risk predictor for all-cause and cardiovascular mortality beyond the contribution of the classical somatic risk factors in men. *Atherosclerosis*. 2017;257:224-231.
121. Healy D. Serotonin and depression. *Br Med J*. 2015;350:h1771.
122. Andrews PW. Is serotonin an upper or a downer? The functional role of serotonin in depression and a possible mechanism of antidepressant action. *Neurosci Biobehav Rev*. 2015;51:1-45.
123. National Center for Health Statistics. Health, United States, 2015: With Special Feature on Racial and Ethnic Health Disparities. <https://www.cdc.gov/nchs/data/health/us/15.pdf>. Accessed June 9, 2017.
124. Serretti A, Artioli P. The pharmacogenomics of selective serotonin reuptake inhibitors. *Pharmacogenomics J*. 2004;4:233-244.
125. U. S. Food and Drug Administration. Information by Drug Class - Selective Serotonin Reuptake Inhibitors (SSRIs) Information. <https://www.fda.gov/Drugs/DrugSafety/InformationbyDrugClass/ucm283587.htm>. Accessed April 23, 2018.
126. Hiemke C, Härtter S. Pharmacokinetics of selective serotonin reuptake inhibitors. *Pharmacol Ther*. 2000;85:11-28.
127. Sanchez C, Reines EH, Montgomery SA. A comparative review of escitalopram, paroxetine, and sertraline. *Int Clin Psychopharmacol*. 2014;29:185-196.
128. Coleman JA, Gouaux E. Structural basis for recognition of diverse antidepressants by the human serotonin transporter. *Nat Struct Mol Biol*. 2018;25:170-175.
129. Baumann P, Hiemke C, Ulrich S, Eckermann G, Gaertner I, Gerlach M, Kuss H-J, Laux

REFERENCES

- G, Müller-Oerlinghausen B, Rao ML, Riederer P, Zernig G. The AGNP-TDM Expert Group Consensus Guidelines: Therapeutic Drug Monitoring in Psychiatry. *Pharmacopsychiatry*. 2004;37:243-265.
130. Caron MG, Gether U. Antidepressant at work. *Nat News Views*. 2016;532:320-321.
131. Blardi P, Lalla A De, Leo A, Auteri A, Iapichino S, Muro A Di, Dell'erba A, Castrogiovanni P. Serotonin and Fluoxetine Levels in Plasma and Platelets After Fluoxetine Treatment in Depressive Patients. *J Clin Psychopharmacol*. 2002;22:131-136.
132. de Abajo FJ, Rodríguez LA, Montero D. Association between selective serotonin reuptake inhibitors and upper gastrointestinal bleeding: population based case-control study. *BMJ*. 1999;319:1106-1109.
133. Vidal X, Ibáñez L, Vendrell L, Conforti A, Laporte J-R, Spanish-Italian Collaborative Group for the Epidemiology of Gastrointestinal Bleeding. Risk of upper gastrointestinal bleeding and the degree of serotonin reuptake inhibition by antidepressants: a case-control study. *Drug Saf*. 2008;31:159-168.
134. Hergovich N, Aigner M, Eichler HG, Entlicher J, Drucker C, Jilma B. Paroxetine decreases platelet serotonin storage and platelet function in human beings. *Clin Pharmacol Ther*. 2000;68:435-442.
135. Taylor CB, Youngblood ME, Catellier D, Veith RC, Carney RM, Burg MM, Kaufmann PG, Shuster J, Mellman T, Blumenthal JA, Krishnan R, Jaffe AS, ENRICHD Investigators. Effects of Antidepressant Medication on Morbidity and Mortality in Depressed Patients After Myocardial Infarction. *Arch Gen Psychiatry*. 2005;62:792-798.
136. Kimmel SE, Schelleman H, Berlin JA, Oslin DW, Weinstein RB, Kinman JL, Sauer WH, Lewis JD. The effect of selective serotonin re-uptake inhibitors on the risk of myocardial infarction in a cohort of patients with depression. *Br J Clin Pharmacol*. 2011;72:514-517.
137. William H. Sauer, MD; Jesse A. Berlin, ScD; Stephen E. Kimmel, MD M. Effect of Antidepressants and Their Relative Affinity for the Serotonin Transporter on the Risk of Myocardial Infarction. *Circulation*. 2003;108:32-36.
138. Mortensen JK, Larsson H, Johnsen SP, Andersen G. Post Stroke Use of Selective Serotonin Reuptake Inhibitors and Clinical Outcome Among Patients With Ischemic Stroke A Nationwide Propensity Score-matched Follow-up Study. *Stroke*. 2013;44:420-426.
139. Sherwood A, Blumenthal JA, Smith PJ, Watkins LL, Hoffman BM, Hinderliter AL. Effects of Exercise and Sertraline on Measures of Coronary Heart Disease Risk in Patients With

REFERENCES

- Major Depression: Results From the SMILE-II Randomized Clinical Trial. *Psychosom Med.* 2016;78:602-609.
140. He Y, Cai Z, Zeng S, Chen S, Tang B, Liang Y, Chang X, Guo Y. Effect of fluoxetine on three-year recurrence in acute ischemic stroke: A randomized controlled clinical study. *Clin Neurol Neurosurg.* 2018;168:1-6.
141. McFarlane A, Kamath M V., Fallen EL, Malcolm V, Cherian F, Norman G. Effect of sertraline on the recovery rate of cardiac autonomic function in depressed patients after acute myocardial infarction. *Am Heart J.* 2001;142:617-623.
142. Rieckmann N, Kronish I. Serotonin Reuptake Inhibitor Use, Depression, and Long-Term Outcomes After an Acute Coronary Syndrome: A Prospective Cohort Study. *JAMA Intern Med.* 2013;173:1150-1151.
143. Smoller JW, Allison M, Cochrane BB, Curb JD, Perlis RH, Robinson JG, Rosal MC, Wenger NK, Wassertheil-Smoller S. Antidepressant Use and Risk of Incident Cardiovascular Morbidity and Mortality Among Postmenopausal Women in the Women's Health Initiative Study. *Arch Intern Med.* 2009;169:2128.
144. Tata LJ, West J, Smith C, Farrington P, Card T, Smeeth L, Hubbard R. General population based study of the impact of tricyclic and selective serotonin reuptake inhibitor antidepressants on the risk of acute myocardial infarction. *Heart.* 2005;91:465-471.
145. Chen V, Guo JJ, Li H, Wulsin L, Patel NC. Risk of Cerebrovascular Events Associated with Antidepressant Use in Patients with Depression: A Population-Based, Nested Case-Control Study. *Ann Pharmacother.* 2008;42:177-184.
146. Weeke P, Jensen A, Folke F, et al. Antidepressant Use and Risk of Out-of-Hospital Cardiac Arrest: A Nationwide Case-Time-Control Study. *Clin Pharmacol Ther.* 2012;92:72-79.
147. Bak S, Tsiropoulos I, Kjaersgaard JO, Andersen M, Møllerup E, Hallas J, García Rodríguez LA, Christensen K, Gaist D. Selective serotonin reuptake inhibitors and the risk of stroke: a population-based case-control study. *Stroke.* 2002;33:1465-1473.
148. Meier CR, Schlienger RG, Jick H. Use of selective serotonin reuptake inhibitors and risk of developing first-time acute myocardial infarction. *Br J Clin Pharmacol.* 2001;52:179-184.
149. Hamer M, David Batty G, Seldenrijk A, Kivimaki M. Antidepressant medication use and future risk of cardiovascular disease: The Scottish Health Survey. *Eur Heart J.* 2011;32:437-442.

REFERENCES

150. Camacho Á, McClelland RL, Delaney JA, Allison MA, Psaty BM, Rifkin DE, Rapp SR, Szklo M, Stein MB, Criqui MH. Antidepressant Use and Subclinical Measures of Atherosclerosis The Multi-Ethnic Study of Atherosclerosis. *J Clin Psychopharmacol*. 2016;36:340-346.
151. Wang M-T, Chu C-L, Yeh C-B, Chang L-C, Malone DC, Liou J-T. Antidepressant Use and Risk of Recurrent Stroke. *J Clin Psychiatry*. 2015;76:e877-e885.
152. Angermann CE, Gelbrich G, Störk S, et al. Effect of Escitalopram on All-Cause Mortality and Hospitalization in Patients With Heart Failure and Depression. *JAMA*. 2016;315:2683.
153. Hanash JA, Hansen BH, Hansen JF, Nielsen OW, Rasmussen A, Birket-Smith M. Cardiovascular Safety of One-Year Escitalopram Therapy in Clinically Nondepressed Patients With Acute Coronary Syndrome: Results From the DEpression in Patients With Coronary ARtery Disease (DECARD) Trial. *J Cardiovasc Pharmacol*. 2012;60:397-405.
154. Glassman AH, O'Connor CM, Califf RM, et al. Sertraline Treatment of Major Depression in Patients With Acute MI or Unstable Angina. *JAMA*. 2002;288:701.
155. O'Connor CM, Jiang W, Kuchibhatla M, Silva SG, Cuffe MS, Callwood DD, Zakhary B, Stough WG, Arias RM, Rivelli SK, Krishnan R. Safety and Efficacy of Sertraline for Depression in Patients With Heart Failure: Results of the SADHART-CHF (Sertraline Against Depression and Heart Disease in Chronic Heart Failure) Trial. *J Am Coll Cardiol*. 2010;56:692-699.
156. *DEPRESSION: A Global Crisis*; 2012. http://www.who.int/mental_health/management/depression/wfmh_paper_depression_wmhd_2012.pdf. Accessed April 18, 2018.
157. Ladwig K-H, Baumert J, Marten-Mittag B, Lukaschek K, Johar H, Fang X, Ronel J, Meisinger C, Peters A. Room for depressed and exhausted mood as a risk predictor for all-cause and cardiovascular mortality beyond the contribution of the classical somatic risk factors in men. *Atherosclerosis*. 2017;257:224-231.
158. Piedrahita JA, Zhang SH, Hagaman JR, Oliver PM, Maeda N. Generation of mice carrying a mutant apolipoprotein E gene inactivated by gene targeting in embryonic stem cells. *Genetics*. 1992;89:4471-4475.
159. Crane JD, Palanivel R, Mottillo EP, et al. Inhibiting peripheral serotonin synthesis reduces obesity and metabolic dysfunction by promoting brown adipose tissue thermogenesis. *Nat Med*. 2015;21:166-172.

REFERENCES

160. Huang C-C, Yeh C-M, Wu M-Y, Hsu K-S. A single in vivo cocaine administration impairs 5-HT 1B receptor-induced long-term depression in the nucleus accumbens. *J Neurochem.* 2013;125:809-821.
161. Drechsler M, De Jong R, Rossaint J, Viola JR, Leoni G, Wang JM, Grommes J, Hinkel R, Kupatt C, Weber C, Döring Y, Zarbock A, Soehnlein O. Annexin A1 counteracts chemokine-induced arterial myeloid cell recruitment. *Circ Res.* 2015;116:827-835.
162. Radu M, Chernoff J. An in vivo Assay to Test Blood Vessel Permeability Video Link. *J Vis Exp.* 2013;e50062.
163. Corcoran MP, Lichtenstein AH, Meydani M, Dillard A, Schaefer EJ, Lamon-Fava S. The effect of 17 β -estradiol on cholesterol content in human macrophages is influenced by the lipoprotein milieu. *J Mol Endocrinol.* 2011;47:109-117.
164. Sager HB, Dutta P, Dahlman JE, et al. RNAi targeting multiple cell adhesion molecules reduces immune cell recruitment and vascular inflammation after myocardial infarction. *Sci Transl Med.* 2016;8:342ra80.
165. Mauler M, Seyfert J, Haenel D, Seeba H, Guenther J, Stallmann D, Schoenichen C, Hilgendorf I, Bode C, Ahrens I, Duerschmied D. Platelet-neutrophil complex formation—a detailed in vitro analysis of murine and human blood samples. *J Leukoc Biol.* 2016;99:781-789.
166. Schymeinsky J, Then C, Walzog B. The non-receptor tyrosine kinase Syk regulates lamellipodium formation and site-directed migration of human leukocytes. *J Cell Physiol.* 2005;204:614-622.
167. Srinivasan S, Wang F, Glavas S, Ott A, Hofmann F, Aktories K, Kalman D, Bourne HR. Rac and Cdc42 play distinct roles in regulating PI(3,4,5)P₃ and polarity during neutrophil chemotaxis. *J Cell Biol.* 2003;160:375-385.
168. Evans R, Lellouch AC, Svensson L, Mcdowall A, Hogg N. The integrin LFA-1 signals through ZAP-70 to regulate expression of high-affinity LFA-1 on T lymphocytes. *Blood.* 2011;117:3331-3342.
169. Rami M, Guillamat-Prats R, Rinne P, Salvermoser M, Ring L, Bianchini M, Blanchet X, Megens RTA, Döring Y, Walzog B, Soehnlein O, Weber C, Faussner A, Steffens S. Chronic Intake of the Selective Serotonin Reuptake Inhibitor Fluoxetine Enhances Atherosclerosis. *Arterioscler Thromb Vasc Biol.* 2018;38:1007-1019.
170. Dulawa SC, Holick KA, Gundersen B, Hen R. Effects of Chronic Fluoxetine in Animal Models of Anxiety and Depression. *Neuropsychopharmacology.* 2004;29:1321-1330.
171. Fernandez-Ruiz I, Puchalska P, Narasimhulu CA, Sengupta B, Parthasarathy S.

REFERENCES

- Differential lipid metabolism in monocytes and macrophages: influence of cholesterol loading. *J Lipid Res.* 2016;57:574-586.
172. Den Hartigh LJ, Connolly-Rohrbach JE, Fore S, Huser TR, Rutledge JC. Fatty Acids from Very Low-Density Lipoprotein Lipolysis Products Induce Lipid Droplet Accumulation in Human Monocytes. *J Immunol.* 2010;184:3927-3936.
173. Khode V, Sindhur J, Kanbur D, Ruikar K, Nallulwar S. Mean platelet volume and other platelet volume indices in patients with stable coronary artery disease and acute myocardial infarction: A case control study. *J Cardiovasc Dis Res.* 2012;3:272-275.
174. Koch S, Perry KW, Nelson DL, Conway RG, Threlkeld PG, Bymaster FP. R-fluoxetine Increases Extracellular DA, NE, As Well As 5-HT in Rat Prefrontal Cortex and Hypothalamus An in vivo Microdialysis and Receptor Binding Study. *Neuropsychopharmacology.* 2002;27:949-959.
175. Millan MJ, Marin P, Bockaert J, Mannoury la Cour C. Signaling at G-protein-coupled serotonin receptors: recent advances and future research directions. *Trends Pharmacol Sci.* 2008;29:454-464.
176. Schaff UY, Yamayoshi I, Tse T, Griffin D, Kibathi L, Simon SI. Calcium flux in neutrophils synchronizes beta2 integrin adhesive and signaling events that guide inflammatory recruitment. *Ann Biomed Eng.* 2008;36:632-646.
177. Rowin ME, Whatley RE, Yednock T, Bohnsack JF. Intracellular calcium requirements for β 1 integrin activation. *J Cell Physiol.* 1998;175:193-202.
178. Nicholson A, Kuper H, Hemingway H. Depression as an aetiologic and prognostic factor in coronary heart disease: a meta-analysis of 6362 events among 146 538 participants in 54 observational studies. *Eur Heart J.* 2006;27:2763-2774.
179. Carney RM, Blumenthal JA, Catellier D, Freedland KE, Berkman LF, Watkins LL, Czajkowski SM, Hayano J, Jaffe AS. Depression as a risk factor for mortality after acute myocardial infarction. *Am J Cardiol.* 2003;92:1277-1281.
180. Ziegelstein RC, Fauerbach JA, Stevens SS, Romanelli J, Richter DP, Bush DE. Patients With Depression Are Less Likely to Follow Recommendations to Reduce Cardiac Risk During Recovery From a Myocardial Infarction. *Arch Intern Med.* 2000;160:1818-1823.
181. Michelson D, Amsterdam JD, Quitkin FM, Reimherr FW, Rosenbaum JF, Zajecka J, Sundell KL, Kim Y, Beasley CM. Changes in weight during a 1-year trial of fluoxetine. *Am J Psychiatry.* 1999;156:1170-1176.

REFERENCES

182. Beyazyüz M, Albayrak Y, Eğilmez OB, Albayrak N, Beyazyüz E. Relationship between SSRIs and Metabolic Syndrome Abnormalities in Patients with Generalized Anxiety Disorder: A Prospective Study. *Psychiatry Investig.* 2013;10:148-154.
183. Lekakis J, Ikonomidis I, Papoutsis Z, Moutsatsou P, Nikolaou M, Parissis J, Kremastinos DT. Selective serotonin re-uptake inhibitors decrease the cytokine-induced endothelial adhesion molecule expression, the endothelial adhesiveness to monocytes and the circulating levels of vascular adhesion molecules. *Int J Cardiol.* 2010;139:150-158.
184. Scott DW, Vallejo MO, Patel RP. Heterogenic endothelial responses to inflammation: role for differential N-glycosylation and vascular bed of origin. *J Am Heart Assoc.* 2013;2:e000263.
185. León-Ponte M, Ahern GP, O'Connell PJ. Serotonin provides an accessory signal to enhance T-cell activation by signaling through the 5-HT₇ receptor. *Blood.* 2007;109:3139-3146.
186. Hara K, Hirowatari Y, Yoshika M, Komiyama Y, Tsuka Y, Takahashi H. The ratio of plasma to whole-blood serotonin may be a novel marker of atherosclerotic cardiovascular disease. *J Lab Clin Med.* 2004;144:31-37.
187. Carneiro AMD, Cook EH, Murphy DL, Blakely RD. Interactions between integrin α IIb β 3 and the serotonin transporter regulate serotonin transport and platelet aggregation in mice and humans. *J Clin Invest.* 2008;118:1544-1552.
188. Roweth HG, Yan R, Bedwani NH, Chauhan A, Fowler N, Watson AH, Malcor J-D, Sage SO, Jarvis GE. Citalopram inhibits platelet function independently of SERT-mediated 5-HT transport. *Sci Rep.* 2018;8:3494.
189. Ortuño MJ, Robinson ST, Subramanyam P, Paone R, Huang Y, Guo XE, Colecraft HM, Mann JJ, Ducey P. Serotonin-reuptake inhibitors act centrally to cause bone loss in mice by counteracting a local anti-resorptive effect. *Nat Med.* 2016;22:1170-1179.
190. Challa A, Eliopoulos AG, Holder MJ, Burguete AS, Pound JD, Chamba A, Grafton G, Armitage RJ, Gregory CD, Martinez-Valdez H, Young L, Gordon J. Population depletion activates autonomous CD154-dependent survival in biopsylike Burkitt lymphoma cells. *Blood.* 2002;99:3411-3418.
191. Tang K-Y, Lu T, Chang C-H, Lo Y-K, Cheng J-S, Wang J-L, Chang H-T, Jan C-R. Effect of fluoxetine on intracellular Ca²⁺ levels in bladder female transitional carcinoma (BFTC) cells. *Pharmacol Res.* 2001;43:503-507.
192. Khan W, Steinberg G, Rengasamy P. A method of treating obesity. 2015. <https://patents.google.com/patent/US20150366865>.

REFERENCES

193. Karsenty G, Sumara G, Sumara O. Methods of preventing and treating diabetes by inhibiting serotonin synthesis. 2015. <https://patents.google.com/patent/US9150521>.
194. Oh CM, Park S, Kim H. Serotonin as a New Therapeutic Target for Diabetes Mellitus and Obesity. *Diabetes Metab J*. 2016;40:89-98.
195. Karshovska E*, Zhao Z*, Blanchet X, Schmitt MMN, Bidzhekov K, Soehnlein O, von Hundelshausen, Philipp Mattheij NJ, Cosemans, Judith M.E.M. Megens RTA, Koepfel TA, Schober A, Hackeng TM, Weber C, Koenen RR. Hyperreactivity of Junctional Adhesion Molecule A-Deficient Platelets Accelerates Atherosclerosis in Hyperlipidemic Mice. *Circ Res*. 2015;116:587-599.
196. Shively CA, Register TC, Appt SE, Clarkson TB. Effects of long-term sertraline treatment and depression on coronary artery atherosclerosis in premenopausal female primates. *Psychosom Med*. 2015;77:267-278.
197. Canan F, Ataoglu A. Effect of escitalopram on white blood cells in patients with major depression. *J Clin Med Res*. 2009;1:290-291.
198. Scheiermann C, Kunisaki Y, Frenette PS. Circadian control of the immune system. *Nat Rev Immunol*. 2013;13:190-198.
199. Sánchez C, Hyttel J. Comparison of the effects of antidepressants and their metabolites on reuptake of biogenic amines and on receptor binding. *Cell Mol Neurobiol*. 1999;19:467-489.

8 ACKNOWLEDGEMENTS

*"Remember to look up to the stars and not down at your feet. Try to make sense of what you see [...].
Be curious. And however difficult life may seem, there is always something you can do and succeed at.
It matters that you don't just give up."*

-Stephen Hawking

Wie Stephen Hawking mit seinen Worten sagt, es kommt darauf an neugierig zu bleiben und nicht aufzugeben und nun kann ich es kaum glauben aber hiermit geht die Zeit meiner Promotion dem Ende zu. Vor allem zum Schluss ist sie wie im Flug vergangen und so sehe ich auf ereignisreiche 4,5 Jahre zurück, die durchaus nicht immer einfach waren, aber sehr wertvoll. An dieser Stelle möchte ich all denjenigen danken, die mich in den letzten Jahren auf diesem Weg begleitet haben.

Zuerst möchte ich mich bei Prof. Dr. Christian Weber dafür bedanken, dass er mir die Möglichkeit gegeben hat, am IPEK, eines der weltweit führenden Forschungsinstitute auf dem Gebiet der Herzkreislauferkrankungen, promovieren zu können.

Mein besonderer Dank gilt meiner Betreuerin Prof. Dr. Sabine Steffens. Danke Sabine, dass du mir diesen Neustart ermöglicht hast. Ich habe in der Zeit am IPEK nicht nur fachlich, sondern auch persönlich viel dazugelernt. Du bist mit mir durch alle Höhen und Tiefen gegangen, hast meine vielen „Abers“ ertragen und mir das Gefühl gegeben, dass du meine Arbeit schätzt. Ich habe in den letzten Jahren unfassbar viele neue Sachen gelernt und von deinem ganzen Wissen profitieren können. Du förderst jeden von uns und so hast du mir ermöglicht, meine Forschungsergebnisse auf diversen Kongressen vorzustellen und an vielen Workshops teilzunehmen. Du vereinst fachliche Kompetenz mit Menschlichkeit, was nicht selbstverständlich ist. Daher möchte ich mich besonders bei dir für dein Verständnis, deine Unterstützung und Loyalität bedanken. Unser offenes und ehrliches Verhältnis habe ich immer sehr geschätzt. Egal um welche Uhrzeit oder an welchem Wochentag, du warst immer erreichbar. Ich bin sehr beeindruckt wie du Familie und die Leitung einer Arbeitsgruppe unter einen Hut bringst. Auch der Spaß kam nie zu kurz! Wir hatten immer sehr viel zu lachen, nicht nur bei den diversen Malen, als du bei den großen Versuchen selbst mitgeholfen hast, sondern auch beim Feierabendbier, der Feuerzangenbowle, im Biergarten, auf der Wiesen oder im Zoo. Danke für diese wertvolle Zeit oder mit anderen Worten „Thank you for your time“.☺

Großer Dank gilt auch Prof. Dr. Alexander Faussner, der großen Anteil daran hatte, dass ich mich in unserer Gruppe wohlfühlt habe. Danke Sascha für die vielen Diskussionen bei den Besprechungen und am Kaffeetisch. Ich habe deine Sicht der Dinge immer sehr geschätzt und

ACKNOWLEDGEMENTS

deine kritischen Fragen waren immer sehr hilfreich. Die Arbeit mit dir in der Zellkultur hat immer Spaß gemacht auch wenn uns die ein oder andere Hefe in den Weg gekommen ist.☺ Du hast mir nicht nur fachlich viel beigebracht, ich habe auch von deinem Wissen über Kunst und Politik aber vor allem über Fußball profitiert. Danke auch für die vielen lustigen Momente! Wir haben immer viel miteinander gelacht und hatten viel Spaß bei diversen Feierabendbieren, auch wenn manch nächster Tag wegen dem schlechten Hendl nicht ganz so gut war. Ich bin immer noch stolz drauf, dass auch ich dir mit dem Milch-Einschenken was Neues beibringen konnte.☺

Ich möchte mich auch ganz herzlich bei Diana und Cornelia für die Unterstützung im Labor bedanken. Liebe Cornelia, du hast mich im Labor die längste Zeit begleitet. Vielen Dank für die lustige Zeit, den täglichen Kaffee und deine tollen Geschichten vom Reisen, die mich immer begeistert haben. Danke auch für die sehr amüsanten Male, in denen Sascha und du nicht so ganz einer Meinung wart.☺ Liebe Diana, ich danke auch dir für die schöne Zeit und die vielen vielen Herzen die du geschnitten hast. Die Zusammenarbeit mit dir war immer super, besonders am Anfang haben wir das doch sehr gut zusammen gemeistert finde ich! Wie haben wir dich vermisst, als du in Elternzeit warst! Schön, dass du wieder da bist!

Raquel, no sé que hauria fet sense tu, estic molt contenta d'haver-te conegut i poder treballar juntes al lab! I think (and here the problem starts ☺) we are a great team- it just fits perfectly! We always had so much fun together and laughed a lot (even if I was sometimes *currupia*). I think you are a great scientist and I'm really looking forward to working with you in the next months. Thanks you so much for aaaall the food and dinners you prepared for us. Also for being the beer-person in power.☺ Thanks for sending me the perfectly suiting PhD comics and for all your support especially in the last months. I hope we will have many more dinners with jamón, tortilla, fuet and vino on the balcony in the future. Sóc feliç de tenir-te com amiga!!!

Liebe Larisa, zusammen haben wir uns an die Maus gewagt und vieles neues gelernt, wie z.B. die Antwort auf die Frage was denn das komische, weiße, glibberige Ding da oben ist.☺ Auch haben wir des Öfteren nach CD45 gesucht oder den Multiplex verflucht. Danke für die tolle Zeit und die vielen lustigen Momente!

Auch möchte ich mich sehr bei Sarah, Michi und Petteri für die schöne Zeit bedanken. Liebe Sarah, der frische Wind war dann doch eher ein Wirbelsturm.☺ Danke für die vielen Lacher und die schönen Abende bei dir zuhause! Petteri, I really enjoyed working with you in the lab. Thank you so much for your support! Michi, wegen deiner unkomplizierten und entspannten Art war es einfach so angenehm mit dir im Labor zusammenzuarbeiten.

Auch möchte ich mich bei Daniel, Mario, Michael, Max, Mariaelvy, Remco, Johan, Maria, Katrin, den Riesens mit Thomas, Donato und Virginia und allen anderen Praktikanten und Studenten unserer Arbeitsgruppe für die gute Zusammenarbeit und das angenehme und

ACKNOWLEDGEMENTS

lustige Arbeitsklima bedanken. Remco, immer wenn ich Helene höre muss ich jetzt an dich denken.☺ Danke Thomas für deinen großen Einsatz, vor allem bei der Feuerzangenbowle. Ein großer Dank gilt auch den Sommerhoffs, v.a. Maresa, Erika, Stefan und Annemarie, die trotz der Abgrenzungen der Institute immer ein offenes Ohr hatten, mir mit Tipps und Tricks beiseite standen und für eine gute Atmosphäre gesorgt haben. Maresa, du hast schon eine große Lücke hinterlassen. Danke, dass ich mit allem immer zu dir kommen konnte. Ich schätze dich sehr, fachlich als auch menschlich!

Ich möchte mich auch bei den Tierpflegern allen voran bei Tobi dafür bedanken, dass ihr euch so um die Mäuschen kümmert und mir dadurch so viel Arbeit abgenommen habt. Tobi, mit dir hat sogar das *Tailing* Spaß gemacht.

An dieser Stelle möchte ich mich auch noch bei allen anderen Kollegen am IPEK insbesondere Pati, Janine, Petra, Lucia und auch alldenjenigen die ich jetzt nicht namentlich nenne, für die gute Zusammenarbeit, die Hilfsbereitschaft und den Austausch bedanken. Liebe Gartenhäusler, allen voran Janina, Sigrid, Holger und Norbert, danke, dass ihr mich immer mit einbezogen habt, mir mit Rat und Tat zur Seite standet und wenn es mal nötig war, dass ich zum „Einkaufen“ vorbeikommen durfte. Holger, danke für deine Hilfs- und auch Feierbereitschaft. Immer wenn ich *Angel* hör muss ich an dich denken.☺ Du und Norbert wart zusammen echt ein super Team. Nicht nur fachlich, sondern auch feierlich!

Vielen lieben Dank auch an AG Döring, vor allem Yvonne, Manu, Carlos und Emiel. Danke, dass ihr mich so toll aufgenommen habt. Yvonne, du O-TA, ohne dich wäre ich ziemlich oft aufgeschmissen gewesen. Danke, dass du mir so viel beigebracht hast und so unfassbar hilfsbereit warst! Carlos, ohne dich wäre ich wohl nicht nach Mexiko. Danke, dass du mich überredet hast. In unseren 3 Wochen haben wir's doch ziemlich gut miteinander ausgehalten und hatten sehr viel Spaß auf dem Kongress, der Reise und dem Bayer-Workshop. Danke liebe Manu für die schöne Zeit am IPEK mit dir und dass wir es auch jetzt noch schaffen, uns ab und zu sehen. Ich freu mich schon auf die nächsten Pyjamapartys mit dir, Yvonne und Janina.

Großer Dank gilt auch meinen ehemaligen Betreuern Ricci und Basti. Ihr wart großartig. Erst jetzt wird mir so richtig bewusst, was ich für ein Glück mit euch beiden hatte. Ihr habt mir so vieles beigebracht und mir vertraut und dadurch mein Selbstvertrauen gesteigert.

Auch möchte ich mich bei meinem ehemaligen Labor bedanken, die bei meiner bis dato wichtigsten und auch schwersten Entscheidung total hinter mir standen.

Ein großer Dank gilt all den Uni-Leuten die mich so lange begleitet haben und die das Studium trotz Stress zu einer tollen Zeit haben werden lassen. Besonders möchte ich mich bei den Mädels Julia, Moni, Nadja, Ruth und Kasia bedanken, die mich auch noch nach der Uni-Zeit weiter begleitet haben und das auch hoffentlich weiter noch tun werden. Julia mit dir habe ich

ACKNOWLEDGEMENTS

die meisten Praktika durchgemacht und durchgestanden. Wir haben Papier in Kohlenstoff verwandelt und konzentrierte Säure zum Kochen gebracht. Ich glaube, ich und mein Labor habe es auch dir zu verdanken, dass ich teilweise so „exakt“ bin. ☺ Ruth, bei dir muss ich mich erstmal dafür bedanken, dass du es auf dich genommen hast einen Teil meiner Arbeit Korrektur zu lesen. Wir hatten eine super Zeit, vor allem im Tox-Praktikum, bei dem ich dich jeden Tag aufs Neue mit einer anderen stinkenden Angelegenheit überrascht habe. ☺ Meine liebe Kasia, ich bin überglücklich dich im Studium kennengelernt zu haben. Wir haben so viele lustige Momente zusammen erlebt: „Darf ich auch mal was sagen!? Nein! Ohoh...“ oder unser Marathon-Protokollschreiben mit unseren nächtlichen Aufwach-Jogging-Aktionen, um nur zwei der vielen vielen Beispiele zu nennen. Ich möchte dich nicht mehr missen!

Auch möchte ich mich bei all meinen Freunden, besonders bei den Münchnern, den Burgheimern und den miesen Neuburgern dafür bedanken, dass ihr die Zeit außerhalb des Labors so wertvoll gemacht hab. Mit euch kommt der Spaß nie zu kurz! Ich kann mich glücklich schätzen und bin dankbar, solche Freunde wie euch zu haben!!!

Mein ganz besonderer Dank gilt aber meiner Familie. Meiner Schwester Regina, die immer für mich da ist und meinen Eltern, die nie etwas von mir gefordert, mich aber immer bei allem unterstützt haben. Danke für alles was ihr für mich macht! Ich weiß, dass das nicht selbstverständlich ist. Ich könnte mir keine bessere Familie wünschen!!!

Zu guter Letzt möchte ich Jonas danken, der mich schon so lange - aber nicht zu lange ☺ - auf meinem Weg begleitet. Ohne ihn wäre diese Arbeit nie möglich gewesen. Du warst immer für mich da und hast mich vor allem in den für mich schwierigen Zeiten, wie in Chicago und dem Gruppenwechsel, immer total aufgebaut. Zusammen haben wir die anstrengenden Phasen überstanden und die Erfolgsmomente gefeiert. Ich freu mich auf die Zeit die jetzt kommt und kann es kaum erwarten die nächsten Herausforderungen gemeinsam mit dir zu meistern!

„Wird es einfach sein? NEIN. Wird es das wert sein? ABSOLUT!“